Elucidating the Binding and Inhibition Mechanism of Anti-malarial Drugs by Molecular Modeling and Simulation Studies

Researcher

Mehrin Gul

34-FBAS/MSBI/F09

Supervisors

Dr. Naveeda Riaz

Mrs. Saima Kalsoom

Department of Environmental Sciences
Faculty of Basic and Applied Sciences
International Islamic University Islamabad

(2012)

Elucidating the Binding and Inhibition Mechanism of Anti-malarial Drugs by Molecular Modeling and Simulation Studies

Researcher

Mehrin Gul

34-FBAS/MSBI/F09

Department of Environmental Sciences
Faculty of Basic and Applied Sciences
International Islamic University Islamabad

(2011)

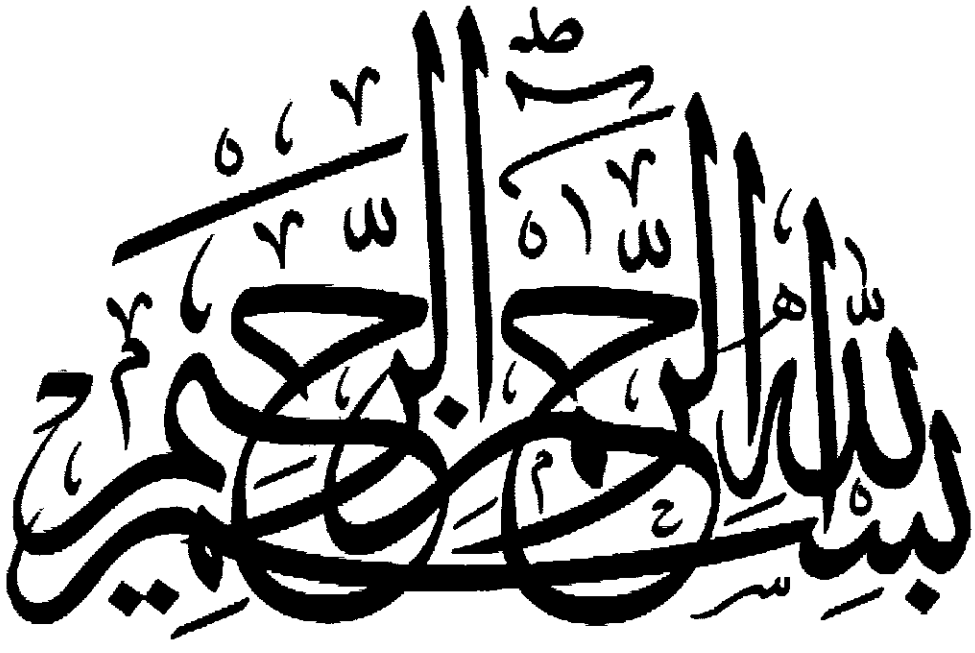

In the name of Allah Most Gracious and Most Beneficial

Department of Environmental Sciences

International Islamic University Islamabad

Dated: _____

FINAL APPROVAL

It is certificate that we have read the thesis submitted by Ms. Mehrin Gul and it is our judgment that this project is of sufficient standard to warrant its acceptance by the International Islamic University. Islamabad for the M.S Degree in Bioinformatics

COMMITTEE

External Examiner
Dr. Muhammad Ashraf
Professor, Principal
National Centre of Virology and Immunology
National University of Science and Technology

Internal Examiner
Dr. Asma Gul
Assistant Professor
Department of Environmental Sciences
International Islamic University Islamabad

Supervisor
Dr. Naveeda Riaz
Assistant Professor
Department of Environmental Sciences
International Islamic University Islamabad

Co-Supervisor
Mrs. Saima Kalsoom
PhD Scholar
Quaid-e-Azam University Islamabad

Dean, FBAS
Dr. Muhammad Irfan Khan
International Islamic University Islamabad

A thesis submitted to Department of Environmental Sciences,
International Islamic University, Islamabad as a partial
fulfillment of requirement for the award of the
degree of MS in Bioinformatics.

Dedicated to ammi, abu and love

ones

DECLARATION

I hereby declare that the work presented in the following thesis is my own effort, except where acknowledged otherwise, and that the thesis is my own composition. No part of the thesis has been previously presented for any other degree.

Date _____

Mehrin Gul

TABLE OF CONTENTS

ACKNOWLEDGMENTS

First and foremost, I thank Allah (subhana wa taala) for endowing me with patience, health and knowledge to complete this thesis. It is His unlimited blessings that I have been able to come this far. I am indebted to His unlimited blessings that He showered upon us. All praises for His Holy Prophet Muhammad (S.A.W) who enabled us to recognize our Lord and Creator and brought to us the real source of knowledge from Allah, The Quran and who is the role model for us in every aspect of life.

I acknowledge, with deep gratitude and appreciation, the inspiration, encouragement, valuable time and guidance given to me by **Mrs. Saima Kalsoom,** PhD Scholar, who served as my major advisor, enabled me to develop an understanding of the project and led to successful completion of the project. I show thanks to my **Dr. Naveeda Riaz,** Assistant Professor, International Islamic University Islamabad for her extensive guidance, continuous support, and personal involvement in all phases of this research.

Special thank goes to my family for their concern, encouragement and support throughout my life. They are one of the most valuable gifts in my life. I also thanks to all my classmates and lab mates that also give me a lot of support and idea to done this project.

Mehrin Gul

LIST OF ABBREVIATIONS

2D	Two Dimensional
3D	Three Dimensional
ACT	Artemisinin-based Combination Therapy
WHO	World Health Organization
Å	Angstrom
COMFA	Comparative Molecular Field Analysis
COMSIA	Comparative Molecular Similarity Indices Analysis
FDA	Food and Drug Administration
HBA	Hydrogen Bond Acceptor
HBD	Hydrogen Bond Donor
HOMO	Highest Occupied Molecular Orbital
DHODH	Dihydroorotate dehydrogenase
PfDHODH	Plasmodium Falciparum Dihydroorotate dehydrogenase
hDHODH	Human Dihydroorotate dehydrogenase

FMN	Flavin Mononucleotide
CoQ	Ubiguinone
DHO	Dihydroorotate
IC_{50}	Half Maximal Inhibitory Concentration
Log P	Partition Coefficient
LUMO	Lowest Unoccupied Molecular Orbital
MOE	Molecular Orbital Environment
PDB	Protein Data Bank
QSAR	Quantitative Structure Activity Relationship
CADD	Computer-aided Drug Designing
AAA	Active Analog Approach
MR	Molar Refractivity
RO5	Rule of Five
MWt	Molecular Weight
Ar	Aromatic
HY	Hydrophobic
IUPAC	International Union of Pure and Applied Chemistry
VMD	Visual Molecular Dynamics

LIST OF FIGURES

LIST OF TABLES

ABSTRACT

Malaria continues to represent a major threat to world health due to the emergence and spread of drug resistant strains but science and technology hold the promise to unlock the mysteries of diseases and to cure them. Ligand-based pharmacophore modeling is carried out on a set of 41 compounds together with the compounds were superimposed and merged into single pharmacophore showing three common features: 5 hydrophobic volume, 2 hydrogen bond acceptor and 1 hydrogen bond donor. *In-silico* approaches have been used to determine the pharmacophore triangle. Lead compound as the dihydroorotate dehydrogenase inhibitors was identified by using AutoDock Vina and the binding interactions of the active conformations of the ligands and the target protein (PDB ID: 3165) have been identified by using VMD. Lead compound showed strong ligand-protein interaction which includes 11 ionic, 13 hydrogen bonds and 55 hydrophobic interactions. Three analogues of the lead compound were made and they were also docked in order to predict their bioactivity. Quantitative structure-activity relationship was established in order to attain the information useful for the design of new compounds acting on a specific target. IC_{50} value was found to be directly related to critical volume, molar refractivity, total energy, heat of formation, E_{HOMO} and E_{LUMO}. Molecular dynamic was performed where the results show that the energy was minimized and the rigid protein structure equilibrate and show stable dynamics in 1ns simulation. On the basis of above computational studies some new compounds were identified and simulate that act as anti-malarial agent and new compounds have been proposed for clinical trials.

CHAPTER 1

INTRODUCTION

1. INTRODUCTION

Disease can be much more devastating than a weapon but the combination of the brightest minds in science and medicine, coupled with modern technology, holds the potential to unlock the mysteries of disease and cure them which elsewhere cause havoc to mankind. Malaria continues to represent a major threat to world health. It is a fatal mosquito-borne infectious disease which is caused by eukaryotic protists of the genus Plasmodium (Greenwood *et al.*, 2005). It occurs in tropical and subtropical regions of the world including much of Sub-Saharan Africa, Asia and the America. The findings indicate that there were 515 (range 300–660) million clinical episodes of *Plasmodium falciparum* malaria in 2002 (Snow *et al.*, 2005) with 0.7 to 2.7 million deaths (Breman, 2001). These estimates are substantially higher than those reported by the World Health Organization (WHO) whose latest malaria report states that in 2003, 350–500 million people worldwide became ill with malaria (Korenromp *et al.*, 2005).

Of the four species of parasite (*Plasmodium falciparum*, *Plasmodium vivax*, *Plasmodium malariae*, and *Plasmodium ovale*) that infect humans, *P. falciparum* is responsible for the majority (95%) of fatalities (Murray and Perkins, 1996) followed by *Plasmodium vivax*. *Plasmodium malarie* can lie dormant in the blood for decades *and Plasmodium vivax* and *Plasmodium ovale* can exist in the liver in a dormant stage called hypnozoites, for months. These parasites have a complex life cycle, involving two different hosts: humans and female mosquitoes of the genus *Anopheles*. The parasite *Plasmodium falciparum* is transmitted to people through the bites of infected mosquitoes. These insects inject sporozoites, which reproduce in human liver cells. After a few days, the liver cells release merozoites which invade red blood cells. Before bursting out they multiply and infect

more red blood cells, causing fever and damaging vital organs. Infected red blood cells also release gametocytes, which also infect mosquitoes when they suck human blood. In the mosquito, the gametocytes multiply and develop into sporozoites, thus parasite's life cycle is completed (Greenwood *et al.*, 2008). The entire genome of Pf was published in 2002 (Gardner *et al.*, 2002). Malaria is classified as a mild or severe form. General symptoms are vomiting, fever and coughing. Severe malaria often manifests itself differently in adults and children (Idro *et al.*, 2005; Schellenberg *et al.*, 1999). In adults, severe malaria often leads to failure of the kidneys and other organs, while children often show extreme weakness, respiratory problems, anaemia and/or cerebral malaria. The latter is a condition in which the patient falls into a coma and is believed to be caused by the sequestration of parasites in the capillaries of the brain (Taylor *et al.*, 2004).

Chloroquine was the first successful synthetic chemotherapy against malaria which was synthesised in 1934. Chloroquinine together with quinine have had a long and successful history in anti-malarial chemotherapy (Slater, 1993). Two other basic quinolines-containing drugs such as quinine and quinidine are the active ingredients in extracts from the bark of the South American cinchona tree, known for hundreds of years to possess anti-malarial properties. Chloroquine together with amodiaquine, mefloquine, halofantrine and lumefantrine acts by inhibiting the detoxification of free heme in the parasite (Kumar *et al.*, 2007; Egan and Kaschula, 2007).

Figure 1.1: *P. falciparum* Malaria Risk Defined by Annual Parasite Incidence (Carlos *et al.*, 2008).

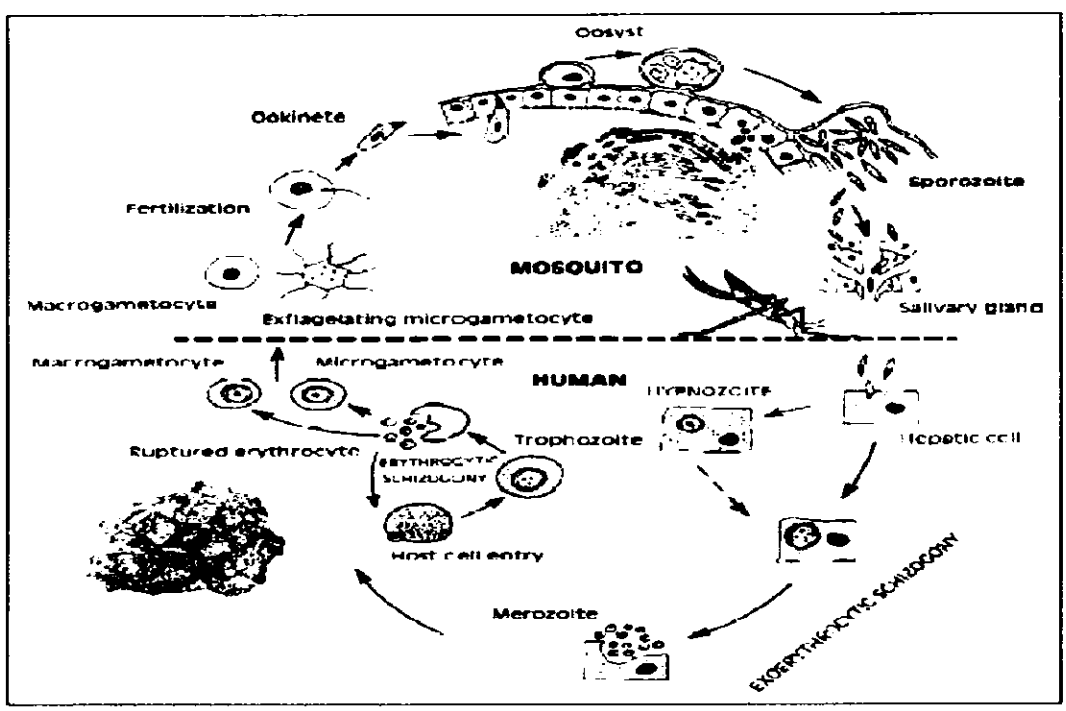

Figure 1.2: Schematic drawing of life cycle of malaria parasites (Fujioka and Aikawa, 2002).

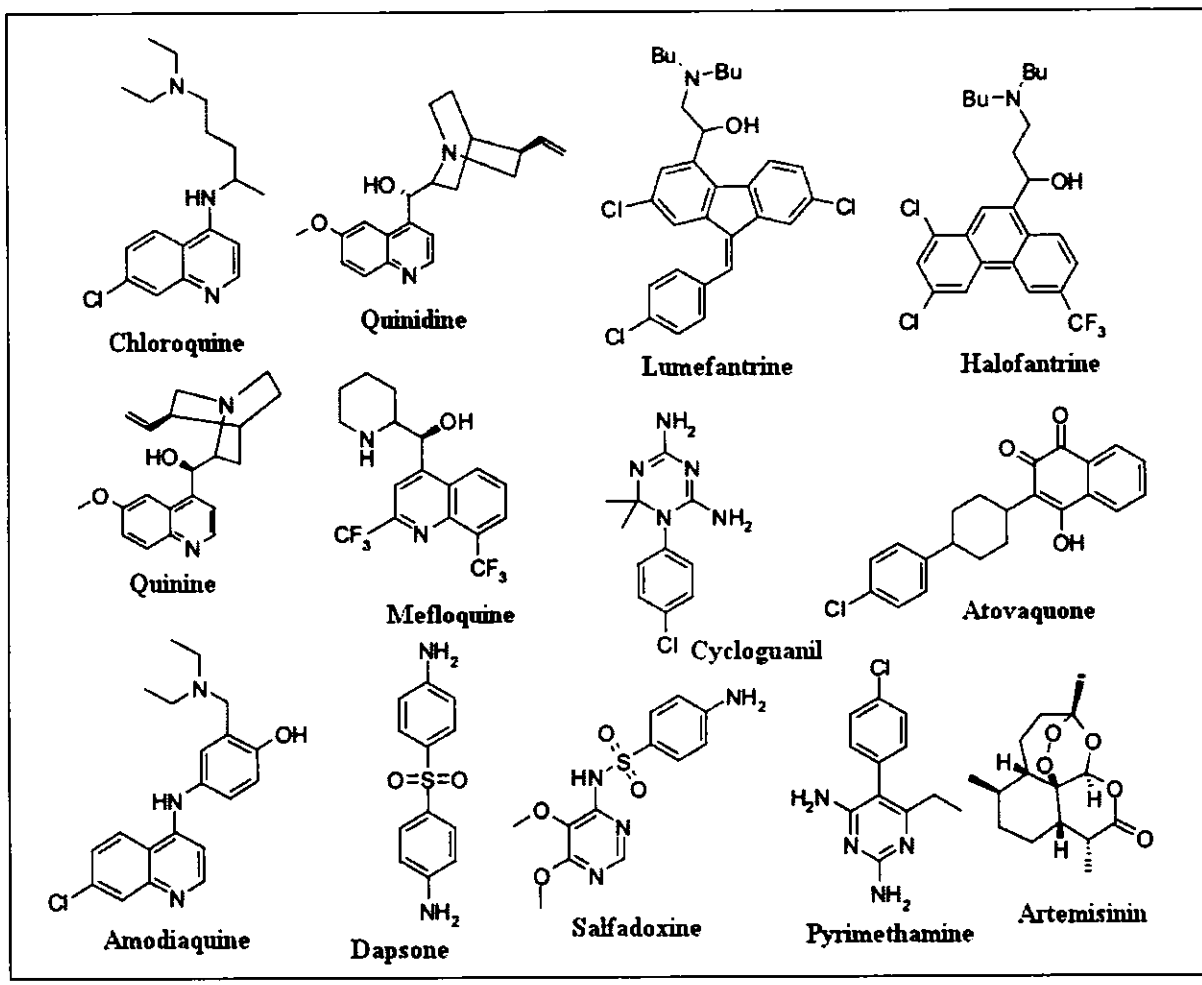

Figure 1.3: Drugs currently used to treat malaria

Drugs that act on specific target enzymes are dapsone (acting on dihydropteroate synthase), pyrimethamine (acting on dihydrofolate reductase), sulfadoxine (acting on dihydropteroate synthase), cycloguanil (acting on dihydrofolate reductase) (Rosenthal, 2001) and atovaquone (acting on the mitochondrial *bc1* complex) (Biagini *et al.,* 2008).The currently recommended first-line therapy employ artemisinin or one of its analogues together with another drug (ACT, artemisinin-based combination therapy) (WHO, 2006).

Artemisinin is a natural product extracted from the flowers and leaves of the traditional Chinese medicinal plant *Artemisia annua (*Balint, 2001*)*. Recent reports of Artemisinin resistance in western Cambodia raise the alarming possibility that this class of drugs may also fall to resistance (Dondorp *et al.,* 2009).There are a number of drugs approved for its treatment but drug resistance has compromised most of them, making the discovering and development of new anti-malarial agents one of the greatest challenge and essential. Anti-malarial drugs will be essential tools along the path towards eradication, including the early control or "attack" phase to drive down transmission and the later stages of maintaining interruption of transmission, preventing malaria reintroduction, and eliminating the last residual foci of infection (Alonso *et al.,* 2011).

The completion of the *Plasmodium falciparum* genome and a growing understanding of parasite biology are fueling the search for novel targets. Despite this, few targets have been validated chemically *in vivo*. De novo pyrimidine biosynthesis represents an attractive and potential target for the identification and development of new chemotherapeutic agents against *P. falciparum*.

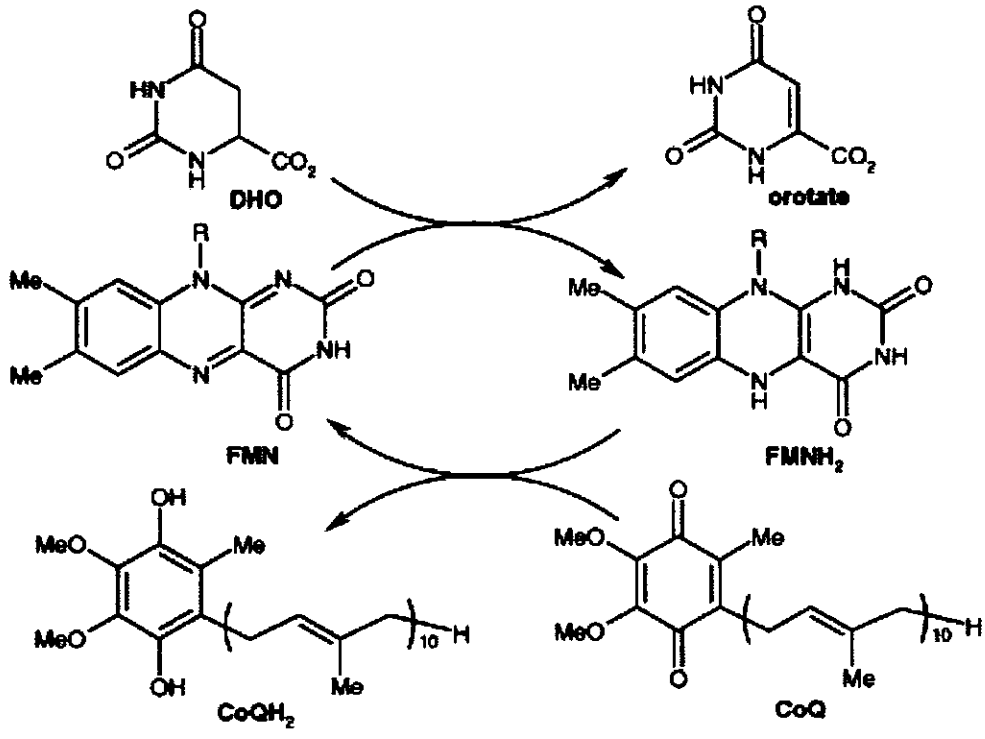

Figure 1.4: Reactions catalyzed by DHODH (Heikkila *et al.*, 2006).

Unlike human cells, which can both synthesise and salvage pyrimidine bases, *P. falciparum* relies completely on a de novo biosynthesis pathway, thus lacking any pathway for the salvage of preformed pyrimidine bases or nucleosides. Dihydroorotate dehydrogenase (DHODH) is the fourth essential mitochondrial enzyme in the pyrimidine biosynthetic pathway. In the presence of the co-factors flavin mononucleotide (FMN) and ubiquinone (CoQ), it catalyses the oxidation of dihydroorotate (DHO) to orotate.

The human version of this enzyme (hDHODH) is the target of a number of inhibitors with proven efficacy in the treatment of arthritis and leflunomide, a pro-drug that is metabolised to the active DHODH inhibitor, A77-1726, is approved for clinical use (Herrmann *et al.,* 2000; Robert *et al.,* 1999; Davis *et al.,* 1996; Greene *et al.,* 1995). Random high-throughput screening of chemical libraries has been used to identify selective inhibitors of *Escherichia coli* (Marcinkeviciene *et al.,* 2000), *Helicobacter pylori* (Copeland *et al.,* 2000) and *P. falciparum* (Baldwin *et al.,* 2005) PfDHODH, respectively. Additionally, Boa *et al.,* have recently shown that selective inhibitors of PfDHODH can be developed from existing inhibitors (Boa *et al.,* 2005). Activated lymphocytes require *de novo* pyrimidine biosynthesis to support their enhanced growth rate, providing a level of selective toxicity towards the target cell population while resting lymphocytes survive on pyrimidine salvage. Other inhibitors of human DHODH with immunosuppressive activity have also been reported, including additional analogs of A77 1726 (Kuo *et al.,* 1969), redoxal (Knecht and Loffler, 2000), S-2678 (Deguchi *et al.,* 2008) and the cinchoninic acid derivative brequinar (Batt *et al.,* 1998; Pitts *et al.,* 1998; Batt *et al.,* 1995; Peters *et al.,* 1990; Chen *et al.,* 1986). Brequinar was evaluated in clinical trials as possible anticancer agent however it was never approved for clinical use.

Figure 1.5: X-ray structure of *Pf*DHODH. Ribbon diagram of an alignment of the structures bound to A77 1726 (tan; pdb 1TV5) and DSM1 (purple; pdb 3I65) (Phillips and Rathod, 2010)

So PfDHODH enzyme is an attractive target for the development of new therapeutic agents against malaria.

Clardy solved the X-ray structures of human DHODH bound to A77 1726 and brequinar providing the first insight into the nature of the inhibitor binding-site in the Class 2 enzymes (Liu *et al.*, 2000). Afterward a number of additional X-ray structures of the human enzyme bound to various inhibitors have been reported (e.g. (Davies *et al.*, 2009; Baumgartner *et al.*, 2006; Walse *et al.*, 2008)), and the X-ray structure of *Pf*DHODH has been solved bound to both A77 1726 (Hurt *et al.*, 2006) and to novel malarial inhibitors from the triazolopyrimidine series (Deng *et al.*, 2009). The central structural element of DHODH from all class types is the core β/α-barrel domain. This domain houses the binding site for the FMN cofactor, which is bound near strand β13 at the top of helix α11 (Figure 1.6). Orotate forms a stacking interaction with FMN on one side, while the oppositeside of the orotate binding-site is formed by β11 and surface loops containing Ser-395 and Thr-459. In addition the class 2 enzymes have a largely hydrophobic N-terminal helical domain (α1 and α2) that presumably sits adjacent to the membrane. The inhibitor binding-site, as illustrated for A77 1726, is formed between the N-terminal helices and the β/α-barrel domain, making interactions with helix α3, α11 and strand β5.

Human life is constantly threatened by many diseases but drugs are used in order to prevent and treat them so ideal drugs are always in great demand. To meet the challenges of ideal drugs, an efficient method of drug development is required. The process of drug development is challenging, expensive, time consuming, and requires consideration of many aspects. Several multidisciplinary approaches are required for the process of drug development in order to fulfill these challenges. The first step is to find potential lead

structures with desired biological activity. Computer-aided drug design (CADD) techniques can help increase the pool of interesting compounds that can be evaluated. The rapid increase in computer memory and speed and the decreased cost of personal computers and workstations have brought important computational resources within the reach of most researchers. Inexpensive computer graphics programs offer enhanced methods of organizing and visualizing molecular information. The algorithms underlying molecular modeling have seen a steady improvement, leading to increasing accuracy in the calculation of molecular properties. The fundamental hypothesis of most CADD procedures is that the key biological event, at the molecular level, is the recognition and noncovalent binding of small molecules (ligand) to specific sites on target biological macromolecules (receptors).

A drug target is a biomolecule which is involved in signaling or metabolic pathways that are explicit to a disease process. As a key example, a drug target would be a biomolecule (for example epidermal growth factor receptor) that is frequently mutated or otherwise deregulated in the disease of cancer. Biomolecules play vital roles in disease progression by communicating through either protein–nucleic acid interactions or protein–protein interactions resulting in propagation of signaling events and/or alteration of metabolic processes. Therefore, modulation of biological functions performed by these biomolecules would be beneficial and could be achieved either (i) by inhibiting the bimolecular interactions by small molecules (between the biomolecules, relatively less studied) (Fuller *et al.*, 2009), to stop cross talks between biomolecules, (ii) by inhibiting their function with small molecules whose competitive binding affinity would be greater than their natural ligands that bind to the active sites (within the biomolecules), or (iii) by activating biomolecules (for normal functions) that are functionally deregulated in some diseases such as cancer. Developing a lead structure and

an effective drug is challenging even for known targets. Recently, drug development has significantly increased due to the availability of 3D X-ray or NMR structures of biomolecules, docking tools, and the development of computer aided methodologies (Greer *et al.,* 1994; Muller, 2009; Henry, 2001). Moreover currently, the Protein Data Bank (PDB) has been developed that holds about 57,558 3D structures. Mainly Computer-Assisted drug designing incorporate following basic steps for the development of novel drug: Pharmacophore Identification, Molecular Docking and QSAR studies.

Pharmacophore Modeling is a three-dimensional computational approach which rationalizes distributions of activities within groups of molecules exhibiting a similar pharmacological profile and believed to be recognized by the same site of a target protein. IUPAC working party leaded by Camille G. Wermuth defines pharmacophore to be "an ensemble of steric and electronic features that is necessary to ensure the optimal supramolecular interactions with a specific biological target and to trigger (or block) its biological response (Wermuth *et al.,* 1998). This "structure-based" definition directly relates pharmacophores to the microscopic phenomenon of molecular recognition of bioactive compounds (potential drugs) by their biological targets and enlightens about the main utility of pharmacophore modeling in drug design. Pharmacophores were historically established by Lemont Kier, who first mentions the concept in 1967 (Kier, 1967) and uses the term in a publication in 1971 (Kier, 1971). The development of the concept is often accredited to Paul Ehrlich but neither the alleged source (Ehrlich, 1909) nor any of his other works mention the term "pharmacophore" or make use of the concept (Drie, 2007). A pharmacophore was firstly described as a molecular framework that carries the essential features that are responsible for a drug's biological activity, with no reference to any microscopic biological target. Peter Gund

(Gund, 1979) and more effectively Garland Marshall with its Active Analog Approach (AAA) (Marshall *et al.*, 1979), developed the basis of present computational three-dimensional "ligand-based" pharmacophore modeling in the late seventies. A computer programs was developed that facilitated the process of determining putative pharmacophoric patterns in different congeneric series of a drug. In computer-assisted early drug research, the most frequent application of pharmacophore models is in multi-step virtual screening or in silico screening workflows, where they filter down the number of compounds for selection. Several programs for pharmacophore modeling are widely used mainly because of their availability in commercial software packages, such as CATALYST (Barnum *et al.*, 1996), PHASE (Dixon *et al.*, 2006), LIGANDSCOUT (Wolber and Langer, 2005) GALAHAD (Richmond *et al.*, 2006) GASP (Jones et al., 1995) and the pharmacophore module of MOE. Typical pharmacophore features are for where a molecule is aromatic, hydrophobic, a hydrogen bond donor, a hydrogen bond acceptor, a cation, or an anion. In order to identify novel ligands the features need to match different chemical groups with similar properties. Ligands receptor interactions are typically "polar negative, "polar positive"or "hydrophobic". A well-defined pharmacophore model includes both hydrophobic volumes and hydrogen bond vectors. These models are used extensively in medicinal chemistry for hit and lead identification and during the subsequent lead to candidate optimization.

The first algorithm developed to dock small molecules into the binding pocket of a biological macromolecule, **the DOCK algorithm**, was published in 1982 by Kuntz et al. In a review from 2007, thirty scoring functions and more than sixty published docking programs were listed (Moitessier *et al.*, 2007). However, the most widely and earliest used docking programs over the past years are probably DOCK (Moustakas *et al.*, 2006; Ewing and Kuntz,

1997; Shoichet *et al.*, 1992; Leach and Kuntz, 1992; Meng *et al.*, 1992), AutoDOCK (Huey *et al.*, 2007; Morris *et al.*, 1998; Morris *et al.*, 1996; Goodsell and Olson, 1990), GOLD (Verdonk *et al.*, 2005; Verdonk *et al.*, 2003; Jones *et al.*, 1997; Jones *et al.*, 1995) and FlexX (Rarey *et al.*, 1999; Rarey *et al.*, 1999; Rarey *et al.*, 1997; Rarey *et al.*, 1996; Rarey *et al.*, 1996) and in recent years also e.g. ICM (Totrov and Abagyan, 1997; Abagyan and Totrov, 1994; Abagyan *et al.*, 1994), Glide (Friesner *et al.*, 2006; Friesner *et al.*, 2004; Halgren *et al.*, 2004), FRED (McGann *et al.*, 2003) and Surflex (Jain, 2003). NMR structures are suggested as the best source for drug discovery and multiple crystal structures with bound ligands can be used to create a composite binding site, which is more likely to find possible ligands from a database of drug-like molecules. The challenge of docking a flexible ligand into a rigid target has been taken up by a number of groups; one particularly good outcome is the FlexX algorithm (Kramer *et al.*, 1999). Access to activity data for a large library of compounds is rare outside of industrial institutions, but can provide an outstanding source for improving and testing docking algorithms, as is the case for Knegtel and Wagener (Knegtel and Wagener, 1999) at Vertex Pharmaceuticals. Using both 'chemical' and energy scoring functions in DOCK 4.0, and an incremental construction algorithm (docks a rigid fragment from the ligand, adding the remaining fragments in a stepwise fashion) for ligand flexibility, only a limited number of ligand conformations were sufficient to rank the actives against the nonactives. Different protein systems require different scoring functions owing to the variation in the hydrophobicity of their binding sites. The possibility of multiple binding modes for a given ligand docked into a particular protein is the focus of the theoretical paper by Brem and Dill (Brem and Dill, 1999). Substituting a simplified model for a protein–ligand

system, purely two-state model (bound/unbound) is not sufficient for predicting binding strengths.

All docking programs contain two components, a scoring function, whose global minimum is intended to coincide with the global free energy minimum of the target-ligand system, and a search method which is used to sample the search space in which the scoring function is optimised. This search space can be very large, combining all ligand rotations and positions with all possible conformations of the ligand and probably also the target protein. In DOCK, the ligand and the protein were initially treated as a rigid body and an incremental construction algorithm has since been adopted to include ligand flexibility. In this version, the ligand is partitioned into rigid fragments placed incrementally in the active site of the target. The fitness function is the sum of the van der Waals and Coulomb interactions between the ligand and the target atoms. By using geometrical methods, ligand positions and orientations are sampled through matching of spheres describing the active site and the ligand. The fitness function is estimated using a pre-calculated grid covering the active site, to reduce the CPU time required to dock each ligand. AutoDOCK also treats the target as a rigid body, and uses a pre-calculated grid to evaluate the fitness function. This function is again force-field based and also includes intramolecular interactions of the ligand. The ligand conformations, orientations and positions were sampled by simulated annealing, but now genetic algorithms are also used. AutoDock Vina is an upgraded version of Auto Dock 4 which is compatible with the Auto Dock PDBQT file format and offers the following advantages over Auto Dock 4:

- grid computation is not necessary which was a complex process elsewhere,
- gives higher accuracy of binding mode, and it is considerably faster

- available for each operating system and use iterated local search algorithm (Chang MW *et al.*, 2010).

Quantitative structure–activity relationships are the most important applications of chemometrics, giving information useful for the design of new compounds acting on a specific target. QSAR attempts to find a consistent relationship between biological activity and molecular properties. In the 1960s, methods to quantitatively approximate the activity of possible lead compounds' analogues began to develop. The field of complement inhibitors benefited from the work of Corwin Hansch (Kutter and Hansch, 1969) who is the founder of QSAR methods. Hansch established quantitative SARs for several classes of compounds which display complement-inhibiting activity (Hansch and Yoshimoto, 1974). Softwares such as COMFA and COMSIA (Klebe G *et al.*, 1998), Chem Draw (Zielesny A *et al.*, 2005), Hyper Chem (Tsuji M, 2010) and many more are used for finding molecular descriptors. Chem draw software package is a chemical structure drawing tool which enables several features upon the drawing of structure which includes boiling point, melting point, critical volume, heat of formation, Log P and molar refractivity (MR). Energy minimization of the compound is done by using Hyper Chem which alters molecular geometry to lower the energy of the system, and yields a more stable conformation. It generates a log file using computational chemistry techniques such as semi-empirical formula, molecular mechanics etc (hypercube *et al.*, 2002). Thus, QSAR models can be used to predict the activity of new compounds.

Molecular dynamics simulations are one of the most versatile and widely applied computational techniques for the study of biological macromolecules (Norberg and Nilsson, 2003; Hansson et al., 2002; Karplus and McCammon, 2002). They are very valuable for

understanding the dynamic behavior of proteins at different timescales, from fast internal motions to slow conformational changes or even protein folding processes (Snow et al., 2005). It is also possible to study the effect of explicit solvent molecules on protein structure and stability to obtain time-averaged properties of the biomolecular system, such as density, conductivity, and dipolar moment, as well as different thermodynamic parameters, including interactions energies and entropies. It is useful not only for rationalizing experimentally measured properties at the molecular level, but it is well known that most structures determined by X-ray or NMR methods have been refined using MD methods. Therefore, the interplay between computational and experimental techniques in the area of MD simulations is longstanding, with the theoretical methods assisting in understanding and analyzing experimental data. These, in turn, are vital for the validation and improvement of computational techniques and protocols. Commonly used programs for MD simulations of biomolecules include Amber CHARMM (Brooks et al., 1983), (Cornell et al., 1996), NAMD (Nelson et al., 1996) and GROMOS (Gunsteren, 1999)). Molecular dynamics was first introduced by Alder and Wainwright in the late 1950s (Alder and Wainwright, 1957), this method is used to study the interaction hard spheres. From these studies, they learn about behavior of simple liquids. In 1964, Rahman did the first simulations using realistic potential for liquid argon (Rahman, 1964). And in 1974, Rahman and Stillinger performed the first molecular dynamics simulations using a realistic system that is simulation of liquid water (Stillinger and Rahman 1974). The first protein simulations appeared in 1977 with the simulation of the bovine pancreatic trypsin inhibitor (BPTI). Today molecular dynamics simulations are well established in the scientific community and this technique is applied to

wide range of application including chemical, biophysical, or medicinal problem such as enzyme catalysis, protein-protein interactions and protein/ligand design.

The static view of the protein-ligand interaction is unrealistic since the proteins interact with ligands in a solvated environment and positioning of water molecules in crystallographic structure are limited to X-ray diffraction resolution parameters. One way to overcome this problem and obtain a more realistic view of protein-ligand interaction comes from molecular dynamic simulations (Punkvang et al., 2010). Commonly used programs for MD simulations of biomolecules include Amber, CHARMM, GROMACS, and NAMD. Gromacs is an application that was first developed by department of chemistry in Groningen University. The aim of GROMACS is to provide a versatile and efficient MD program with source code, especially directed towards the simulation of biological molecules in aqueous and membrane environments, and able to run on single processors as well as on parallel computer systems.

The main purposes of the molecular dynamics simulation is:

- Generate trajectory molecules in the limited time period.
- Become the bridge between theory and experiments.
- Allow the chemist to make simulation that can't be done in the laboratory.

CHAPTER 2

MATERIALS AND METHODS

2. Materials and Methods

In an effort to reduce the cost of developing new medicines and their time to market, the drug discovery process has now been streamlined by computational tools. Today, virtually every drug company has adopted computational methodology in most stages of the design process (Jorgensen, 2004; Barril *et al.*, 2006; Tramontano, 2006). Many computational methods complement one another and may be combined to rationalize the drug discovery process.

2.1 Anti-Malarial Drugs

The data set consisted of anti-malarial agents along with some standard inhibitors are shown in Table 2.1. Chemdraw was used to draw the anti-malarial agents for further application which were then saved in pdb file format.

2.2 Pharmacophore Modeling

The study was carried out using the software Ligand Scout (version 3.02). It is a software tool that allows to model 3D chemical feature-based pharmacophore models from structural data of macromolecule/ligand complexes. It integrate a complete definition of 3D chemical features that describe the interaction of a ligand with the protein (Wolber and Langer, 2005). By using pattern-matching based alignment algorithm these pharmacophores can be superimposed (Wolber *et al.*, 2007). Shared features can be intercalated to create "shared-feature pharmacophore" that shares all common interactions of several binding sites/ligands or extended to create "merged-feature" pharmacophore. The software has been successfully used in drug designing to predict new lead structures, e.g. for the prediction of biological activity of novel HIV reverse transcriptase inhibitors (Barreca et al., 2007).

Table 2.1 Anti-malarial agents along with IC50 value.

Compound	**Structure**	**IC50 (μM)**	**Compound**	**Structure**	**IC50 (μM)**
GUL1	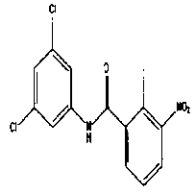	0.016	GUL22	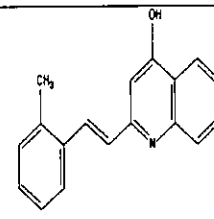	0.93 ± 0.1
GUL2	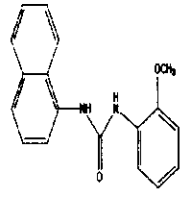	0.23	GUL23	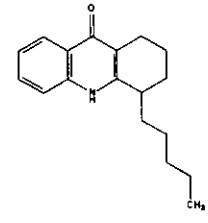	0.34 ± 0.1
GUL3	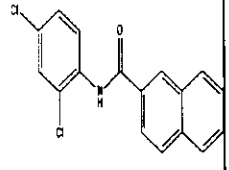	0.05	GUL24	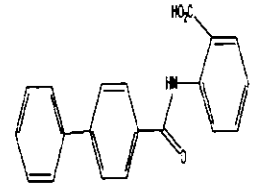	13.2
GUL4	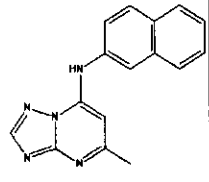	0.047	GUL25	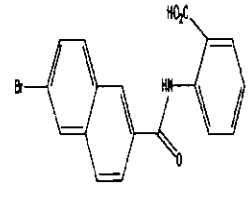	14.2
GUL5	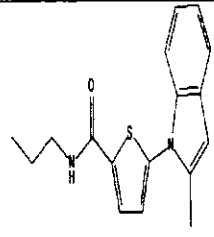	0.042	GUL26	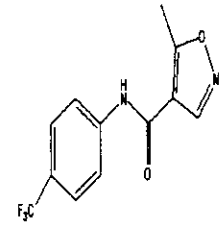	0.06

GUL6	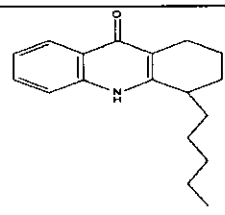	0.34	GUL27	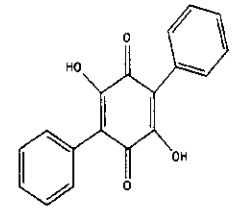	0.89
GUL7	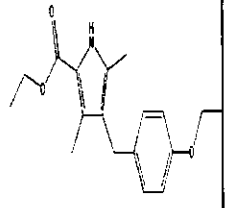	0.083	GUL28	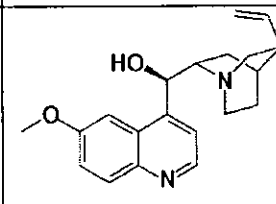	0.97
GUL8	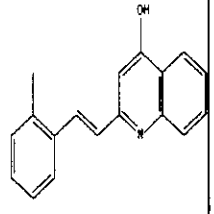	0.93	GUL29	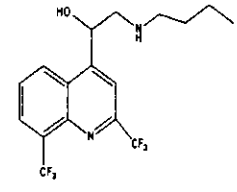	1.8
GUL9	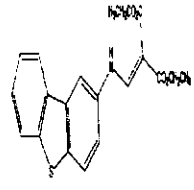	0.16	GUL30	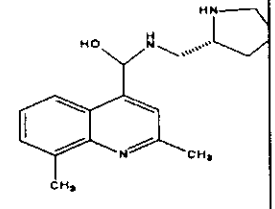	3.2
GUL10	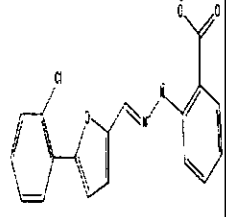	0.5	GUL31	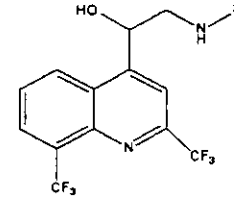	3.7

GUL11	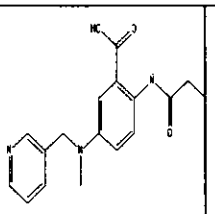	5.5	GUL32	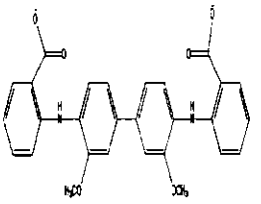	0.43 ±0.2
GUL12	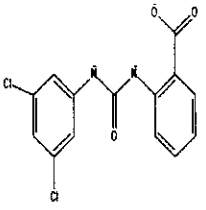	0.7	GUL33	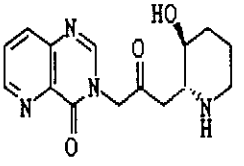	3.1
GUL13	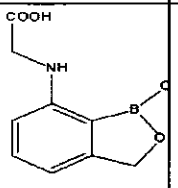	0.95	GUL34	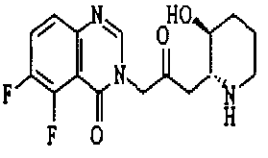	1.8
GUL14	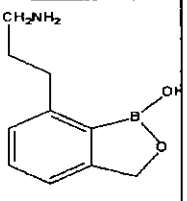	0.52	GUL35	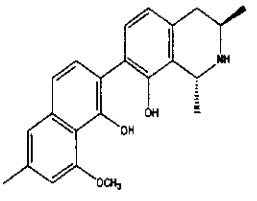	1.9
GUL15	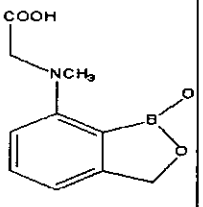	>5	GUL36	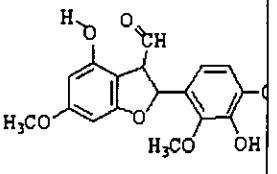	4.1
GUL16	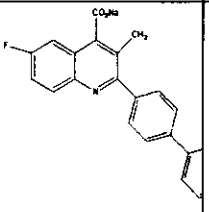	888	GUL37	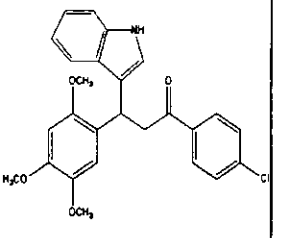	2.4

GUL17	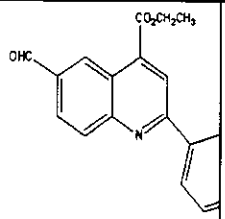	>200	GUL38	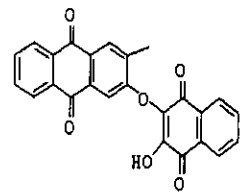	4.1
GUL18	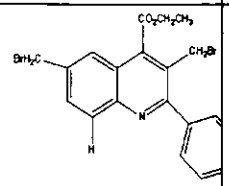	>200	GUL39	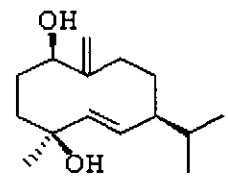	2.8
GUL19	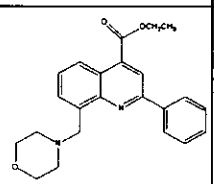	>200	Atovaquone	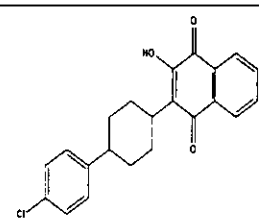	27.4
GUL20	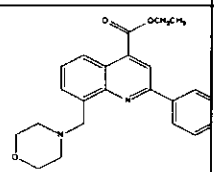		A771726	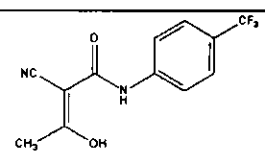	4.7
GUL21	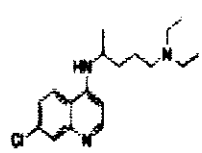	0.39			

The training set consisted of 40 compounds of which 3 were standard compounds. It was selected to generate the ligand based pharmacophore model. The compounds present in the set were different groups of Chloroquinine, Quinine, atovaquone, alkoids, sesquiterpenoid, Quinone, DHOH, Andidermal, chalcone, benzoxaborole, quinoline methanols, brequinar, amino-Benzoic Acid, polyporic acid, DHOD, A771726, Leflunomide and ureas. Ligand based pharmacophore model generation was performed using default settings of Ligand Scout 3.02. The pharmacophore for each group of compounds has been generated and the distances among the pharmacophoric features of the ligands have been calculated using the software VMD. It is a molecular graphics program designed for the display and analysis of molecular assemblies such as proteins and nucleic acids (Humphrey *et al.*, 1996). The pharmacophore of the above mentioned groups have been superimposed in order to get the common pharmacophore of anti-malarial DHODH inhibitors. The distances among the pharmacophoric features of the common and unique pharmacophore were then calculated.

2.3 Molecular Docking

In the perspective of molecular modeling, docking means predicting the bioactive conformation of a molecule in the binding site of a target (Blaney *et al.*, 1993). This is equivalent to finding the global free energy minimum of the system consisting of the target and the ligand (Verkhivker *et al.*, 2000; Totrov *et al.*, 1997). Docking is used as important tool in structure-based drug design. AutoDOCK treats the target as a rigid body, and evaluate the fitness function by using a pre-calculated grid. This function is force-field based which includes intramolecular interactions of the ligand. The ligand conformations, positions and orientations were initially sampled by simulated annealing, but today genetic algorithms are also used.

As target protein and ligands is two important constituent in the process of molecular docking so in order to perform docking studies a suitable target protein for selected anti-malarial agents was identified. The target protein *plasmodium falciparum* Dihydroorate Dehydrogenase pfDHODH (Protein Data Bank ID: 3I65) was chosen for current study. It is the fourth enzyme in the *de novo* pyrimidine biosynthetic pathway of *P. falciparum*, dihydroorotate dehydrogenase and consisted of 415 amino acids.

Docking studies on the dataset of 41 anti-malarial agents were carried out by using the latest docking software AutoDock Vina (Trott *et al.*, 2010), which accept the pdb files of ligand and target. Water molecules were removed from the text file of 3I65. The pdb files of ligand and target were placed in a newly formed folder, in the directory of installed software. All the missing hydrogens and atoms of protein were checked, repaired and added by using autodock tools and saved in pdb file format. Autodock perform operation within pregenerated grid map so the conformational flexibility of the receptor was not considered. The ADT package was also used to prepare the docking input files of ligands which automatically compute gasteiger charges, merge non polar hydrogen to carbon atom and define torsions. The ligand file was saved in .pdbqt file format. For preparing the target file and to be saved as .pdbqt file, opened the target file from grid which automatically added hydrogen and charges. Proper area and dimension for docking was provided by setting the properties of grid box. Grid parameter file for 3I65 was prepared by centered the affinity grid on the predefined active site of protein with dimensions of 20Å×20Å× 20Å and grid spacing of 0.375. Log parameter files was generated by running the command ("\Program Files\The Scripps Research Institute\Vina\vina.exe" --config conf.txt --log log.txt) on the command prompt. The docking conformation of ligand was analyzed and all structures generated were evaluated on

the basis of the lowest energy. The lowest energy conformation was obtained among all the observed conformation. The overall procedure was repeated for all the 41 compounds. The log parameter files for all ligands docked into 3I65 were obtained and analyzed.

2.3.1 Ligand Protein Interactions

The ligand protein interactions were predicted using Visual Molecular Dynamics VMD (Humphrey *et al.,* 1996). The target protein and the active conformation of ligand obtained from docking were taken as input to the VMD. The interactions were studied between the ligand and the active site of target by selecting atoms within 5Å.

2.3.2 Lead Identification

Binding interactions of all docked protein ligand complexes have been observed thoroughly and the compound showing the best interactions among all has been identified as lead compound.

2.3.3 Analogue Designing

Three structural analogues of the lead compound were made by the introduction or elimination of various functional groups. Docking studies were applied on the analogue by the same procedure mentioned above by using AutoDock Vina and the ligand–protein interactions of the analogues have also been obtained by using VMD.

2.4 Quantitative Structure Activity Relationship

The fundamental theory of QSAR modeling is that molecular structure can be correlated to physical or biological properties thus the requirement is some method to encode various structural features in a molecule. Molecular descriptors fulfill this requirement as they are numerical representations of specific molecular features. A number of steric and electronic

descriptors can be calculated by using ChemDraw and HyperChem. ChemDraw was used to calculate steric descriptors like Molecular weight, hydrophobicity, molar volume, heat of formation and molar refractivity. Electronic descriptors like total binding energy, HUMO and LUMO were calculated by HyperChem.

2.5 Molecular Dynamic Simulation

Molecular dynamics (MD) simulations were performed using the GROMACS 4.5.4 package and the molecular graphics for analysis was produced by GRACE. The *plasmodium falciparum* dehydroorotate dehydrogenase bound with triazolopyrimidine-based inhibitor DSM2 were used for performing MD simulations. Topology file for protein was prepared with pdb2gmx by using the standard GROMOS96 43A1 force field and the ligand topology file and force field parameters were generated using the PRODRG program. A unit cell was defined and was filled with water in order to get the solvated system. The system was neutralized by adding 6 Cl counterions by replacing water molecules, respectively. The energy of this complex was minimized using the steepest descent minimization algorithm. Then, a 100 ps position restraining dynamics simulation was carried out to restrain the complex and to relieve close contacts before the actual simulation. Finally, 1 ns MD simulations were performed at the NPT canonical ensemble and the periodic boundary conditions were used in all three dimensions. Berendsen's temperature coupling method and Parrinello-Rahman's pressure coupling methods were used. Water molecules, ions, receptor, and ligand were coupled separately in a temperature bath at 300 K, with a coupling constant tt = 0.1 ps. The pressure coupling is on for NPT with a constant pressure of 1 bar and a coupling constant tp of 2 ps. The particle mesh Ewald (PME) method for long-range electrostatics, a

14A° cutoff for van der Walls interactions, a 9A° cutoff for Coulomb interactions and the Lincs algorithm for covalent bond constraints were used.

CHAPTER 3

RESULT AND DICUSSION

3. Results and Discussions

3.1 Data Set Formation

Anti-malarial agents were taken into account for Computer-Aided drug designing. It incorporated different classes as the functional groups, making the total of 41 compounds in the data set. These compounds included 2 FDA Approved drugs (A771726, Atovaquone) which were taken as standard drugs and rest 39 as the potential hits for this study. These various compounds belong to following classes: Chloroquine, Quinine, Andidermal B, Sesquiterpenoid, Alkoid, Quinone, Chalcone, Quinoline methanols, Benzoxaborole, Brequinar, Polyporic acid, Amino-Benzoic acid, Redoxal, Leflunomide and Ureas (McLean et al., 2010; Zhang et al., 2011; Boa et al., 2005; Patel et al., 2008; Milner et al., 2010; Knecht and Loffler., 2000; Kaur et al., 2009; Heikkila et al., 2006; Kuo et al., 1996).

3.2 Rule of Five

The rule of five (RO5) deals with orally active compounds and defines four simple physicochemical parameter ranges (MWt $\leq$ 500, log $P \leq 5$, H-bond donors $\leq$ 5, H-bond acceptors $\leq$ 10) associated with 90% of orally active drugs that have achieved phase II clinical status. These physicochemical parameters are associated with acceptable aqueous solubility and intestinal permeability and comprise the first steps in oral bioavailability. The results are given in Table 3.1.

Table 3.1: Lipinski's rule (Rule of Five) applied to complete data set

Compound	HBA	HBD	Molecular Weight (amu)	Log P
GUL1	3	1	278.27	4.56
GUL2	2	2	292.34	3.38
GUL3	1	1	269.30	4.88
GUL4	4	1	275.31	2.86
GUL5	2	1	298.40	3.95
GUL6	2	1	269.39	3.45
GUL7	4	1	301.39	3.86
GUL8	2	1	261.32	4.83
GUL9	3	1	369.44	4.03
GUL10	2	2	317.32	3.88
GUL11	4	1	313.36	1.83
GUL12	3	2	278.27	3.19
GUL13	4	1	206.99	2.69
GUL14	2	1	191.04	1.11
GUL15	4	1	221.02	3.06
GUL16	4	1	388.37	4.88
GUL17	3	2	305.33	4.12
GUL18	2	2	324.98	5.92
GUL19	3	3	376.46	3.92
GUL20	3	3	376.46	3.92
GUL21	1	2	296.44	2.64
GUL22	2	1	261.32	4.83
GUL23	2	1	269.39	3.45
GUL24	3	1	317.34	4.07

GUL25	3	1	301.11	4.22
GUL26	6	1	270.21	2.27
GUL27	4	2	292.29	0.34
GUL28	3	2	324.42	2.37
GUL29	8	2	380.33	4.65
GUL30	2	3	285.39	2.72
GUL31	8	2	324.23	2.89
GUL32	5	2	484.51	5
GUL33	4	3	302.33	3.54
GUL34	5	3	337.33	4.86
GUL35	2	2	393.48	3.07
GUL36	6	2	332.31	1.21
GUL37	4	1	426.49	4.84
GUL38	6	1	410.00	1.64
GUL39	2	2	238.00	2.87
Atovaquone	3	2	343.40	3.68
A771726	6	1	270.21	1.27

The results of RO5 shows that all the compounds follow the rule so all the potential hits have druggable properties.

Table 3.2: Detailed Analysis of Rule of Five in percentage form

RULE OF FIVE CONSTRAINT	PERCENTAGE
Hydrogen Bond Acceptor	100%
Hydrogen Bond Donor	100%
Molecular Weight	100%
Log P	100%

3.3 Pharmacophore Modeling

The pharmacophore model of anti-malarial agents has not been reported yet therefore it is an attempt to generate the general pharmacophore model. The pharmacophore generated by Ligand Scout for the training set showed five main features as hydrogen bond acceptors, hydrogen bond donors, aromatic ring, hydrophobic and positive ionizable. The pharmacophore generated for the chosen group of compounds showed consistency in the above features. The features identified in green colors are the HBDs, red colored are HBAs and the aromatic rings are shown in blue color. The pharmacophores of all these compounds were then coordinated and a unique pharmacophore was identified after a detailed analysis. Similar features were identified after analyzing the pharmacophores of all compounds. The similar features of all the compounds were then analyzed, superimposed and merged into a single pharmacophore. The pharmacophoric features for each are shown in Table 3.3.

The distance ranges from minimum to maximum and have been measured between the HBA and HBD, HBA and aromatic ring and HBD and aromatic ring as shown in Figure 3.1. The distances between HBA and HBD range from 4.0 to 4.99 (Å), between HBD and Ar/HY range from 3.70 to 4.75 (Å) and between Ar/HY to HBA range from 3.70 to 4.6 (Å). The distances were calculated with the help of VMD software.

To generate a pharmacophore model, 17 ligands were superimposed along with a two standard drug (Teriflunomide and Atovaquone) and the shared pharmacophore was produced as shown in Figure 3.2 This shared pharmacophore represent that every candidate compound must have 5 hydrophobic volumes, 2 hydrogen bond acceptors (HBA) and 1hydrogen bond donors (HBD).

Table 3.3: Pharmacophore features of each compound.

Compounds	**Ar**	**HY**	**HBA**	**HBD**	**Positive Ionizable**
Chloroquine	2	4	1	2	1
Quinine	2	3	3	2	1
Sesquiterpenoid		1	2	2	1
Andidermal B	1	1	6	2	1
Alkoids	2	3	5	3	2
Quinone	2	3	6	3	-
DHOH	3	4	3	1	1
Chalcone	4	3	4	1	-
Benzoxaborole	1	1	4	1	1
Quinoline methanols	2	4	8	2	1
Brequinar	3	6	4	1	1
Polyporic acid	2	2	4	2	-
Amino-Benzoic acid	3	4	2	2	1
Redoxal	4	3	5	2	-
DHOD1	3	3	2	1	-
Leflunomide	2	3	6	1	-
Ureas	3	3	2	2	-
Teriflunomide(A771726)	1	2	6	1	-
Atvaquone(Malarone)	2	3	3	2	-

Table 3.4: 2D Pharmacophore Model of anti-malarial agents.

Compounds	HBA-HBD	HBD-C	C-HBA
Chloroquinine	4.26	4.29	4.20
Quinine	4.98	3.90	3.70
Sesquiterpenoid1	4.27	3.93	4.68
Andidermal B	4.81	3.7	3.7
Alkoids1	4.06	4.10	4.26
Quinone1	4.68	4.64	4.6
DHOH6	4.06	4.18	4.25
Chalcone1	4.09	3.71	4.49
Benzoxaborole3	4.67	4.30	3.64
Quinoline methanols	4.94	4.2	3.57
Brequinar	4.99	3.70	4.13
Polyporic acid	4.70	4.63	4.21
Amino-Benzoic Acid	4.06	4.18	4.25
Redoxal	4.10	4.30	4.41
DHOD2	4.06	4.42	4.18
Leflunomide	4.29	4.04	3.91
Ureas	4.06	4.42	4.18
Teriflunomide(A771726)	4.89	4.19	3.55
Atovaquone(Malarone)	4.31	3.76	3.74

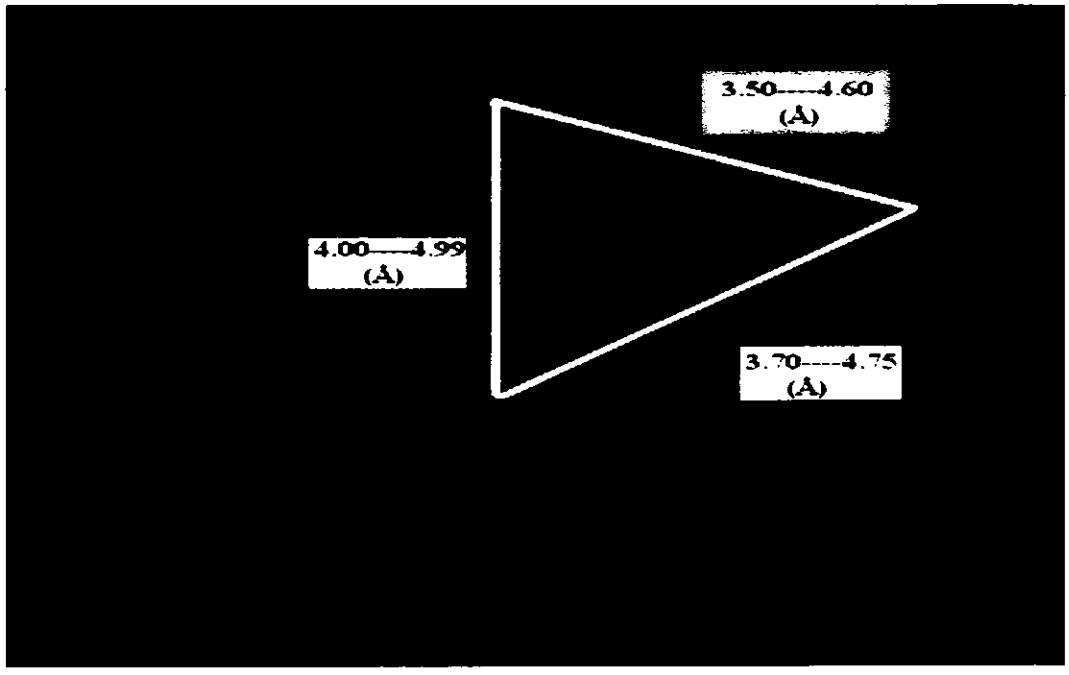

Figure 3.1: Pharmacophore Triangle of anti-malarial agents.

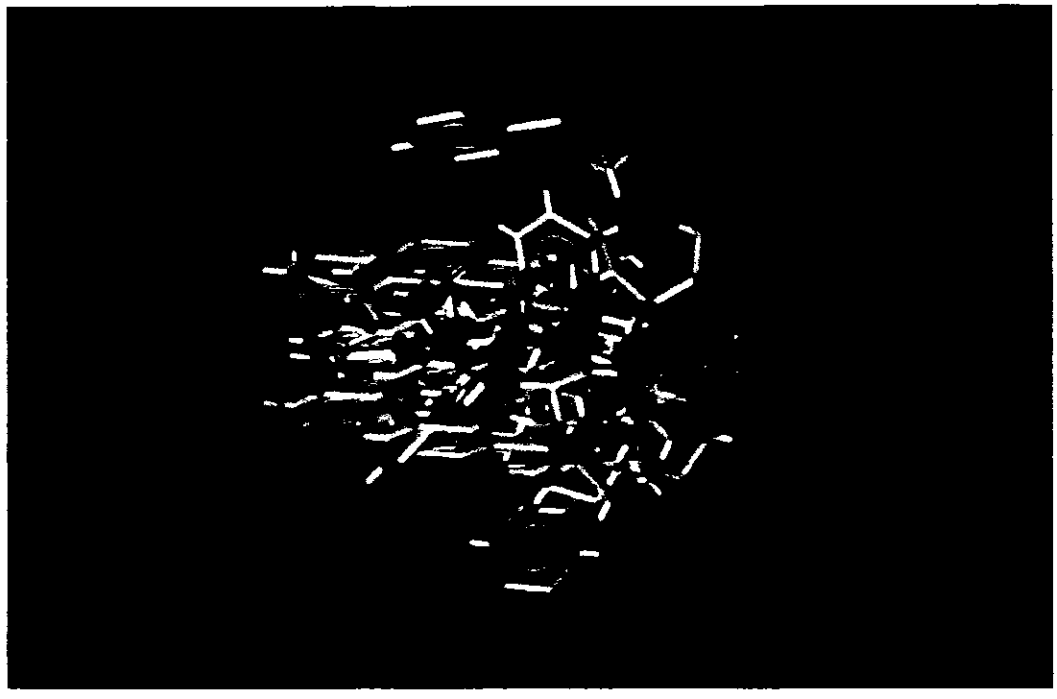

Figure 3.2: Merged Pharmacophore of compounds generated by LigandScout.

3.4 Molecular Docking

3.4.1 Docking of data set compounds

The data set compounds were docked into the active site of DHODH by using AutoDOCK Vina. The docked files were visualized in VMD software in order to get the binding interactions e.g hydrogen bonding, ionic bonding and hydrobhobic interactions. To predict compound activeness IC50 value and binding interaction was also incorporated. The active site of 3I65 was searched by docking the test set compounds and standard compound with the protein 3I65 and amino acid within 5A was identified. Table 3.1 shows amino acid within 5A°. The residues found were ALA225, ALA259, ALA224, ASN347, ASN342, ASN347, ASN458, ASN274, ASN279, CYS276, GLY226, GLY507, GLY506, GLY248, GLY478, GLY475, GLY226, GLY277, ILE272, ILE263, LYS429, LYS229, LYS459, LYS473, LEU527, LEU481, PRO346, PHE227, PHE278, PHE509 SER311, SER477, SER275, SER505, SER529, SER345, SER344, SER529, SER457, TYR528, THR459, THR249, ILE508, GLN526, HIS185. Amino acids like ALA225, CYS276, THR459, LYS429, LYS229, PHE278, SER477, SER505, SER345, TYR528, ASN458 ASN274 were major involved in binding interactions with the ligands.

Table 3.5: Amino acids Present within the 5 Å Vicinity of the Ligand where + and – signs indicate the presence and absence of amino acid.

A.A	1	2	3	4	5	6	7	8	9	10	11	12	13	14	15	16	17	18
ALA225	+	+	+	+	+	+	+	+	+	+	+	+	+	+	+	+	+	+
ALA259	-	-	-	-	-	-	-	-	-	-	-	-	-	-	-	-	-	-
ALA224	-	-	-	-	+	+	+	-	-	+	+	-	-	+	+	+	-	+
ASN347	+	-	+	-	-	-	+	-	+	-	-	-	-	+	+	-	-	-
ASN342	+	+	+	+	+	-	-	+	+	+	-	+	-	+	+	+	+	+
ASN347	-	+	+	-	+	+	-	+	-	-	+	+	+	-	-	-	+	-
ASN458	+	+	-	+	+	+	+	+	+	+	+	+	+	+	+	+	+	+
ASN274	+	+	-	+	+	+	+	+	+	+	+	+	+	+	+	+	+	+
ASN279	-	-	-	-	-	-	-	-	-	-	+	-	-	-	-	-	-	+
CYS276	+	+	+	+	+	+	+	+	+	+	+	+	+	+	+	+	+	+
GLY226	+	-	+	-	-	-	-	-	+	+	-	+	-	-	-	+	-	+
GLY507	-	+	+	+	+	-	+	+	+	+	+	+	+	+	-	-	-	+
GLY506	-	+	+	+	+	-	+	+	+	+	+	+	+	+	-	-	-	+
GLY248	-	-	-	-	-	-	-	-	+	-	-	-	-	-	+	-	-	-
GLY478	-	+	+	+	+	-	+	+	+	+	-	+	+	-	-	-	-	+
GLY475	-	-	-	-	-	-	-	-	-	-	-	-	-	-	-	-	-	-
GLY226	+	+		+	+	+	+	+	-	-	+	-	+	+	+	-	+	-
GLY277	+	-	+	-	-	+	+	+	-	-	+	+	+	+	+	-	+	+
ILE272	+	-	-	-	-	+	-	-	-	-	-	-	-	-	-	+	-	-
ILE263	+	-	-	-	-	-	-	-	-	-	-	-	+	-	-	-	-	-
LYS429	+	+	+	-	+	+	-	+	+	+	+	+	+	+	+	+	+	+
LYS229	+	+	+	+	+	+	+	+	+	+	+	+	+	+	+	+	+	+
LYS459	-	-	-	-	-	-	-	-	-	-	-	-	-	-	-	-	-	-
LYS473	-	-	-	-	-	-	-	-	-	-	-	-	-	-	-	-	-	-
LEU527	-	-	-	-	+	-	+	-	-	+	+	-	-	+	-	-	-	+
LEU481	-	+	+	+	+	+	+	+	+	+	+	+	+	+	+	-	-	-
PRO346	+	+	+	-	+	+	+	+	-	-	+	+	+	+	-	-	+	-
PHE227	-	-	-	-	-	+	-	-	-	-	-	-	-	-	-	-	-	-
PHE278	+	+	+	+	+	+	+	+	+	+	+	+	+	+	+	-	+	+
PHE509	-	-	-	-	-	-	-	-	-	-	-	-	-	-	-	-	-	-
SER311	+	-	-	-	-	-	-	-	+	-	-	+	-	+	-	-	-	+
SER477	+	+	+	+	+	+	+	+	+	+	-	+	+	-	+	+	+	+
SER275	-	-	-	-	-	-	-	-	-	-	-	-	-	-	-	-	-	+
SER505	-	+	+	+	+	+	+	+	+	+	+	+	+	+	+	-	-	+
SER529	+	+	-	+	-	-	-	+	+	-	+	+	+	+	-	-	-	-
SER345	+	+	+	+	+	+	+	+	-	+	+	+	+	+	+	-	+	+
SER344	-	-	-	-	+	-	-	+	-	-	+	-	-	+	-	-	+	-
SER529	-	-	+	-	+	-	+	-	-	+	-	-	-	-	-	-	-	+
SER457	-	+	-	+	+	+	+	+	+	+	+	+	+	+	+	-	-	-
TYR528	+	+	+	+	+	+	+	+	+	+	+	+	+	+	+	+	+	+
THR459	+	+	-	+	+	+	+	+	+	+	+	+	+	+	+	+	+	+
THR249	+	-	+	-	-	-	-	-	+	+	-	+	-	+	+	+	-	+
ILE508	-	-	-	-	-	-	-	-	-	-	-	-	-	-	-	-	-	-
GLN526	-	-	-	-	+	+	-	-	+	-	+	-	-	-	-	-	-	+
HIS185	+	-	-	-	-	-	-	-	-	-	-	-	-	-	-	-	-	-

A.A	19	20	21	22	23	24	25	26	27	28	29	30	31	32	33
ALA225	+	+	+	+	+	+	+	-	+	+	+	+	+	+	+
ALA259	-	-	-	-	-	-	-	+	-	-	-	-	-	-	-
ALA224	+	+	+	-	+	+	-	-	-	+	-	+	+	+	+
ASN347	+	-	-	-	-	+	+	-	+	-	-	+	-	+	-
ASN342	+	+	+	+	+	+	-	-	-	+	+	+	+	+	+
ASN347	-	-	+	+	+	+	-	+	-	-	+	+	-	-	-
ASN458	+	+	+	+	+	+	+	-	+	+	+	+	+	+	+
ASN274	+	+	-	+	+	+	+	-	-	+	+	-	+	+	+
ASN279	-	-	+	+	-	+	-	-	-	-	+	-	+	-	-
CYS276	+	-	+	+	+	+	+	-	+	+	+	+	+	+	+
GLY226	+	+	-	+	+	-	+	-	+	-	-	+	+	+	-
GLY507	+	+	-	+	-	-	-	-	+	+	-	+	-	-	-
GLY506	+	+	+	+	-	+	+	-	+	+	-	+	-	-	-
GLY248	-	-	+	+	-	-	-	-	-	-	-	-	+	+	-
GLY478	+	+	+	+	+	+	+	-	+	+	-	+	-	-	-
GLY475	-	-	-	+	+	-	-	-	-	-	-	-	-	-	-
GLY226	-	-	+	-	-	+	-	-	-	+	+	+	+	-	+
GLY277	+	-	+	-	-	+	+	-	+	-	+	-	-	+	-
ILE272	-	+	+	-	+	-	+	-	-	-	+	-	-	+	-
ILE263	-	-	+	+	-	-	-	-	-	-	-	-	+	-	+
LYS429	+	+	+	+	-	+	+	-	+	+	-	+	-	+	+
LYS229	+	+	+	+	+	+	+	-	+	+	+	+	+	+	+
LYS459	-	-	-	-	-	-	-	-	-	-	-	-	+	-	-
LYS473	-	-	-	-	-	-	-	+	-	-	-	-	-	-	-
LEU527	-	+	-	-	+	-	-	-	-	+	-	-	-	-	-
LEU481	-	-	+	+	-	+	+	-	+	+	+	+	-	-	+
PRO346	-	-	-	+	+	+	+	+	+	-	+	+	-	+	-
PHE227	-	-	-	-	+	-	+	-	-	-	-	-	+	-	+
PHE278	+	+	+	+	+	+	+	-	+	+	+	+	+	+	+
PHE509	-	-	-	-	-	-	-	-	-	-	-	-	-	-	-
SER311	-	-	+	-	-	-	-	-	-	-	-	-	+	-	+
SER477	+	+	+	+	+	+	+	-	+	+	+	+	+	-	+
SER275	-	-	-	-	-	-	-	+	-	-	-	-	+	-	-
SER505	+	+	+	+	-	+	+	-	+	+	+	+	+	+	+
SER529	+	-	+	-	-	+	+	-	-	+	+	+	-	+	-
SER345	+	-	-	+	+	+	+	-	+	+	+	+	+	+	+
SER344	-	-	-	+	+	+	-	-	-	-	+	+	-	-	-
SER529	-	+	-	-	+	-	-	-	+	-	-	-	-	-	-
SER457	+	+	+	+	-	+	+	-	+	+	-	+	+	+	+
TYR528	+	+	+	+	+	+	+	-	+	+	+	+	+	+	+
THR459	+	+	+	-	+	+	+	-	+	+	+	+	+	+	+
THR249	+	+	+	+	-	+	-	-	-	+	-	+	+	+	+
ILE508	-	-	-	-	-	-	-	-	-	-	-	-	-	-	-
GLN526	-	+	-	-	+	-	-	-	-	+	-	-	-	-	-
HIS185	-	-	-	-	-	-	-	-	-	-	-	-	+	-	-

A.A	34	35	36	37	38	39	40	41
ALA225	+	+	+	+	+	+	+	+
ALA259	-	-	-	-	-	-	-	-
ALA224	+	+	+	+	-	+	+	-
ASN347	+	-	-	-	-	+	-	-
ASN342	+	+	+	+	+	-	+	-
ASN347	-	-	+	-	+	+	+	+
ASN458	-	+	+	+	+	+	+	+
ASN274	+	+	+	+	+	+	+	+
ASN279	-	-	-	-	-	+	-	-
CYS276	+	+	+	+	+	+	+	+
GLY226	+	-	-	+	+	+	+	+
GLY507	+	+	+	+	+	-	+	-
GLY506	+	+	+	+	+	+	+	-
GLY248	+	-	-	+	-	+	-	+
GLY478	-	+	+	+	+	-	+	-
GLY475	-	-	-	-	-	-	-	-
GLY226	-	+	+	-	+	-	-	-
GLY277	+	+	+	-	-	+	+	-
ILE272	-	-	-	+	+	+	+	-
ILE263	-	-	-	+	-	+	-	-
LYS429	+	+	+	+	-	+	+	+
LYS229	+	+	+	+	+	+	+	+
LYS459	-	-	-	-	-	-	-	-
LYS473	-	-	-	-	-	-	-	-
LEU527	+	-	-	-	-	-	-	-
LEU481	+	+	+	-	+	+	-	-
PRO346	+	+	+	-	+	-	+	+
PHE227	-	-	-	-	-	-	+	-
PHE278	+	+	+	+	+	+	+	+
PHE509	+	-	-	-	-	-	-	-
SER311	+	-	-	-	-	+	-	+
SER477	-	+	+	+	+	+	+	+
SER275	+	+	-	-	-	-	+	-
SER505	+	+	+	+	+	+	+	-
SER529	-	+	+	+	+	+	-	-
SER345	+	+	+	+	+	-	+	+
SER344	+	+	+	+	-	-	+	-
SER529	+	-	-	-	+	-	-	-
SER457	+	+	+	+	+	+	+	-
TYR528	+	+	+	+	+	+	+	+
THR459	-	+	+	+	-	+	+	+
THR249	+	+	+	+	-	+	+	+
ILE508	+	-	-	+	-	-	+	-
GLN526	+	-	-	-	-	-	-	-
HIS185	-	-	-	-	-	-	-	-

3.4.2 Docking of standard drugs

Standard drugs were selected and docked with DHODH using the same molecular docking software and parameters. A detailed 3D analysis indicated that these compounds bind to the same active site. In case of A771726 and atovaquone, it showed three active binding interactions. In A771726, the N of ASN458 at 3.14 A° and of ASN274 at 3.61 A°, in different conformations form ionic bond with oxygen of the ligand. Two more ionic interactions were between O of ASN458 at 3.45 A°and of ASN274 at 3.53 with nitrogen. Two hydrogen bonds were formed with ASN458 at distances of 2.69 and 2.61. The hydrophobic interactions include the C's of ligand with the Cs of TYR528 at 3.71 A°, at 3.86 A°, at 3.94 A°, at 3.71 A°, at 3.86 A°, and at 3.94 A°, of SER477 at 3.68A ° , of PHE278 at 3.70 and 3.73 A ° and last of the THR459 at 3.57 A°, at 3.76 A°and at 3.78 A° . Atovaquone also showed three binding interaction in which there were 33 hydrobhobic interactions, 4 ionic bonds and 4 hydrogen bonds. The hydrobhobic interactions were with Cs of GLY506, SER529, TYR528, SER477, THR459, ASN274, CYS276, ALA224, LEU527, PHE278, and SER505. Ten hydrobhobic interactions of atovaquone were with TYR528 at distances of 3.91 A°, 3.92 A°, 3.44 A°, 3.46 A°, 3.59 A°, 3.62 A°, 3.75 A°, 3.765 A°, 3.971 A° and 3.397 A°, eight with PHE278 at distances of 3.80 A°, 3.34 A°, 3.97 A°, 3.89 A°, 3.83 A°, 3.56 A°, 3.84 A° and 3.630 A°, three with GLY506 at distances of 3.79 A°, 3.70 A° and 3.84 A°, three with THR459 at 2.73 A°, 3.02 A°and 3.90 A°and one with SER505 A°, LEU527 A°, CYS276 A°, ASN274 A°and SER529 A° at distances of 3.99, 3.73, 3.57, 3.68 and 3.95 respectively. Ionic bonding was between O of ligand and ASN342, ASN458, LYS429, ASN274 having distances 2.73 A°, 3.23 A°, 2.71 A°, and 3.30 respectively. Two hydrogen bond were with ASN458 at

distances 2.47 A°and 3.13 A°and one was with ASN342 and LYS429 having distances 3.70 A° and 3.00 A° respectively.

3.4.3 Lead Compound Identification

Six active compounds were chosen from the data set on the basis of showing strong binding interaction with the target. Along with their strong binding interaction, IC50 value is much lower which is a positive sign toward their being activeness. So, GUL32, GUL12, GUL13, GUL37, GUL35, GUL36 were showing strong binding interaction. GUL32 had 55 hydrophobic interactions, 11 ionic interaction and 13 hydrogen bonding. The compound GUL12 showed 23 hydrophobic, 8 hydrogen and 5 ionic interactions. There were 9 hydrophobic, 6 ionic and 9 hydrogen bonds in case of GUL13. 67 hydrophobic, 9 ionic and 7 hydrogen bond interactions were shown by GUL37. GUL35 showed 40 hydrophobic, 10 hydrogen and 3 ionic interactions. 22 hydrophobic, 7 ionic and 9 hydrogen bonds interaction were shown by GUL36. As IC50 value has 30% role in identifying the lead compound so on the basis of this criteria and strong binding interaction, the data set consisting of six active compounds is further reduced to two i.e., GUL32 and GUL37. GUL36 have the lowest binding affinity but it can't be selected as lead because neither the IC50 value is lowest nor the binding interaction is strongest as compared to other compounds in the group. GUL37 shows more hydrophobicity but when the IC50 value of GUL32 and GUL37 are compared than there is remarkable difference as IC50 value of redoxal is 0.43±0.2 and that of chalcones is 2.9. Moreover the no. of ionic and hydrogen bonds are more in GUL32 as compared to GUL37. So GUL32 was selected as a lead compound having strong binding interactions and lowest IC50 value.

Table 3.6: Binding interactions and distances of data set showing all the three kinds of interactions including hydrophobic interactions, ionic and hydrogen bonds.

Compounds	Hydrophobic Interactions		Ionic Bond		Hydrogen Bond	
	Amino Acid	Distance	Amino Acid	Distance	Amino Acid	Distance
GUL1	ILE272:CG2—UNKO:C	3.203	TRY528:OH—UNKO:N	3.766	ASN274:ND2—UNKO:H	3.185
	ILE272:CG2—UNKO:C	3.811	ASN274:OD—UNKO:N	3.825		
	ILE272:CG2—UNKO:C	3.845				
	ILE272:CB—UNKO:C	3.768				
	ILE272:CD1—UNKO:C	3.272				
	TYR528:CZ—UNKO:C	3.487				
	TYR528:CZ—UNKO:C	3.855				
	TYR528:CZ—UNKO:C	3.039				
	TYR528:CZ—UNKO:C	3.303				
	TYR528:CZ—UNKO:C	3.516				
	TYR528:CZ—UNKO:C	3.880				
	TYR528:CE2—UNKO:C	3.684				
	TYR528: CE2—UNKO:C	3.994				
	TYR528: CE2—UNKO:C	3.295				
	TYR528: CE2—UNKO:C	3.243				
	TYR528: CE2—UNKO:C	3.590				
	TYR528: CE2—UNKO:C	3.949				
	TYR528: CD2—UNKO:C	3.730				
	TYR528: CD2—UNKO:C	3.840				
	TYR528: CE'—UNKO:C	3.903				
	SER477:CB—UNKO:C	3.813				
	ASN274:CG—UNKO:C	3.660				
	ASN274:CG—UNKO:C	3.836				
	ILE263:CG2—UNKO:C	3.807				
	ILE263:CG1—UNKO:C	3.721				
	ILE263:CG1—UNKO:C	3.219				
	PHE278:CZ—UNKO:C	3.870				
	PHE278:CZ—UNKO:C	3.787				
	PHE278:CE2—UNKO:C	3.738				
	PHE278:CG—UNKO:C	3.925				
	PHE278:CD'—UNKO:C	3.572				
	PHE278:CE1—UNKO:C	3.513				
GUL2	SER477:CB—UNKO:C	3.345	SER477:OG—UNKO:N	3.589	ASN458:OD—UNKO:H	3.093
	SER477:CB—UNKO:C	3.452				
	SER477:CB—UNKO:C	3.874				
	LEU481:CD2—UNKO:C	3.950				
	GLY506:CA—UNKO:C	3.966				
	GLY506:CA—UNKO:C	3.426				
	THR459:CG'—UNKO:C	3.680				
	THR459:CG'—UNKO:C	3.916				
	ASN458:C—UNKO:C	3.465				
	ASN458:CA—UNKO:C	3.416				
	PHE278:CE2—UNKO:C	3.780				
	PHE278:CZ—UNKO:C	3.679				
	TRY528CG—UNKO:C	3.529				
	TRY528CG—UNKO:C	3.919				
	TRY528CG—UNKO:C	3.088				

	TRY528CG—UNKO:C TRY528CG—UNKO:C	3.985 3.138				
GUL3	PHE278:CZ—UNKO:C PHE278:CE1—UNKO:C PHE278:CD'—UNKO:C PHE278:CG—UNKO:C PHE278:CD2—UNKO:C PHE278:CE2—UNKO:C PHE278:CA—UNKO:C ASN458:C—UNKO:C THR459:CG—UNKO:C THR459:CG—UNKO:C THR459:CG—UNKO:C THR459:CG—UNKO:C ASN274:CG—UNKO:C ASN274:CG—UNKO:C LEU481:CD2—UNKO:C SER505:C—UNKO:C GLY506:CA—UNKO:C GLY506:CA—UNKO:C GLY506:C—UNKO:C SER477:CB—UNKO:C SER477:CB—UNKO:C SER477:CB—UNKO:C SER529:CB—UNKO:C TYR528:CA—UNKO:C TYR528:CB—UNKO:C TYR528:CB—UNKO:C TYR528:CB—UNKO:C TYR528:CB—UNKO:C TYR528:CG—UNKO:C TYR528:CG—UNKO:C TYR528:CD—UNKO:C	3.612 3.527 3.389 3.370 3.423 3.552 3.575 3.972 3.448 3.350 3.783 3.901 3.725 3.963 3.774 3.896 3.059 3.479 3.684 3.509 3.654 3.882 3.908 3.949 2.960 3.596 3.620 3.821 3.752 3.717 3.747	ASN274:ND2—UNKO: O ASN458:OD—UNKO:N	3.873 3.251	ASN458:OD—UNKO:H ASN458:ND2—UNKO:H	2.355 3.836
GUL4	PHE278:CZ—UNKO:C PHE278:CE2—UNKO:C ASN274:CG—UNKO:C ASN274:CG—UNKO:C ASN458:CG—UNKO:C THR459:CG—UNKO:C THR459:CG—UNKO:C THR459:CG—UNKO:C ASN458:C—UNKO:C ASN458:CA—UNKO:C LYS429:CE—UNKO:C GLY506:CA—UNKO:C SER477:CB—UNKO:C SER477:CB—UNKO:C SER477:CB—UNKO:C SER477:CB—UNKO:C SER529:CB—UNKO:C TYR528:CA—UNKO:C TYR528:CB—UNKO:C TYR528:CB—UNKO:C TYR528:CB—UNKO:C	3.688 3.807 3.867 3.902 3.916 3.606 3.639 3.992 3.772 3.516 3.753 3.886 3.281 3.290 3.885 3.909 3.823 3.980 3.080 3.154 3.932	ASN458:OD—UNKO:N ASN458:OD—UNKO:N ASN274:OD—UNKO:N	2.819, 3.595, 3.545,	ASN458:OD—UNKO:H ASN458:ND2—UNKO:H ASN274:NZ—UNKO:H	2.122 3.147 3.435

	TYR528:CB—UNKO:C	3.849				
	TYR528:CG—UNKO:C	3.385				
	TYR528:CG—UNKO:C	3.809				
	TYR528:CD2—UNKO:C	3.902				
	TYR528:CD—UNKO:C	3.859				
	TYR528:CE'—UNKO:C	3.761				
	TYR528:CZ—UNKO:C	3.510				
GUL5	PHE278:CE2—UNKO:C	3.453	SER505:OG—UNKO:N	3.427	TRY528:N—UNKO:H	3.880
	PHE278:CZ—UNKO:C	3.210			SER505:OG—UNKO:H	3.553
	PHE278:CZ—UNKO:C	3.565				
	PHE278:CE2—UNKO:C	3.784				
	PHE278:CE1—UNKO:C	3.587				
	SER345:CB—UNKO:C	3.645				
	SER345:CB—UNKO:C	3.937				
	ASN458:CG—UNKO:C	3.980				
	ASN274:CG—UNKO:C	3.541				
	THR459:CG—UNKO:C	3.929				
	SER477:CB—UNKO:C	3.986				
	GLY506:CA—UNKO:C	3.395				
	GLY506:CA—UNKO:C	3.638				
	GLY506:CA—UNKO:C	3.043				
	GLY506:C—UNKO:C	3.671				
	ALA225:C—UNKO:C	3.819				
	TYR528:CZ—UNKO:C	3.460				
	TYR528:CE'—UNKO:C	3.576				
	TYR528:CE'—UNKO:C	3.924				
	TYR528:CE'—UNKO:C	3.659				
	TYR528:CD—UNKO:C	3.208				
	TYR528:CD—UNKO:C	3.449				
	TYR528:CG—UNKO:C	3.750				
	TYR528:CB—UNKO:C	3.853				
	TYR528:CB—UNKO:C	3.632				
	TYR528:CA—UNKO:C	3.817				
	LEU527:CA—UNKO:C	3.801				
	LEU527:CA—UNKO:C	3.772				
	LEU527:C—UNKO:C	3.590				
GUL6	ASN347:CB—UNKO:C	3.437	ALA225:O—UNKO:N	2.578	ALA225:O—UNKO:H	1.768
	ASN347:CG—UNKO:C	3.697	ASN274:ND2—UNKO: O	3.443	GLY226:N—UNKO:H	3.371
	PRO346:C—UNKO:C	3.871				
	SER345:CB—UNKO:C	3.697				
	PHE278:CZ—UNKO:C	3.612				
	PHE278:CE1—UNKO:C	3.324				
	PHE278:CD'—UNKO:C	3.929				
	LYS229:CE—UNKO:C	3.698				
	LYS229:CE—UNKO:C	3.967				
	PRO346:CD—UNKO:C	3.926				
	ASN274:CG—UNKO:C	3.285				
	ASN274:CG—UNKO:C	3.588				
	ASN274:CB—UNKO:C	3.841				
	SER477:CB—UNKO:C	3.409				
	THR459:CG—UNKO:C	3.651				
	THR459:CG—UNKO:C	3.924				
	TYR528:CG—UNKO:C	3.948				

	TYR528:CD—UNKO:C	3.393				
	TYR528:CD—UNKO:C	3.898				
	TYR528:CD—UNKO:C	3.677				
	TYR528:CD—UNKO:C	3.846				
	TYR528:CE'—UNKO:C	3.254				
	TYR528:CE'—UNKO:C	3.570				
	TYR528:CE'—UNKO:C	3.945				
	TYR528:CE'—UNKO:C	3.781				
	TYR528:CE'—UNKO:C	3.736				
	TYR528:CZ—UNKO:C	3.833				
	TYR528:CZ—UNKO:C	3.745				
	GLY226:CA—UNKO:C	2.629				
	GLY226:CA—UNKO:C	3.370				
	GLY226:CA—UNKO:C	3.651				
	GLY226:CA—UNKO:C	3.259				
	GLY226:C—UNKO:C	3.355				
	GLY226:C—UNKO:C	3.578				
	ALA224:CB—UNKO:C	3.791				
GUL7	TYR528:CB—UNKO:C	3.588	GLY506:N—UNKO:O	3.661	TRY528:OH—UNKO:H	3.259
	TYR528:CB—UNKO:C	3.110	GLY507:N—UNKO:O	3.956		
	TYR528:CB—UNKO:C	3.869	LYS229:NZ—UNKO:O	3.969		
	TYR528:CB—UNKO:C	3.847	LYS229:NZ—UNKO:O	3.660		
	TYR528:CG—UNKO:C	3.800				
	TYR528:CG—UNKO:C	3.460				
	ALA224:CB—UNKO:C	3.945				
	TYR528:CD—UNKO:C	3.221				
	TYR528:CD—UNKO:C	3.963				
	TYR528:CD—UNKO:C	3.760				
	TYR528:CD—UNKO:C	3.936				
	TYR528:CE'—UNKO:C	3.984				
	TYR528:CE'—UNKO:C	3.694				
	GLY507:CA—UNKO:C	3.968				
	GLY506:C—UNKO:C	3.919				
	GLY506:CA—UNKO:C	3.678				
	LEU481:CD2—UNKO:C	3.653				
	ASN458:C—UNKO:C	3.716				
	ASN458:CA—UNKO:C	3.969				
	ASN458:CG—UNKO:C	3.710				
	ASN458:CG—UNKO:C	3.804				
	THR459:CG—UNKO:C	3.617				
	THR459:CG—UNKO:C	3.545				
	THR459:CG—UNKO:C	3.782				
	THR459:CG—UNKO:C	3.434				
	SER529:CB—UNKO:C	3.797				
	SER529:CB—UNKO:C	3.982				
	PHE278:CG—UNKO:C	3.874				
	PHE278:CD'—UNKO:C	3.515				
	PHE278:CE1—UNKO:C	3.580				
	PHE278:CZ—UNKO:C	3.965				
	ASN347:CB—UNKO:C	3.951				
	GLY277:CA—UNKO:C	3.982				
	CYS276:CB—UNKO:C	3.434				

GUL8	PHE278:CE2—UNKO:C	3.870	SER477:OG—UNKO:N	3.138	SER505:OG—UNKO:H	2.753
	PHE278:CZ—UNKO:C	3.790	LYS429:NZ—UNKO:O	3.155	SER457:O—UNKO:H	2.426
	SER345:CB—UNKO:C	3.868	ASN458:N—UNKO:O	3.865	ASN458:N—UNKO:H	3.840
	LYS229:CE—UNKO:C	3.768	THR459:N—UNKO:O	3.684	LYS429:NZ—UNKO:H	3.650
	LYS229:CE—UNKO:C	3.991				
	CYS276:CB—UNKO:C	3.590				
	CYS276:CB—UNKO:C	3.924				
	ASN458:CG—UNKO:C	3.694				
	THR459:CG'—UNKO:C	3.524				
	THR459:CG'—UNKO:C	3.562				
	THR459:CG'—UNKO:C	3.822				
	THR459:CG'—UNKO:C	3.984				
	SER477:CB—UNKO:C	3.284				
	SER477:CB—UNKO:C	3.720				
	SER477:CB—UNKO:C	3.734				
	GLY506:CA—UNKO:C	3.677				
	ASN274:CG—UNKO:C	3.821				
	TYR528:CB—UNKO:C	3.332				
	TYR528:CB—UNKO:C	3.009				
	TYR528:CB—UNKO:C	3.686				
	SER505:OG—UNKO:C	3.541				
	TYR528:CG—UNKO:C	3.480				
	TYR528:CG—UNKO:C	3.879				
GUL9	LEU481:CD2—UNKO:C	3.694	ASN342:ND2—UNKO: O	3.207	ALA225:O—UNKO:C	3.297
	GLY478:CA—UNKO:C	3.950	ASN342:ND2—UNKO: O	2.807		
	GLY506:C—UNKO:C	3.480	ASN342:ND2—UNKO: O	3.354		
	GLY506:CA—UNKO:C	2.936	LYS229:NZ—UNKO: O	3.863		
	GLY506:CA—UNKO:C	3.635				
	GLY506:CA—UNKO:C	3.966				
	ASN458:C—UNKO:C	3.757				
	ASN458:CA—UNKO:C	3.471				
	ASN458:CG—UNKO:C	3.839				
	LYS429:CE—UNKO:C	3.655				
	LYS429:CE—UNKO:C	3.847				
	SER477:CB—UNKO:C	3.043				
	SER477:CB—UNKO:C	3.228				
	SER477:CB—UNKO:C	3.454				
	ALA225:CB—UNKO:C	3.234				
	THR249:CB—UNKO:C	2.977				
	THR249:CB—UNKO:C	3.820				
	THR249:CA—UNKO:C	3.479				
	GLY248:C—UNKO:C	3.886				
	ASN274:CG—UNKO:C	3.801				
	GLY226:CA—UNKO:C	3.888				
	SER529:CB—UNKO:C	2.819				
	SER529:CB—UNKO:C	3.959				
	SER529:CA—UNKO:C	3.445				
	TYR528:CB—UNKO:C	3.197				
	TYR528:CB—UNKO:C	3.822				
	TYR528:CB—UNKO:C	3.783				
	TYR528:CG—UNKO:C	3.792				
	TYR528:CD—UNKO:C	3.850				
	TYR528:CD—UNKO:C	3.705				
	TYR528:CE—UNKO:C	3.415				
	TYR528:CE'—UNKO:C	3.823				

	TYR528:CZ—UNKO:C	3.405				
	TYR528:CE2—UNKO:C	3.837				
GUL10	CYS276:CB—UNKO:C	3.327	ASN347:ND2—UNKO:O	3.211	PRO346:N—UNKO:H	3.625
	CYS276:CB—UNKO:C	3.907	ASN458:ND2—UNKO:O	3.452	SER345:OG—UNKO:H	3.040
	LYS229:CE—UNKO:C	3.502	ASN458:OD—UNKO:N	3.236	ASN458:OD—UNKO:H	2.349
	LYS229:CE—UNKO:C	3.379	ASN458:OD—UNKO:N	3.577	ASN458:ND2—UNKO:H	3.459
	GLY226:CA—UNKO:C	3.835			ASN458:ND2—UNKO:H	3.323
	GLY226:CA—UNKO:C	3.892			ASN458:OD—UNKO:H	2.951
	PRO346:CD—UNKO:C	3.910			THR459:OG—UNKO:H	3.916
	THR459:CG—UNKO:C	3.527				
	LEU481:CD2—UNKO:C	2.721				
	GLY506:CA—UNKO:C	3.792				
	GLY506:CA—UNKO:C	3.517				
	GLY506:CA—UNKO:C	3.592				
	GLY506:CA—UNKO:C	3.931				
	GLY506:C—UNKO:C	3.493				
	GLY506:C—UNKO:C	3.662				
	GLY507:CA—UNKO:C	3.548				
	GLY507:CA—UNKO:C	3.558				
	GLY507:N—UNKO:C	3.939				
	ALA224:CB—UNKO:C	3.639				
	ALA224:CB—UNKO:C	3.298				
	TYR528:CB—UNKO:C	3.625				
	TYR528:CB—UNKO:C	3.532				
	TYR528:CB—UNKO:C	2.999				
	TYR528:CB—UNKO:C	3.938				
	TYR528:CB—UNKO:C	3.804				
	TYR528:CA—UNKO:C	3.402				
	TYR528:CA—UNKO:C	3.689				
	TYR528:C—UNKO:C	3.983				
	LEU527:C—UNKO:C	3.743				
	LEU527:C—UNKO:C	3.649				
	LEU527:CA—UNKO:C	3.872				
	SER477:CB—UNKO:CL	3.074				
	SER477:CB—UNKO:C	3.789				
	SER477:CA—UNKO:CL	3.102				
	SER477:C—UNKO:CL	3.824				
	GLY478:CA—UNKO:C	3.621				
	SER529:CB—UNKO:C	3.744				
GUL11	SER477:CB—UNKO:C	3.667	ASN347:ND2—UNKO:O	3.449	ASN342:ND2—UNKO:H	3.560
	SER477:CB—UNKO:C	3.496	ASN274:ND2—UNKO:O	3.863	SER311:OG—UNKO:H	3.970
	LEU481:CD2—UNKO:C	3.711	SER477:OG—UNKO:N	3.604	THR249:OG—UNKO:H	3.532
	GLY506:CA—UNKO:C	3.357	SER505:OG—UNKO:N	3.186	LYS429:NZ—UNKO:H	3.387
	GLY506:C—UNKO:C	3.887	ASN342:ND2—UNKO:O	3.149		
	TYR528:CE'—UNKO:C	3.684	LYS429:NZ—UNKO:O	2.919		
	TYR528:CD—UNKO:C	3.235				
	TYR528:CG—UNKO:C	3.323				
	TYR528:CG—UNKO:C	3.947				
	TYR528:CD2—UNKO:C	3.821				

	TYR528:CB—UNKO:C	3.748				
	TYR528:CB—UNKO:C	3.370				
	TYR528:CB—UNKO:C	3.381				
	TYR459:CG—UNKO:C	3.736				
	TYR459:CG—UNKO:C	3.516				
	TYR459:CG—UNKO:C	3.455				
	ASN274:CG—UNKO:C	3.858				
	ASN347:CB—UNKO:C	3.458				
	PHE278:CE1—UNKO:C	3.557				
	PHE278:CE1—UNKO:C	3.373				
	PHE278:CD'—UNKO:C	3.376				
	PHE278:CD'—UNKO:C	3.503				
	PHE278:CG—UNKO:C	3.867				
	PHE278:CG—UNKO:C	3.710				
	PHE278:CD2—UNKO:C	3.721				
	PHE278:CE2—UNKO:C	3.594				
	PHE278:CZ—UNKO:C	3.426				
	PHE278:CA—UNKO:C	3.934				
	GLY277:C—UNKO:C	3.636				
	GLY277:CA—UNKO:C	3.399				
GUL12	PHE278:CZ—UNKO:CL	3.887	ASN458:OD—UNKO:N	3.545	ASN458:O —UNKO:H	2.826
	PHE278:CE2—UNKO:CL	3.942	SER477:OG—UNKO:N	3.654	SER505:OG—UNKO:H	3.879
	CYS276:CB—UNKO:C	3.937	THR459:N—UNKO:O	3.105	SER457:O—UNKO:H	2.117
	LYS229:CE—UNKO:C	3.653	ASN458:N—UNKO:O	3.772	THR459:N—UNKO:H	2.905
	ASN274:CG—UNKO:C	3.813	GLY506:N—UNKO:O	3.138	ASN458:N—UNKO:H	2.829
	SER477:CB—UNKO:C	3.463			ASN458:OD—UNKO:H	3.639
	SER477:CB—UNKO:C	3.347			ASN458:OD—UNKO:H	2.558
	SER477:CB—UNKO:C	3.674			ASN458:OD—UNKO:H	3.367
	SER477:CB—UNKO:C	3.883				
	LEU481:CD2—UNKO:C	3.718				
	GLY506:CA—UNKO:C	3.933				
	THR459:CG—UNKO:C	3.488				
	THR459:CG—UNKO:C	3.821				
	ASN458:C—UNKO:C	3.756				
	TYR528:CD—UNKO:C	3.728				
	TYR528:CD2—UNKO:C	3.982				
	TYR528:CD2—UNKO:C	3.832				
	TYR528:CB—UNKO:C	2.812				
	TYR528:CB—UNKO:C	3.287				
	TYR528:CB—UNKO:C	3.513				
	TYR528:CA—UNKO:C	3.849				
	TYR528:CG—UNKO:C	3.382				
	TYR528:CG—UNKO:C	3.406				
GUL13	PHE278:CE1—UNKO:C	3.949	ASN347:ND2—UNKO:O	3.120	ASN274:OD—UNKO:H	3.252
	PHE278:CZ—UNKO:C	3.881	ASN347:ND2—UNKO:O	3.702	THR459:OG—UNKO:H	2.905
	PHE278:CZ—UNKO:C	3.802	ASN274:ND2—UNKO:O	3.243	ASN274:ND2—UNKO:H	3.146
	PHE278:CZ—UNKO:C	3.904	ASN458:ND2—UNKO:O	3.052	ASN347:ND2—UNKO:H	2.924
	PHE278:CE2—UNKO:C	3.374	LYS429:NZ—UNKO:O	3.895	GLY475:N—UNKO:H	3.957
	PHE278:CE2—UNKO:C	3.785	THR459:N—UNKO:O	3.284	ASN458:OD—UNKO:H	2.876
	PHE278:CD2—UNKO:C	3.849			THR459:OG—UNKO:H	3.776
	ALA225:C—UNKO:C	3.957			THR459:N—UNKO:H	3.269
	THR459:CG—UNKO:C	3.907			ASN458:OD—UNKO:H	3.677

GUL14	THR459:CG—UNKO:C	3.709	GLY226:N—UNKO:O	3.884	SER505:OG—UNKO:H	3.171
	ASN274:CG—UNKO:C	3.701	LYS229:NZ—UNKO:O	3.233	SER505:OG—UNKO:H	3.716
	ASN274:CG—UNKO:C	3.947	SER505:OG—UNKO:N	2.963	ALA225:O—UNKO:H	3.839
	LYS229:CE—UNKO:C	3.849			ALA225:O—UNKO:H	3.633
	TYR528:CE2—UNKO:C	3.774			GLY226:N—UNKO:H	3.909
	TYR528:CZ—UNKO:C	3.691			LYS429:NZ—UNKO:H	2.917
	TYR528:CZ—UNKO:C	3.512				
	TYR528:CZ—UNKO:C	3.830				
	TYR528:CE'—UNKO:C	3.722				
	TYR528:CE'—UNKO:C	3.888				
	TYR528:CE'—UNKO:C	3.691				
	TYR528:CE'—UNKO:C	3.828				
	TYR528:CE'—UNKO:C	3.990				
	TYR528:CD—UNKO:C	3.832				
	TYR528:CD—UNKO:C	3.800				
GUL15	TYR528:CD—UNKO:C	3.687	ASN274:ND2—UNKO:O	3.250	SER345:OG—UNKO:H	2.406
	TYR528:CD—UNKO:C	3.817	ASN347:ND2—UNKO:O	3.374	PRO346:O—UNKO:H	2.764
	TYR528:CD—UNKO:C	3.915	PHE278:N—UNKO:O	3.264	ASN347:ND2—UNKO:H	3.486
	TYR528:CE'—UNKO:C	3.612	LYS229:NZ—UNKO:O	3.154	ASN274:OD—UNKO:H	2.951
	TYR528:CE'—UNKO:C	3.600	LYS229:NZ—UNKO:O	3.786		
	TYR528:CE'—UNKO:C	3.946				
	TYR528:CZ—UNKO:C	3.712				
	ASN458:CG—UNKO:C	3.927				
	ASN458:CG—UNKO:C	3.761				
	SER345:CB—UNKO:C	3.942				
	PHE278:CZ—UNKO:C	3.973				
GUL16	SER477:CB—UNKO:C	3.763	ASN274:ND2—UNKO: O	3.172		
	THR459:CG—UNKO:C	3.554	LYS229: NZ—UNKO: O	3.665		
	ASN342:CG—UNKO:C	3.742				
	PHE278:CE2—UNKO:C	3.813				
	GLY506:CA—UNKO:C	2.917				
	GLY506:CA—UNKO:C	3.300				
	GLY506:CA—UNKO:C	3.990				
	GLY506:CA—UNKO:C	3.340				
	GLY506:C—UNKO:C	3.584				
	GLY506:C—UNKO:C	3.746				
	GLY507:CA—UNKO:C	3.717				
	GLY507:CA—UNKO:C	3.882				
	GLY506:C—UNKO:C	3.788				
	ILE508:CA—UNKO:C	3.955				
	SER529:CB—UNKO:C	3.598				
	SER529:CB—UNKO:C	3.340				
	SER529:CA—UNKO:C	3.913				
	TYR528:CD—UNKO:C	3.740				
	TYR528:CD—UNKO:C	3.670				
	TYR528:CD—UNKO:C	3.990				
	TYR528:CG—UNKO:C	3.639				
	TYR528:CG—UNKO:C	3.968				
	TYR528:CG—UNKO:C	3.780				
	TYR528:CB—UNKO:C	3.822				
	TYR528:CB—UNKO:C	3.048				
	TYR528:CB—UNKO:C	3.186				
	TYR528:CB—UNKO:C	3.609				
	TYR528:CA—UNKO:C	3.913				

	LEU527:CA—UNKO:C	3.985				
	LEU527:CA—UNKO:C	3.677				
	GLN526:C—UNKO:C	3.918				
	ALA225:C—UNKO:C	3.705				
	ALA224:CB—UNKO:C	3.165				
	ALA224:CB—UNKO:C	3.178				
	ALA225:CB—UNKO:C	3.570				
GUL17	TYR528:CB—UNKO:C	3.252	ALA225: O—UNKO:N	3.404		
	TYR528:CB—UNKO:C	3.581	LYS229:NZ—UNKO:O	2.730		
	TYR528:CB—UNKO:C	3.813				
	TYR528:CB—UNKO:C	3.742				
	TYR528:CB—UNKO:C	3.429				
	TYR528:CB—UNKO:C	3.169				
	TYR528:CG—UNKO:C	3.499				
	TYR528:CG—UNKO:C	3.853				
	TYR528:CG—UNKO:C	3.734				
	TYR528:CD—UNKO:C	3.815				
	TYR528:CD—UNKO:C	3.717				
	TYR528:C—UNKO:C	3.787				
	SER477:CB—UNKO:C	3.120				
	SER477:CB—UNKO:C	3.400				
	ASN458:CG—UNKO:C	3.803				
	PHE278:CZ—UNKO:C	3.769				
	PHE278:CE2—UNKO:C	3.327				
	PHE278:CCD2—UNKO:C	3.866				
	LYS229:CE—UNKO:C	3.843				
	CYS276:CB—UNKO:C	3.517				
	LYS429:CE—UNKO:C	3.817				
	ALA224:CB—UNKO:C	3.927				
GUL18	TYR528:CD2—UNKO:C	3.069	ASN274:ND2—UNKO:O	2.502		
	TYR528:CE2—UNKO:C	3.529	ASN458:OD—UNKO:N	3.836		
	TYR528:CG—UNKO:C	3.651	ALA225:O—UNKO:N	3.470		
	TYR528:CB—UNKO:C	3.363				
	TYR528:CB—UNKO:C	3.317				
	TYR528:CB—UNKO:C	3.685				
	TYR528:CB—UNKO:C	3.770				
	SER529:CB—UNKO:C	3.976				
	SER477:CB—UNKO:C	3.319				
	SER477:CB—UNKO:C	3.676				
	SER477:CB—UNKO:C	3.440				
	THR459:CG—UNKO:C	3.917				
	PHE278:CE2—UNKO:C	3.563				
	LYS229:CE—UNKO:C	3.849				
	LYS229:CE—UNKO:C	3.817				
	THR249:CB—UNKO:C	3.803				
	ILE272:CD1—UNKO:C	3.102				
	ILE272:CG1—UNKO:C	3.987				
	ILE272:CB—UNKO:C	3.962				
	ASN274:CG—UNKO:C	3.943				

GUL19	TYR528:CB—UNKO:C	3.839	LYS229:NZ—UNKO:O	3.630		
	TYR528:CB—UNKO:C	3.913	ASN274:ND2—UNKO:O	3.187		
	TYR528:CB—UNKO:C	3.656	GLY506:N—UNKO:O	3.773		
	TYR528:CG—UNKO:C	3.622	SER505:OG—UNKO:N	3.906		
	TYR528:CG—UNKO:C	3.295				
	TYR528:CG—UNKO:C	3.736				
	TYR528:CD2—UNKO:C	3.581				
	TYR528:CD2—UNKO:C	3.559				
	TYR528:CE2—UNKO:C	3.572				
	TYR528:CE2—UNKO:C	3.906				
	TYR528:CZ—UNKO:C	3.743				
	TYR528:CZ—UNKO:C	3.607				
	TYR528:CZ—UNKO:C	3.989				
	TYR528:CD—UNKO:C	3.645				
	TYR528:CD—UNKO:C	3.381				
	TYR528:CD—UNKO:C	3.512				
	TYR249:CB—UNKO:C	3.933				
	TYR249:CB—UNKO:C	3.400				
	CYS276:CB—UNKO:C	3.097				
	CYS276:CB—UNKO:C	3.692				
	LYS229:CE—UNKO:C	3.832				
	LYS429:CD—UNKO:C	3.440				
	LYS429:CE—UNKO:C	3.719				
	LYS229:CE—UNKO:C	3.582				
	THR459:CG—UNKO:C	3.262				
	SER505:CB—UNKO:C	3.640				
	SER505:CB—UNKO:C	3.923				
	LEU481:CD2—UNKO:C	3.376				
	SER505:C—UNKO:C	3.922				
	SER477:CB—UNKO:C	3.500				
	SER477:CB—UNKO:C	3.826				
	SER477:CA—UNKO:C	3.795				
	SER477:CA—UNKO:C	3.821				
	GLY226:CA—UNKO:C	3.751				
	GLY226:CA—UNKO:C	3.884				
	GLY226:CA—UNKO:C	3.325				
	ALA225:C—UNKO:C	3.559				
	ASN274:CG—UNKO:C	3.362				
	ASN274:CG—UNKO:C	3.696				
GUL20	LYS429:CD—UNKO:C	3.418	SER505:OG—UNKO:N	3.960		
	LYS429:CE—UNKO:C	3.710	GLY506:N—UNKO:O	3.782		
	LYS429:CE—UNKO:C	3.557	ALA225:O—UNKO:N	3.247		
	ASN342:CG—UNKO:C	3.397	LYS229:NZ—UNKO:O	3.600		
	THR249:CB—UNKO:C	3.404	ASN274:ND2—UNKO:O	3.180		
	THR249:CB—UNKO:C	3.958				
	ALA225:CB—UNKO:C	3.792				
	ALA225:CB—UNKO:C	3.489				
	ALA225:CB—UNKO:C	3.491				
	ALA225:CB—UNKO:C	3.795				
	LYS229:CE—UNKO:C	3.863				
	CYS276:CB—UNKO:C	3.148				
	CYS276:CB—UNKO:C	3.710				
	ASN274:CG—UNKO:C	3.357				
	ALA225:C—UNKO:C	3.764				
	ALA225:C—UNKO:C	3.555				

	GLY226:CA—UNKO:C	3.326				
	GLY226:CA—UNKO:C	3.880				
	GLY226:CA—UNKO:C	3.764				
	THR459:CG'—UNKO:C	3.266				
	SER505:CB—UNKO:C	3.662				
	SER505:CB—UNKO:C	3.979				
	LEU481:CD2—UNKO:C	3.401				
	SER505:C—UNKO:C	3.943				
	SER477:CB—UNKO:C	2.986				
	SER477:CB—UNKO:C	3.512				
	SER477:CB—UNKO:C	3.857				
	SER477:CB—UNKO:C	3.473				
	SER477:CA—UNKO:C	3.783				
	SER477:CA—UNKO:C	3.796				
	TYR528:CB—UNKO:C	3.808				
	TYR528:CB—UNKO:C	3.913				
	TYR528:CB—UNKO:C	3.674				
	TYR528:CG—UNKO:C	3.293				
	TYR528:CG—UNKO:C	3.608				
	TYR528:CG—UNKO:C	3.761				
	TYR528:CD2—UNKO:C	3.575				
	TYR528:CD2—UNKO:C	3.565				
	TYR528:CE2—UNKO:C	3.569				
	TYR528:CE2—UNKO:C	3.925				
	TYR528:CD—UNKO:C	3.365				
	TYR528:CD—UNKO:C	3.506				
	TYR528:CD—UNKO:C	3.901				
	TYR528:CD—UNKO:C	3.644				
	TYR528:CE'—UNKO:C	3.740				
	TYR528:CE'—UNKO:C	3.652				
	TYR528:CE'—UNKO:C	3.725				
	TYR528:CE'—UNKO:C	3.882				
	TYR528:CE'—UNKO:C	3.966				
	TYR528:CZ—UNKO:C	3.617				
	TYR528:CZ—UNKO:C	3.730				
GUL21	PRO346:CD—UNKO:CL	3.437	ASN274:OD—UNKO:N	3.804	ASN274:ND2—UNKO:H	1.697
	PHE278:CZ—UNKO:CL	3.478			ASN274:ND2—UNKO:H	3.042
	SER345:CB—UNKO:CL	2.464				
	LYS229:CE—UNKO:C	3.782				
	GLY226:C—UNKO:C	3.232				
	GLY226:C—UNKO:C	3.826				
	GLY226:CA—UNKO:C	2.437				
	GLY226:CA—UNKO:C	3.505				
	ALA225:C—UNKO:C	3.914				
	ASN274:CG—UNKO:C	3.595				
	ASN274:CG—UNKO:C	3.895				
	ASN274:CG—UNKO:C	3.787				
	THR459:CG—UNKO:C	3.761				
	SER477:CB—UNKO:C	3.432				
	SER477:CB—UNKO:C	3.706				
	SER477:CB—UNKO:C	3.429				
	ILE272:CG2—UNKO:C	3.799				
	GLY506:CA—UNKO:C	3.186				
	SER529:CB—UNKO:C	3.479				
	SER529:CA—UNKO:C	3.948				

	TYR528:CB—UNKO:C	3.764				
	TYR528:CB—UNKO:C	3.490				
	TYR528:CB—UNKO:C	3.429				
	TYR528:CB—UNKO:C	3.296				
	TYR528:CB—UNKO:C	3.806				
	TYR528:CZ—UNKO:C	3.515				
	TYR528:CZ—UNKO:C	3.772				
	TYR528:CE2—UNKO:C	3.919				
	TYR528:CD2—UNKO:C	3.600				
	TYR528:CE'—UNKO:C	3.969				
	TYR528:CE'—UNKO:C	3.850				
	TYR528:CE'—UNKO:C	3.308				
	TYR528:CE'—UNKO:C	3.859				
	TYR528:CD—UNKO:C	3.320				
	TYR528:CD—UNKO:C	3.884				
	TYR528:CD—UNKO:C	3.810				
	SER345:CA—UNKO:CL	3.243				
	ASN458:CG—UNKO:CL	3.958				
	TYR528:CG—UNKO:C	3.107				
	TYR528:CG—UNKO:C	3.768				
GUL22	PHE278:CZ—UNKO:C	3.468	ASN274:OD—UNKO:N	3.481	SER345:OG—UNKO:H	3.754
	PHE278:CZ—UNKO:C	3.701	ASN458:ND2—UNKO:O	2.806	ASN342:ND2—UNKO:H	3.130
	PHE278:CE1—UNKO:C	3.646	ASN342:ND2—UNKO:O	3.649	ASN458:ND2—UNKO:H	3.197
	PHE278:CE1—UNKO:C	3.861			ASN458:OD—UNKO:H	3.816
	PHE278:CE2—UNKO:C	3.570				
	PHE278:CE2—UNKO:C	3.754				
	PHE278:CD—UNKO:C	3.657				
	PHE278:CG—UNKO:C	3.754				
	PHE278:CD2—UNKO:C	3.770				
	CYS276:CB—UNKO:C	3.394				
	CYS276:CB—UNKO:C	3.240				
	ASN274:CG—UNKO:C	3.823				
	THR459:CG—UNKO:C	3.623				
	THR459:CG—UNKO:C	3.850				
	THR459:CG—UNKO:C	3.844				
	SER477:CB—UNKO:C	3.166				
	SER477:CB—UNKO:C	3.547				
	SER477:CB—UNKO:C	3.742				
	TYR528:CB—UNKO:C	3.201				
	TYR528:CB—UNKO:C	3.020				
	TYR528:CB—UNKO:C	3.924				
	TYR528:CB—UNKO:C	3.626				
	TYR528:CG—UNKO:C	3.347				
	TYR528:CG—UNKO:C	3.485				
	TYR528:CD—UNKO:C	3.781				
	TYR528:CD—UNKO:C	3.987				
	TYR528:CD—UNKO:C	3.983				
	TYR528:CD—UNKO:C	3.641				
	LYS429:CE—UNKO:C	3.867				
GUL23	PHE278:CG—UNKO:C	3.830	ASN458:OD—UNKO:N	3.789	ASN458:OD—UNKO:H	3.158
	PHE278:CD—UNKO:C	3.152			LYS429:NZ—UNKO:H	3.414
	PHE278:CD—UNKO:C	3.892				
	PHE278:CE1—UNKO:C	3.133				
	PHE278:CE1—UNKO:C	3.885				
	PHE278:CZ—UNKO:C	3.779				

	GLY277:CA—UNKO:C	3.632				
	ASN347:CB—UNKO:C	3.119				
	ASN347:CG—UNKO:C	3.784				
	ASN274:CG—UNKO:C	3.682				
	ASN458:C—UNKO:C	3.908				
	ASN458:C—UNKO:C	3.917				
	ASN458:CA—UNKO:C	3.757				
	ASN458:CA—UNKO:C	3.979				
	LEU481:CD2—UNKO:C	3.713				
	SER477:CB—UNKO:C	3.471				
	SER477:CB—UNKO:C	3.869				
	THR459:CG—UNKO:C	3.758				
	THR459:CG—UNKO:C	3.664				
	GLY226:CA—UNKO:C	3.452				
	GLY226:CA—UNKO:C	3.988				
	GLY226:C—UNKO:C	3.955				
	TYR528:CB—UNKO:C	3.916				
	TYR528:CG—UNKO:C	3.567				
	TYR528:CD—UNKO:C	3.550				
	TYR528:CD—UNKO:C	3.598				
	TYR528:CD—UNKO:C	3.816				
	TYR528:CE'—UNKO:C	3.294				
	TYR528:CE'—UNKO:C	3.487				
	TYR528:CE'—UNKO:C	3.971				
	TYR528:CE'—UNKO:C	3.588				
	TYR528:CZ—UNKO:C	3.182				
	TYR528:CZ—UNKO:C	3.963				
	TYR528:CZ—UNKO:C	3.912				
	TYR528:CZ—UNKO:C	3.882				
	TYR528:CE2—UNKO:C	3.627				
	TYR528:CD2—UNKO:C	3.980				
GUL24	ALA259:CB—UNKO:C	3.540	LYS473:N—UNKO:O	3.387	LYS473:O —UNKO:H	2.117
	ASN347:CA—UNKO:C	3.973	LYS473:N—UNKO:O	3.841	LYS473:N—UNKO:H	2.570
	PRO346:CB—UNKO:C	3.736	ASN258:ND2—UNKO:O	3.707	GLY474:N—UNKO:H	3.809
	PRO346:CB—UNKO:C	3.935	SER275:OG—UNKO:N	3.063	SER275:OG—UNKO:H	2.803
	LYS473:CG—UNKO:C	3.509			SER275:OG—UNKO:H	3.620
	LYS473:CG—UNKO:C	3.922				
	LYS473:CB—UNKO:C	3.650				
	LYS473:CB—UNKO:C	3.695				
	SER275:CB—UNKO:C	3.304				
	SER275:CB—UNKO:C	3.760				
	SER275:CB—UNKO:C	3.899				
GUL25	CYS276:CB—UNKO:C	3.953	LYS429:NZ—UNKO:O	3.094	LYS429:NZ—UNKO:H	2.454
	ASN274:CG—UNKO:C	3.727	LYS429:NZ—UNKO:O	3.645	THR459:N—UNKO:H	3.841
	ASN274:CG—UNKO:C	3.901	ASN458:N—UNKO:O	3.731	ASN458:OD—UNKO:H	2.847
	ASN274:CG—UNKO:C	3.619	SER477:OG—UNKO:N	3.490	SER457:O—UNKO:H	3.798
	ASN458:CA—UNKO:C	3.892			ASN458:ND2—UNKO:H	3.918
	LEU481:CD2—UNKO:C	3.856				
	GLY506:CA—UNKO:C	3.869				
	GLY506:CA—UNKO:C	3.932				
	SER477:CA—UNKO:C	3.988				
	SER477:CB—UNKO:C	3.077				
	SER477:CB—UNKO:C	3.029				
	SER477:CB—UNKO:C	3.793				

	SER477:CB—UNKO:C	3.869				
	TYR528:CB—UNKO:C	3.625				
	TYR528:CB—UNKO:C	3.331				
	TYR528:CB—UNKO:C	3.917				
	TYR528:CG—UNKO:C	3.670				
	TYR528:CD—UNKO:C	3.976				
	TYR528:CE'—UNKO:C	3.682				
	TYR528:CE'—UNKO:C	3.573				
	TYR528:CZ—UNKO:C	3.691				
	TYR528:CE'—UNKO:C	3.590				
	TYR528:CD—UNKO:C	3.442				
	TYR528:CG—UNKO:C	3.774				
	SER529:CB—UNKO:C	3.889				
GUL26	ASN274:CG—UNKO:C	3.588	LYS229:NZ—UNKO:O	2.797	ASN274:ND2—UNKO:H	3.854
	PHE278:CE2—UNKO:C	3.933	ASN458:ND2—UNKO:O	3.724		
	TYR528:CB—UNKO:C	3.739	LYS429:NZ—UNKO:O	3.452		
	TYR528:CB—UNKO:C	3.654	ALA225:O—UNKO:N	3.891		
	TYR528:CB—UNKO:C	3.600				
	TYR528:CD—UNKO:C	3.607				
	TYR528:CD—UNKO:C	3.634				
GUL27	GLY277:CA—UNKO:C	3.941	ASN274:ND2—UNKO:O	3.271	ASN274:ND2—UNKO:H	3.138
	PHE278:CD'—UNKO:C	3.817	ASN274:ND2—UNKO:O	2.869	SER477:OG—UNKO:H	3.016
	PHE278:CD'—UNKO:C	3.794	ASN458:ND2—UNKO:O	3.179	ASN458:OD—UNKO:H	3.321
	PHE278:CE1—UNKO:C	3.415	LYS429:NZ—UNKO:O	2.735	ASN458:ND2—UNKO:H	3.505
	PHE278:CE1—UNKO:C	3.953				
	PHE278:CZ—UNKO:C	3.560				
	ASN274:CG—UNKO:C	3.800				
	CYS276:CB—UNKO:C	2.939				
	CYS276:CB—UNKO:C	3.840				
	CYS276:CB—UNKO:C	3.735				
	CYS276:CA—UNKO:C	3.870				
	THR459:CG—UNKO:C	3.503				
	THR459:CG—UNKO:C	3.474				
	THR459:CG—UNKO:C	3.422				
	THR459:CG—UNKO:C	3.492				
	SER477:CB—UNKO:C	3.994				
	SER477:CB—UNKO:C	3.830				
	TYR528:CB—UNKO:C	3.033				
	TYR528:CB—UNKO:C	3.514				
	TYR528:CG—UNKO:C	3.602				
	TYR528:CG—UNKO:C	3.495				
	TYR528:CD—UNKO:C	3.531				
	TYR528:CD—UNKO:C	3.809				
GUL28	SER345:CB—UNKO:C	2.956	ASN458:ND2—UNKO:O	3.720	LYS429:NZ—UNKO:H	2.367
	ASN342:CG—UNKO:C	3.696	ASN274:OD—UNKO:N	3.604	ALA225:O—UNKO:H	3.210
	PHE278:CZ—UNKO:C	3.181	LYS429:NZ—UNKO:O	3.156		
	PHE278:CE2—UNKO:C	3.477	SER477:OG—UNKO:N	3.616		
	ASN274:CG—UNKO:C	3.819				
	ASN274:CG—UNKO:C	3.833				
	THR459:CG—UNKO:C	3.354				
	THR459:CG—UNKO:C	3.910				
	THR459:CG—UNKO:C	3.661				

	THR459:CG—UNKO:C	3.820				
	LEU481:CD2—UNKO:C	3.854				
	LEU481:CD2—UNKO:C	3.952				
	GLY506:CA—UNKO:C	3.223				
	ASN458:CA—UNKO:C	3.886				
	SER477:CB—UNKO:C	3.206				
	SER477:CB—UNKO:C	3.603				
	SER477:CB—UNKO:C	3.603				
	ALA224:CB—UNKO:C	3.556				
	ALA224:CB—UNKO:C	3.786				
	TYR528:CZ—UNKO:C	3.480				
	TYR528:CZ—UNKO:C	3.799				
	TYR528:CE'—UNKO:C	3.363				
	TYR528:CE'—UNKO:C	3.230				
	TYR528:CD—UNKO:C	3.583				
	TYR528:CD—UNKO:C	3.133				
	TYR528:CG—UNKO:C	3.459				
	TYR528:CB—UNKO:C	3.343				
	TYR528:CB—UNKO:C	3.679				
GUL29	HIS185:CD2—UNKO:C	3.575	TYR528:OH—UNKO:N	3.583	ASN274:ND2—UNKO:H	2.880
	PHE227:C—UNKO:C	3.198	GLY226:O—UNKO:N	3.232	ASN274:OD—UNKO:H	2.531
	PHE227:CA—UNKO:C	3.804	ASN274:ND2—UNKO:O	2.705	GLY226:O—UNKO:H	2.887
	GLY226:C—UNKO:C	2.762	ASN458:OD—UNKO:N	3.932	LYS229:NZ—UNKO:H	3.848
	GLY226:C—UNKO:C	3.653				
	GLY226:C—UNKO:C	3.524				
	GLY226:C—UNKO:C	3.591				
	GLY226:CA—UNKO:C	3.793				
	GLY226:CA—UNKO:C	3.488				
	LYS229:CB—UNKO:C	3.830				
	LYS229:CG—UNKO:C	3.359				
	LYS229:CG—UNKO:C	3.875				
	LYS229:CG—UNKO:C	3.937				
	LYS229:CD—UNKO:C	3.223				
	LYS229:CD—UNKO:C	3.628				
	LYS229:CD—UNKO:C	3.134				
	LYS229:CE—UNKO:C	2.290				
	LYS229:CE—UNKO:C	3.227				
	LYS229:CE—UNKO:C	3.399				
	LYS229:CE—UNKO:C	3.242				
	CYS276:CB—UNKO:C	3.317				
	ASN274:CG—UNKO:C	2.991				
	ASN274:CB—UNKO:C	3.971				
	TYR528:CZ—UNKO:C	3.771				
	TYR528:CZ—UNKO:C	3.545				
	TYR528:CE2—UNKO:C	3.644				
	TYR528:CD2—UNKO:C	3.806				
	TYR528:CD2—UNKO:C	3.708				
	TYR528:CE'—UNKO:C	3.857				
	TYR528:CE'—UNKO:C	3.571				
	TYR528:CE'—UNKO:C	3.517				
	TYR528:CE'—UNKO:C	3.757				
	TYR528:CD—UNKO:C	3.501				
	TYR528:CD—UNKO:C	3.168				
	TYR528:CD—UNKO:C	3.587				
	TYR528:CG—UNKO:C	3.312				
	TYR528:CG—UNKO:C	3.701				

	TYR528:CB—UNKO:C	3.796				
GUL30	ASN347:CB—UNKO:C	3.776	ALA225:O —UNKO:N	3.961	ASN458:OD—UNKO:H	2.819
	ASN347:CG—UNKO:C	3.551	SER477:OG—UNKO:N	2.620	LYS429:NZ—UNKO:H	2.691
	PHE278:CA—UNKO:C	3.978	LYS429:NZ—UNKO:O	2.739	SER477:OG—UNKO:H	3.188
	PHE278:CD'—UNKO:C	3.438	ASN458:ND2—UNKO:O	3.664	ALA225:O—UNKO:H	2.951
	PHE278:CG—UNKO:C	3.712				
	PHE278:CD2—UNKO:C	3.926				
	PHE278:CE1—UNKO:C	3.466				
	PHE278:CZ—UNKO:C	3.734				
	PHE278:CE2—UNKO:C	3.946				
	PRO346:CD—UNKO:C	3.153				
	PRO346:CD—UNKO:C	3.693				
	PRO346:CG—UNKO:C	3.144				
	PRO346:CG—UNKO:C	3.692				
	ASN458:CG—UNKO:C	3.857				
	THR459:CG—UNKO:C	3.906				
	THR459:CG—UNKO:C	3.885				
	SER477:CB—UNKO:C	3.273				
	ILE272:CG2—UNKO:C	3.855				
	ILE272:CD1—UNKO:C	3.865				
	TYR528:CZ—UNKO:C	3.708				
	TYR528:CZ—UNKO:C	3.544				
	TYR528:CZ—UNKO:C	3.542				
	TYR528:CE2—UNKO:C	3.262				
	TYR528:CE2—UNKO:C	3.676				
	TYR528:CE2—UNKO:C	3.819				
	TYR528:CE2—UNKO:C	3.478				
	TYR528:CD2—UNKO:C	3.083				
	TYR528:CD2—UNKO:C	3.449				
	TYR528:CD2—UNKO:C	3.869				
	TYR528:CE'—UNKO:C	3.304				
	TYR528:CE'—UNKO:C	3.864				
	TYR528:CD—UNKO:C	3.369				
	TYR528:CD—UNKO:C	3.891				
	TYR528:CG—UNKO:C	3.675				
	TYR528:CG—UNKO:C	3.325				
	TYR528:CB—UNKO:C	3.815				
	LYS229:CE—UNKO:C	3.746				
	GLY248:C—UNKO:C	3.826				
	GLY226:CA—UNKO:C	3.418				
	GLY226:CA—UNKO:C	2.615				
	GLY226:CA—UNKO:C	3.763				
	ALA225:C—UNKO:C	3.444				
	ALA225:C—UNKO:C	3.758				
GUL31	ASN274:CG—UNKO:C	3.791	ALA225: O—UNKO:N	3.429	ASN458:OD—UNKO:H	2.686
	ASN458:CA—UNKO:C	3.896	ASN458:OD—UNKO:N	3.342	ASN458:OD—UNKO:H	3.083
	LYS429:CE—UNKO:C	3.875			THR459:OG—UNKO:H	3.861
	TYR528:CG—UNKO:C	3.680			ASN458:OD—UNKO:H	3.084
	TYR528:CG—UNKO:C	3.864			SER457:O—UNKO:H	3.536
	TYR528:CD2—UNKO:C	3.791			SER505:OG—UNKO:H	3.623
	TYR528:CE2—UNKO:C	3.870			THR459:N—UNKO:H	2.220
	TYR528:CE2—UNKO:C	3.738			THR459:N—UNKO:H	3.020
	TYR528:CZ—UNKO:C	3.815			ASN458:N—UNKO:H	3.876

	TYR528:CZ—UNKO:C	3.529				
	TYR528:CZ—UNKO:C	3.735				
	TYR528:CE'—UNKO:C	3.721				
	TYR528:CE'—UNKO:C	3.774				
	TYR528:CE'—UNKO:C	3.792				
	TYR528:CE'—UNKO:C	3.760				
	TYR528:CE'—UNKO:C	3.708				
	TYR528:CE'—UNKO:C	3.689				
	TYR528:CD—UNKO:C	3.618				
	TYR528:CD—UNKO:C	3.846				
	TYR528:CD—UNKO:C	3.480				
GUL32	SER529:CB—UNKO:C	2.784	GLY478:N—UNKO:O	2.283	ASN342:ND2—UNKO:H	3.167
	SER529:CB—UNKO:C	2.679	GLY507:N—UNKO:O	2.914	ASN458:ND2—UNKO:H	3.083
	SER529:CB—UNKO:C	3.748	GLY478:N—UNKO:O	3.834	THR249:OG—UNKO:H	2.934
	SER529:CB—UNKO:C	3.898	GLY506:N—UNKO:O	3.970	THR249:N—UNKO:H	2.470
	SER529:CB—UNKO:C	3.814	LYS229:NZ—UNKO:O	2.130	THR249:O—UNKO:H	3.497
	SER529:CB—UNKO:C	3.238	THR249:N—UNKO:O	3.364	ASN458:OD—UNKO:H	3.645
	SER529:CB—UNKO:C	3.738	ASN342:ND2—UNKO:O	3.275	LYS229:NZ—UNKO:H	2.843
	SER529:CB—UNKO:C	3.641	LYS429:NZ—UNKO:O	3.288	GLY478:N—UNKO:H	2.657
	TYR528:C—UNKO:C	3.867	ASN458:OD—UNKO:N	3.462	GLY478:O—UNKO:H	3.585
	TYR528:CA—UNKO:C	3.917	SER505:OG—UNKO:N	2.796	SER505:OG—UNKO:H	2.468
	TYR528:CB—UNKO:C	3.425	GLN526:O—UNKO:N	3.862	GLY506:N—UNKO:H	2.678
	LEU527:C—UNKO:C	3.550			GLY507:N—UNKO:H	3.660
	LEU527:C—UNKO:C	2.857			GLN526:O—UNKO:H	3.290
	TYR528:CA—UNKO:C	3.761				
	PHE509:CZ—UNKO:C	3.860				
	PHE509:CE1—UNKO:C	3.926				
	LEU481:CD2—UNKO:C	3.455				
	GLY478:CA—UNKO:C	3.149				
	GLY478:CA—UNKO:C	3.987				
	GLY478:CA—UNKO:C	3.890				
	GLY507:CA—UNKO:C	3.786				
	GLY507:CA—UNKO:C	3.563				
	GLY506:C—UNKO:C	3.720				
	GLY506:C—UNKO:C	3.646				
	GLY506:C—UNKO:C	3.711				
	GLY506:CA—UNKO:C	3.089				
	GLY506:CA—UNKO:C	3.514				
	GLY506:CA—UNKO:C	3.631				
	GLY506:CA—UNKO:C	3.834				
	SER505:CB—UNKO:C	3.670				
	SER505:CB—UNKO:C	3.418				
	LEU527:CA—UNKO:C	3.315				
	LEU527:CA—UNKO:C	3.419				
	LEU527:CA—UNKO:C	3.888				
	GLN526:C—UNKO:C	3.201				
	SER477:CB—UNKO:C	3.734				
	SER477:CA—UNKO:C	3.800				
	SER477:C—UNKO:C	3.910				
	ALA224:CB—UNKO:C	2.683				
	ALA224:CB—UNKO:C	3.114				
	ALA224:CB—UNKO:C	3.110				
	ALA224:CA—UNKO:C	3.882				
	THR459:CG—UNKO:C	3.079				
	THR459:CG—UNKO:C	3.580				

	THR459:CG—UNKO:C	3.858				
	ASN274:CG—UNKO:C	3.471				
	CYS276:CB—UNKO:C	3.323				
	LYS229:CE—UNKO:C	3.697				
	THR249:CB—UNKO:C	3.830				
	PHE278:CE2—UNKO:C	3.523				
	PHE278:CD2—UNKO:C	3.771				
	ASN458:CG—UNKO:C	3.484				
	ASN458:CG—UNKO:C	3.287				
	ASN458:CG—UNKO:C	3.688				
	LYS459:CE—UNKO:C	3.649				
GUL33	PHE278:CE1—UNKO:C	3.562	SER345:OG—UNKO:N	3.067	SER457:O —UNKO:H	2.802
	PHE278:CZ—UNKO:C	3.826	PRO346:O—UNKO:N	3.970	SER505:OG—UNKO:H	2.834
	PHE278:CD'—UNKO:C	3.776	ASN458:ND2—UNKO:O	2.811		
	ASN347:CB—UNKO:C	3.899	ASN342:ND2—UNKO:O	3.184		
	CYS276:CB—UNKO:C	3.386	ASN458:OD—UNKO:N	3.882		
	CYS276:CB—UNKO:C	3.482	SER457:O—UNKO:N	3.777		
	CYS276:CA—UNKO:C	3.967	SER505:OG—UNKO:N	2.940		
	ASN458:CG—UNKO:C	3.775				
	THR459:CG'—UNKO:C	3.745				
	LYS429:CE—UNKO:C	3.755				
	LEU481:CD2—UNKO:C	3.652				
	SER477:CB—UNKO:C	3.640				
	SER477:CB—UNKO:C	3.336				
	GLY226:CA—UNKO:C	3.538				
	TYR528:CB—UNKO:C	3.697				
	TYR528:CB—UNKO:C	3.400				
	TYR528:CB—UNKO:C	3.717				
	TYR528:CG—UNKO:C	3.774				
	TYR528:CG—UNKO:C	3.670				
	TYR528:CD—UNKO:C	3.613				
GUL34	CYS276:CB—UNKO:C	3.219	SER457:O —UNKO:N	3.852	GLY506:N—UNKO:H	3.771
	CYS276:CB—UNKO:C	3.751	SER505:OG—UNKO:N	2.799	SER505:OG—UNKO:H	2.665
	GLY506:CA—UNKO:C	3.877	ASN458:ND2—UNKO:O	2.934	SER457:O—UNKO:H	2.872
	LEU481:CD2—UNKO:C	3.256	ASN458:OD—UNKO:N	3.993	SER477:OG—UNKO:H	3.731
	PHE278:CZ—UNKO:C	3.974	ALA225:O—UNKO:N	3.465		
	ALA225:C—UNKO:C	3.607	ALA225:O—UNKO:N	3.900		
	GLY226:CA—UNKO:C	3.382	ASN342:ND2—UNKO:O	3.671		
	TYR528:CB—UNKO:C	3.461				
	TYR528:CB—UNKO:C	3.376				
	TYR528:CG—UNKO:C	3.717				
	TYR528:CG—UNKO:C	3.988				
	TYR528:CD—UNKO:C	3.851				
	THR459:CG'—UNKO:C	3.931				
	SER477:CB—UNKO:C	3.607				
	SER477:CB—UNKO:C	3.025				
	LYS229:CE—UNKO:C	3.903				
	ASN274:CG—UNKO:C	3.781				
GUL35	ASN458:CG—UNKO:C	3.499	LYS429:NZ—UNKO:O	3.110	ASN458:OD—UNKO:H	3.098
	LYS429:CE—UNKO:C	3.760	LYS429:NZ—UNKO:O	3.200	ASN458:ND2—UNKO:H	3.706
	PHE278:CE2—UNKO:C	3.407	THR249:OG—UNKO:N	3.379	LYS429:NZ—UNKO:H	2.682
	PHE278:CD2—UNKO:C	3.728			LYS429:NZ—UNKO:H	3.271
	THR249:CB—UNKO:C	3.686			ALA225O—UNKO:H	2.492
	THR249:CB—UNKO:C	3.450			TYR528:OH—UNKO:H	3.362
	THR249:CA—UNKO:C	3.739			SER345:OG—UNKO:H	3.974

	GLY248:C—UNKO:C	3.739			ASN342:ND2—UNKO:H	3.006
	LYS229:CE—UNKO:C	3.846			ASN458:ND2—UNKO:H	3.912
	LYS229:CE—UNKO:C	3.890			ASN274:ND2—UNKO:H	3.951
	GLY226:CA—UNKO:C	3.507				
	ASN274:CG—UNKO:C	3.914				
	ASN274:CG—UNKO:C	3.763				
	SER477:CB—UNKO:C	3.106				
	SER477:CB—UNKO:C	3.371				
	SER477:CB—UNKO:C	3.230				
	SER529:CB—UNKO:C	3.613				
	SER529:CB—UNKO:C	3.977				
	GLY506:CA—UNKO:C	3.965				
	ALA224:CB—UNKO:C	3.609				
	ALA224:CB—UNKO:C	3.979				
	TYR528:CB—UNKO:C	3.504				
	TYR528:CB—UNKO:C	3.648				
	TYR528:CB—UNKO:C	3.558				
	TYR528:CB—UNKO:C	3.127				
	TYR528:CB—UNKO:C	3.267				
	TYR528:CB—UNKO:C	3.253				
	TYR528:CD2—UNKO:C	3.914				
	TYR528:CD2—UNKO:C	3.673				
	TYR528:CZ—UNKO:C	4.012				
	TYR528:CE'—UNKO:C	4.176				
	TYR528:CD—UNKO:C	3.643				
	TYR528:CD—UNKO:C	3.663				
	TYR528:CD—UNKO:C	3.753				
	TYR528:CD—UNKO:C	3.716				
	TYR528:CD—UNKO:C	3.793				
	TYR528:CD—UNKO:C	3.822				
	TYR528:CG—UNKO:C	3.706				
	TYR528:CG—UNKO:C	3.378				
	TYR528:CG—UNKO:C	3.549				
GUL36	PHE278:CE2—UNKO:C	3.705	THR459:N—UNKO:O	3.460	SER505:OG—UNKO:H	2.280
	PHE278:CZ—UNKO:C	3.621	LYS429:NZ—UNKO:O	3.621	SER505:O—UNKO:H	3.186
	PHE278:CE1—UNKO:C	3.869	GLY507:N—UNKO:O	3.154	GLY506:N—UNKO:H	2.815
	THR459:CG—UNKO:C	3.725	GLY506:N—UNKO:O	2.946	GLY506:N—UNKO:H	3.501
	THR459:CG—UNKO:C	3.743	GLY506:N—UNKO:O	3.554	GLY507:N—UNKO:H	2.805
	ASN274:CG—UNKO:C	3.861	ASN274:ND2—UNKO:O	2.419	ASN274:OD—UNKO:H	2.841
	ASN458;CG—UNKO:C	3.739	ASN274:ND2—UNKO:O	3.361	ASN274:ND2—UNKO:H	3.514
	LEU481:CD2—UNKO:C	3.853			SER457:O—UNKO:H	2.492
	LEU481:CD2—UNKO:C	3.763			GLY478:N—UNKO:H	3.307
	SER477:CB—UNKO:C	3.705				
	SER477:CB—UNKO:C	3.590				
	TYR528:CB—UNKO:C	3.492				
	TYR528:CB—UNKO:C	3.107				
	TYR528:CG—UNKO:C	3.456				
	TYR528:CG—UNKO:C	3.911				
	TYR528:CD—UNKO:C	3.281				
	TYR528:CD—UNKO:C	3.650				
	TYR528:CD—UNKO:C	3.806				
	TYR528:CE'—UNKO:C	3.073				
	TYR528:CE'—UNKO:C	3.869				
	TYR528:CZ—UNKO:C	3.837				
	TYR528:CZ—UNKO:C	3.548				

GUL37	LEU481:CD2—UNKO:CL	2.426	ASN458:OD—UNKO:N	3.069	ASN342:OD—UNKO:H	3.023
	LEU481:CD2—UNKO:C	3.775	ASN342:OD—UNKO:N	3.908	ASN342:ND2—UNKO:H	2.908
	LEU481:CD2—UNKO:C	3.252	SER344:O—UNKO:N	3.574	ASN458:ND2—UNKO:H	2.300
	LEU481:CG—UNKO:CL	3.547	SER345:OG—UNKO:N	3.689	SER345:OG—UNKO:H	3.343
	GLY506:CA—UNKO:CL	3.325	LYS429:NZ—UNKO:O	2.140	SER344:O—UNKO:H	2.697
	GLY506:C—UNKO:CL	3.619	ASN458:ND2—UNKO:O	3.711	ASN458:OD—UNKO:H	3.593
	SER477:CB—UNKO:C	3.359	LYS229:NZ—UNKO:O	3.058	SER345:N—UNKO:H	3.964
	THR459:CG—UNKO:C	3.458	GLY226:N—UNKO:O	3.694		
	THR459:CG—UNKO:C	3.845	LYS229:NZ—UNKO:O	3.656		
	THR459:CG—UNKO:C	3.752				
	SER505:CB—UNKO:C	3.961				
	ASN458:C—UNKO:C	3.671				
	ASN458:C—UNKO:C	3.813				
	ASN458:CA—UNKO:C	3.458				
	ASN458:CA—UNKO:C	3.977				
	SER457:C—UNKO:C	3.915				
	SER457:C—UNKO:C	3.967				
	LYS429:CE—UNKO:C	3.796				
	ASN458:CG—UNKO:C	3.623				
	ASN458:CG—UNKO:C	3.984				
	ASN458:CG—UNKO:C	3.374				
	ASN458:CG—UNKO:C	3.855				
	ASN458:CG—UNKO:C	3.959				
	PRO346:CG—UNKO:C	2.414				
	PRO346:CG—UNKO:C	3.071				
	PRO346:CG—UNKO:C	3.555				
	PRO346:CD—UNKO:C	2.318				
	PRO346:CD—UNKO:C	2.439				
	PRO346:CD—UNKO:C	3.796				
	PRO346:CD—UNKO:C	3.651				
	PRO346:CB—UNKO:C	3.786				
	SER345:CB—UNKO:C	3.221				
	SER345:CB—UNKO:C	3.567				
	SER345:CA—UNKO:C	3.418				
	SER345:C—UNKO:C	3.804				
	CYS276:CB—UNKO:C	3.456				
	ASN274:CG—UNKO:C	3.506				
	ASN274:CG—UNKO:C	3.867				
	LYS229:CE—UNKO:C	2.311				
	LYS229:CE—UNKO:C	2.887				
	LYS229:CE—UNKO:C	3.522				
	LYS229:CD—UNKO:C	3.732				
	LYS229:CE—UNKO:C	1.613				
	LYS229:CD—UNKO:C	2.630				
	LYS229:CG—UNKO:C	3.779				
	ASN279:CG—UNKO:C	3.986				
	TYR528:CD—UNKO:C	3.914				
	TYR528:CE'—UNKO:C	2.898				
	TYR528:CE'—UNKO:C	3.658				
	TYR528:CE'—UNKO:C	3.919				
	TYR528:CZ—UNKO:C	2.159				
	TYR528:CZ—UNKO:C	3.869				
	TYR528:CE2—UNKO:C	2.823				
	TYR528:CD2—UNKO:C	3.841				
	GLY226:CA—UNKO:C	3.061				
	GLY226:CA—UNKO:C	2.947				

	GLY226:CA—UNKO:C	3.368				
	GLY226:CA—UNKO:C	3.832				
	GLY226:CA—UNKO:C	3.564				
	GLY226:CA—UNKO:C	3.920				
	GLY226:CA—UNKO:C	2.931				
	GLY226:C—UNKO:C	3.880				
	GLY226:C—UNKO:C	3.873				
	ALA225:C—UNKO:C	2.966				
	ALA225:C—UNKO:C	3.944				
	ALA225:CA—UNKO:C	3.814				
	ALA225:CB—UNKO:C	3.469				
GUL38	PHE278:CZ—UNKO:C	3.908	LYS429:NZ—UNKO:O	3.578	LYS429:NZ—UNKO:H	3.073
	PHE278:CE2—UNKO:C	3.929	ASN458:ND2—UNKO:O	3.305	ALA225:O—UNKO:H	3.576
	SER345:CB—UNKO:C	3.891	ASN274:ND2 —UNKO:O	3.046	ASN458:ND2—UNKO:H	3.947
	LYS229:CE—UNKO:C	3.784	ASN347:ND2—UNKO:O	3.550	ASN458:OD—UNKO:H	3.567
	ALA225:CB—UNKO:C	3.723			ASN458:ND2—UNKO:H	3.375
	GLY226:CA—UNKO:C	3.643			ASN458:OD—UNKO:H	2.033
	GLY226:CA—UNKO:C	3.680			ASN458:ND2—UNKO:H	2.360
	GLY226:CA—UNKO:C	3.752				
	GLY226:CA—UNKO:C	3.875				
	ALA225:C—UNKO:C	3.890				
	ASN274:CG—UNKO:C	3.788				
	ASN274:CG—UNKO:C	3.917				
	ASN274:CG—UNKO:C	3.811				
	TYR528:CD—UNKO:C	3.865				
	TYR528:CE'—UNKO:C	3.928				
	TYR528:CE'—UNKO:C	3.860				
	TYR528:CE'—UNKO:C	3.478				
	TYR528:CZ—UNKO:C	3.549				
	TYR528:CZ—UNKO:C	3.902				
	TYR528:CE2—UNKO:C	3.959				
GUL39	PHE278:CE2—UNKO:C	3.696	ASN342:ND2—UNKO:O	3.195	ASN274:ND2—UNKO:H	3.047
	PHE278:CE2—UNKO:C	3.190	ASN458:ND2—UNKO:O	3.071	SER477:OG—UNKO:H	3.884
	PHE278:CZ—UNKO:C	2.989	ASN458:ND2—UNKO:O	3.662		
	PHE278:CZ—UNKO:C	3.481	THR459:N—UNKO:O	3.233		
	PHE278:CD2 —UNKO:C	3.664	LYS429:NZ—UNKO:O	3.502		
	PHE278:CD2—UNKO:C	3.627	ASN274:ND2—UNKO:O	2.742		
	PHE278:CG—UNKO:C	3.433	ASN274:ND2—UNKO:O	3.847		
	PHE278:CG—UNKO:C	3.887				
	PHE278:CD'—UNKO:C	3.152				
	PHE278:CD'—UNKO:C	3.686				
	PHE278:CE1—UNKO:C	3.194				
	PHE278:CE1—UNKO:C	3.258				
	PHE278:CA—UNKO:C	3.818				
	GLY277:CA—UNKO:C	3.954				
	CYS276:C—UNKO:C	3.890				
	CYS276:CB—UNKO:C	3.330				
	CYS276:CB—UNKO:C	3.367				
	CYS276:CA—UNKO:C	3.877				
	ASN458:CG—UNKO:C	3.990				
	THR459:CG—UNKO:C	3.446				
	THR459:CG—UNKO:C	3.540				
	THR459:CG—UNKO:C	3.568				
	ASN274:CG—UNKO:C	3.700				

	ASN274:CG—UNKO:C	3.802				
	SER477:CA—UNKO:C	3.927				
	SER477:CB—UNKO:C	3.326				
	SER477:CB—UNKO:C	3.479				
	SER477:CB—UNKO:C	3.353				
	SER477:CB—UNKO:C	3.985				
	GLY506:CA—UNKO:C	2.714				
	GLY506:CA—UNKO:C	3.296				
	GLY506:CA—UNKO:C	3.719				
	GLY506:C—UNKO:C	2.990				
	GLY506:C—UNKO:C	3.727				
	GLY507:CA—UNKO:C	3.730				
	SER529:CB—UNKO:C	3.836				
	SER529:CB—UNKO:C	3.663				
	SER529:CA—UNKO:C	3.964				
	TYR528:C—UNKO:C	3.872				
	TYR528:CA—UNKO:C	3.718				
	TYR528:CB—UNKO:C	3.531				
	TYR528:CB—UNKO:C	3.097				
	TYR528:CB—UNKO:C	3.310				
	TYR528:CB—UNKO:C	3.632				
	TYR528:CB—UNKO:C	3.694				
	TYR528:CG—UNKO:C	3.302				
	TYR528:CG—UNKO:C	3.777				
	TYR528:CG—UNKO:C	3.454				
	TYR528:CD—UNKO:C	2.704				
	TYR528:CD—UNKO:C	3.660				
	TYR528:CD—UNKO:C	3.815				
	TYR528:CD—UNKO:C	3.691				
	TYR528:CE'—UNKO:C	3.349				
	TYR528:CE'—UNKO:C	3.836				
	TYR528:CE'—UNKO:C	3.326				
	ALA225:C—UNKO:C	3.321				
	GLY226:CA—UNKO:C	3.284				
A771726	TYR528:CB—UNKO:C	3.712	ASN458:ND2—UNKO: O	3.141	ASN458:OD—UNKO:H	2.686
	TYR528:CD—UNKO:C	3.861	ASN458:OD—UNKO:N	3.455	ASN458:OD—UNKO:H	2.605
	TYR528:CD—UNKO:C	3.939	ASN274:ND2—UNKO: O	3.614		
	TYR528:CB—UNKO:C	3.712	ASN274:OD—UNKO:N	3.534		
	TYR528:CD—UNKO:C	3.861				
	TYR528:CD—UNKO:C	3.939				
	SER477:CB—UNKO:C	3.676				
	PHE278:CZ—UNKO:C	3.702				
	PHE278:CE2—UNKO:C	3.729				
	THR459:CG—UNKO:C	3.569				
	THR459:CG—UNKO:C	3.760				
	THR459:CG—UNKO:C	3.783				
Atovaquone	GLY506:CA—UNKO:C	3.794	ASN342:ND2—UNKO: O	2.735	ASN458:ND2—UNKO: H	2.473
	GLY506:CA—UNKO:C	3.700	ASN458:ND2—UNKO: O	3.226	ASN342:ND2—UNKO: H	3.698
	GLY506:CA—UNKO:C	3.842	LYS429: NZ—UNKO: O	2.714	ASN458:ND2—UNKO: H	3.132
	SER529:CB—UNKO:C	3.949	ASN274:ND2—UNKO: O	3.291	LYS429: NZ—UNKO: H	3.004
	TYR528:CA—UNKO:C	3.914				
	TYR528:CA—UNKO:C	3.919				
	TYR528:CB—UNKO:C	3.444				

	TYR528:CB—UNKO:C	3.459				
	TYR528:CB—UNKO:C	3.591				
	TYR528:CB—UNKO:C	3.624				
	TYR528:CB—UNKO:C	3.750				
	TYR528:CB—UNKO:C	3.765				
	TYR528:CG—UNKO:C	3.971				
	TYR528:CD—UNKO:C	3.397				
	SER477:CB—UNKO:C	3.476				
	SER477:CB—UNKO:C	3.874				
	THR459:CG—UNKO:C	2.730				
	THR459:CG—UNKO:C	3.021				
	THR459:CB—UNKO:C	3.904				
	ASN274:CG—UNKO:C	3.675				
	CYS276:CB—UNKO:C	3.570				
	ALA224:CB—UNKO:C	3.649				
	ALA224:CB—UNKO:C	3.556				
	LEU527:C—UNKO:C	3.725				
	PHE278:CA—UNKO:C	3.801				
	PHE278:CE2—UNKO:C	3.341				
	PHE278:CE2—UNKO:C	3.970				
	PHE278:CD'—UNKO:C	3.893				
	PHE278:CG—UNKO:C	3.830				
	PHE278:CD2—UNKO:C	3.562				
	PHE278:CD2—UNKO:C	3.840				
	PHE278:CZ—UNKO:C	3.630				
	SER505:CB—UNKO:C	3.986				

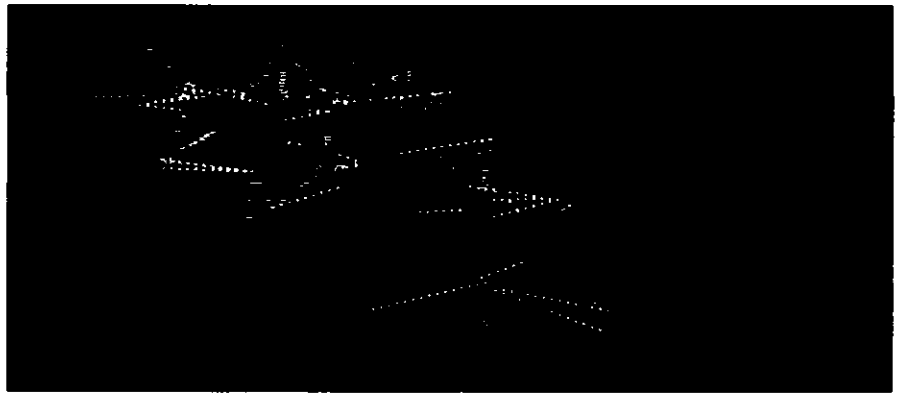

Figure 3.3: Binding interactions of GUL32 (lead compound) showing 55 hydrophobic interactions.

Figure 3.4: Binding interactions of GUL32 (lead compound) showing 11 ionic interactions.

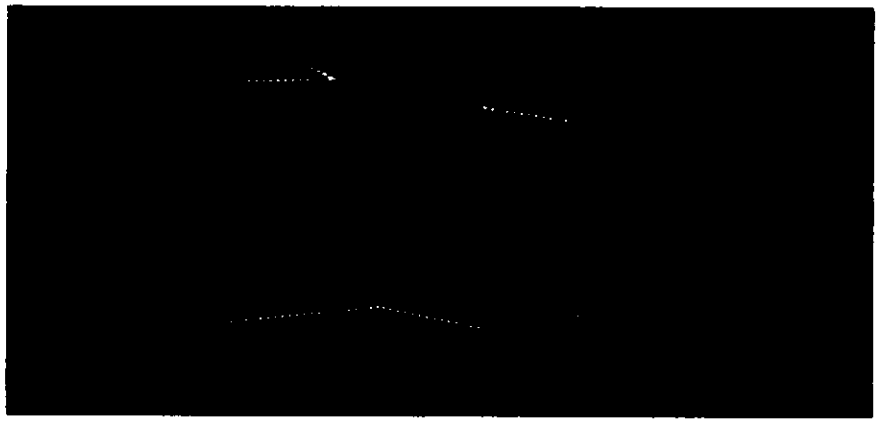

Figure 3.5: Binding interactions of GUL32 (lead compound) showing 13 hydrogen interactions.

Table 3.7: Analogues formed from lead compound along with their IUPAC names

Compound	Structure	Energy Value
Alcohol formation	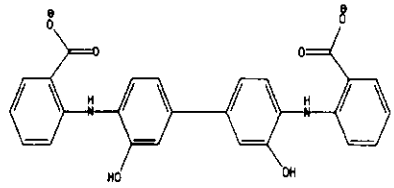 2-[(4-{4-[(2-carboxylatophenyl)amino]-3-hydroxyphenyl}-2-hydroxyphenyl)amino]benzoate	4.3
C-Alkylation	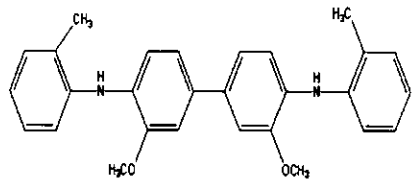 2-methoxy-4-{3-methoxy-4-[(2- methylphenyl) amino]phenyl}-N-(2-methylphenyl)aniline	5.9
Ester formation	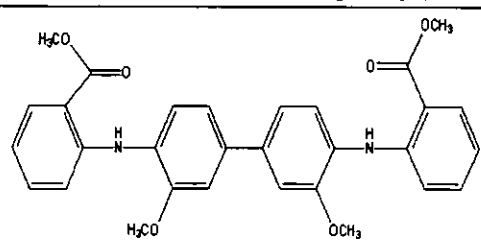 methyl 2-{[2-methoxy-4-(3-methoxy-4-{[2-(methoxycarbonyl)phenyl]amino}phenyl)phenyl]amino}benzoate	24.3

3.4.4 Analogues of Lead Compound

On the basis of binding interactions and IC50 value, GUL32 had been selected as a lead compound, from which three novel structural analogues have been designed in order to get the most active compound to be used as potent DHODH inhibitors. Table 3.7 shows the analogues of the lead compound with their IUPAC names obtained from ChemDraw software. Analogues were designed by introduction or elimination of various functional groups which either increase/decrease the hydrophobicity or hydrophilicity of the designed compound or increase/decrease the polarity as shown in Table 3.7.

All the analogues were docked within the active site and the best conformation was selected and visualized in the VMD software in order to calculate binding interactions. The first analogue of the lead was designed by formation of alcohol, due to which it show strong hydrogen and ionic bonding. It showed three binding interaction in which there were 52 hydrophobic interactions, 13 ionic bond and 13 hydrogen bonds. The hydrophobic interactions include the C's of ligand with the Cs of CYS276 at 2.909 A°, at 3.528 A°, at 3.902 A°, at 3.706 A°, of ASN274 at 3.994 A °, at 3.969 A °, at 3.275 A °, of LYS229 at 3.720 A°, at 3.293, of THR459 at 3.274, at 3.981, at 3.769, of ALA225 at 3.659, at 3.725, of ALA224 at 2.824, at 2.828, of SER477 at 3.809, at 3.911, at 3.950, of GLY478 at 3.164, of TYR528 at 3.762, at 3.944, at 3.824, at 3.874, of SER529 at 3.313, at 3.787, at 3.816, at 2.865, at 2.725, at 3.718, at 3.922, of CYS530 at 3.976, of PHE509 at 3.813, at 3.853, of LEU527 at 3.464, at 3.346, of LEU529 at 3.930, of ASN458 at 3.633, at 3.988, at 3.940, of GLY507 at 3.492, at 3.823, at 3.923, of GLY506 at 3.697, at 3.652, at 3.840, at 3.195, at 3.490, at 3.556, at 3.987 and of SER505 at 3.715 , at 3.782. The ionic interactions include the O's of ligand with the N's of GLY478 at 2.460, at 3.955, of GLY507 at 2.822, of GLY506 at 3.970,

of TYR528 at 3.990, of ALA224 at 3.989, of GLY226 at 3.409, of ASN347 at 3.122, at 3.767,at 3.630, of LYS429 at 3.754 and the N's of ligand with O's of SER505 at 2.829, of GLN526 at 3.740. The hydrogen bond was between H's of ligand and O's of ALA225 having distance 2.029, of GLY226 having distance 2.479, of ALA225 having distance 3.691, of ASN342 having distance 3.328, of ASN458 having distances 3.669 and 3.983, of GLY506 having distance 2.979, of SER505 having distances 2.183 and 2.456, of GLN526 having distances 3.176, 3.087 and 3.625 and between H's of ligand and N's of LEU527 having distance 3.940. This analogue increased the activity and interactions than the lead compound by increasing its ionic and hydrogen bonds.

The 2nd analogue was formed by C-alkylation in which methyl group was introduced on both side of ring, as a result hydrophobic character was increased. All three type of interaction were existed in the 2nd analogue in which there were 59 hydrophobic interactions, 5 ionic and 7 hydrogen bonds. The hydrophobic interactions include the C's of ligand and C's of CYS276 having distances 2.935, 3.586, 3.946, 3.607 and 3.850, of ASN274 at 3.602, of LYS229 having distances 3.904 and 3.511, of PHE278 with distances 3.989 and 3.900, of ASN347 at 3.987, of PRO346 having distances 3.795 and 3.698, of ALA225 at 3.952, of ASN458 at 3.434, 3.812 and 3.570, of THR459 at 3.206, 3.545 and3.894, of LYS429 at 3.951, of LEU481 at 3.084, of SER505 at 3.676 and 3.774, of GLY506 at 3.100, 3.677, 3.536, 3.849, 3.793 and 3.733, of GLY507 at 3.826 and 3.625, of ALA224 at 3.237, 3.064 and 2.440, of GLN526 at 3.875 and 3.614, of LEU527 at 3.079, 3.707, 3.675 and 3.712 , of TYR528 at 3.217, 3.895, 3.722, 3.992 and 3.878, of SER529 at 3.012, 3.162 , 2.625, 3.584, 3.769, 3.346 and 3.950, of GLY478 at 3.885, 3.733 and 2.993, of SER 477 at 3.883, 3.567 and 3.582. The ionic bond include the interactions between O's of ligand and N's of

GLY226, LYS 429 and GLY506 with distances 3.775, 3.872 and 3.264 and between N's of ligand and O's of SER505 and ASN458 with distances 2.525 and 3.988 respectively. The hydrogen bond was between H's of ligand and O's of SER505, GLN 526 and ASN458 with distances 2.030, 3.628, 3.915 and between H of ligand and N of GLY506, ASN458 and ASN342 with distances 2.688, 3.655 and 3.105 respectively.

In case of 3rd analogue, the hydrophobicity was increased by converting COO on both side of ring to $COOCH_3$. The binding interactions observed in this analogue were 81 hydrophobic interactions, 11 ionic and 5 hydrogen bonds. The hydrophobic interaction were between C of ligand and C of PRO346 with distances 2.910, 3.610, 3.781 and 3.939, of ASN347 with distances 3.649, 3.522 and 3.981, of SER345 with distances 3.707, 3.591 and 3.919, of PHE278 with distances 3.763, 3.708, 3.928, 3.933, 3.647, 3.982, 3.772, 3.929, 3.107, 3.525 and 3.967, of GLY277 with distances 3.615, 3.585, 3.326 and 3.886, of CYS276 with distances 3.123, 3.784, 3.220, 3.982, 3.174, 2.819 and 3.839, of LYS229 with distances 3.485 and 3.626, of GLY226 with distance 3.973, of THR459 with distances 3.193 and 3.760, of ALA225 with distances 3.852, 3.718, 3.781 and 3.294, of ALA224 with distances 2.020, 2.630, 3.331, 3.741 and 3.218, of GLN526 with distance 3.300, of TYR528 with distances 3.557, 3.946 , 3.844 and 3.910, of LEU527 with distance 3.805, of SER505 with distances 3.217 and 3.919, of THR459 with distances 3.738 and 3.496, of ASN458 with distances 2.951, 3.767 and 3.333, of LYS429 with distances 3.945 and 3.990, of GLY507 with distance 3.784, of GLY507 with distances 3.871, 3.973, 3.450, 3.641, 3.890, 3.525, 3.782 and 3.957, of GLN526 with distance 3.541, of LEU481 with distances 2.823, 2.809 and 3.811, of GLY478 3.713 and 3.748, of SER477 with distances 3.112, 2.239, 3.958 and 2.027, of VAL476 with distance 3.546. The ionic bond include the interaction between the ligand and

amino acid SER505, GLY506, ALA225, ALA224, GLY226, LYS429, THR249, GLY478, PRO346, ASN458, ASN347 with distances 1.807, 3.905, 3.720, 3.807, 3.932, 3.198, 3.478, 3.984, 3.761, 2.602 and 3.676. The hydrogen bond was formed with ASN342, THR249, SER505, GLY506 and GLN526 with distances 3.064, 3.562, 1.008, 3.639, 3.949.

Docking of the analogues through AutoDock has been performed with the earlier mentioned procedure in order to get the active conformations of the analogues. The binding interactions of each analogue bound into the active site of the protein have been obtained using VMD.

Figure 3.6: Binding interactions of analogue 1 showing 52 hydrophobic interactions

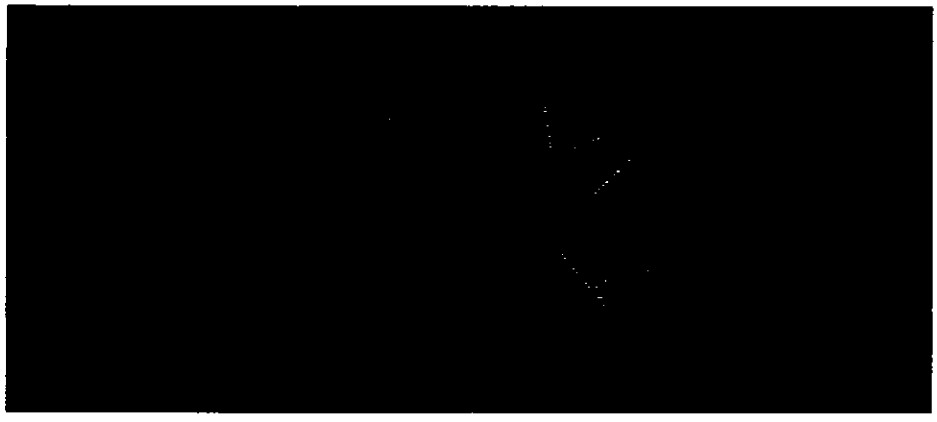

Figure 3.7: Binding interactions of analogue 1 showing 13 ionic interactions.

Figure 3.8: Binding interactions of analogue 1 showing 13 hydrogen bonds.

Figure 3.9: Binding interactions of analogue 2 showing 59 hydrophobic interactions.

Figure 3.10: Binding interactions of analogue 2 showing 5 ionic interactions.

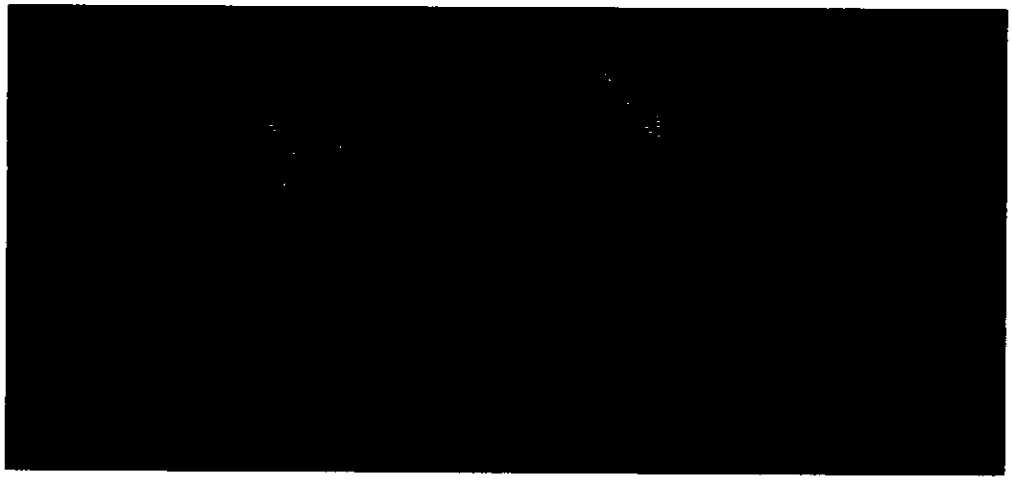

Figure 3.11: Binding interactions of analogue 2 showing 5 hydrogen bonds.

Figure 3.12: Binding interactions of analogue 3 showing 81 hydrophobic interactions.

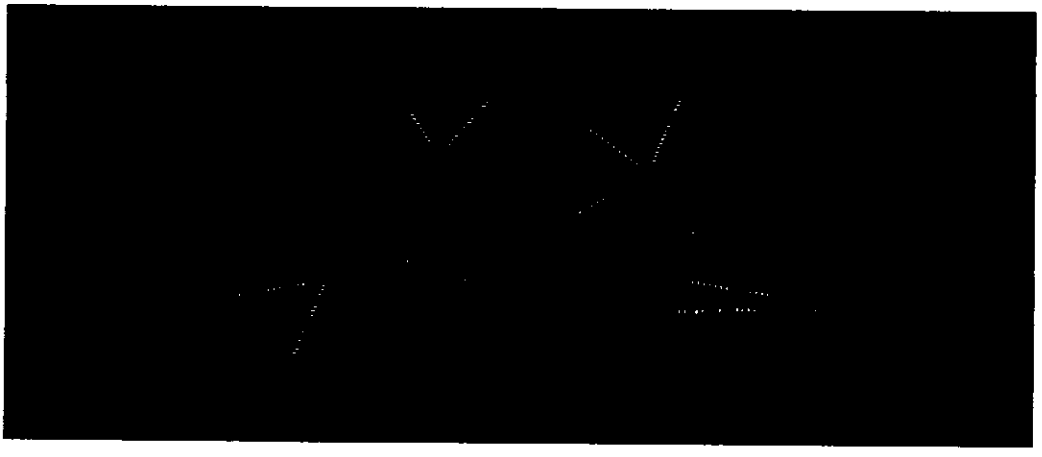

Figure 3.13: Binding interactions of analogue 3 showing 11 ionic interactions.

Figure 3.14: Binding interactions of analogue 3 showing 5 hydrogen bonds.

Table 3.8: Binding interactions of the analogues which include hydrophobic, hydrogen bonding and ionic bonding along with distances in Angstrom.

Compounds	Hydrophobic Interactions		Ionic Bond		Hydrogen Bond	
	Amino Acid	Distance	Amino Acid	Distance	Amino Acid	Distance
Alcohol Formation	CYS276:CB—UNKO:C	2.909	GLY478:N—UNKO:O	2.460	ALA225:O—UNKO:H	2.029
	CYS276:CB—UNKO:C	3.528	GLY478:N—UNKO:O	3.955	GLY226:N—UNKO:H	2.479
	CYS276:CB—UNKO:C	3.902	GLY507:N—UNKO:O	2.822	ALA225:N—UNKO:H	3.691
	CYS276:CA—UNKO:C	3.706	GLY506:N—UNKO:O	3.970	ASN342:ND2—UNKO:H	3.328
	ASN274:CG—UNKO:C	3.994	SER505:OG—UNKO:N	2.829	ASN458:ND2—UNKO:H	3.669
	ASN274:CG—UNKO:C	3.969	GLN526:O—UNKO:N	3.740	ASN458:OD—UNKO:H	3.983
	ASN274:CG—UNKO:C	3.275	TYR528:N—UNKO:O	3.990	GLY506:N—UNKO:H	2.979
	LYS229:CE—UNKO:C	3.720	ALA224:N—UNKO:O	3.989	SER505:OG—UNKO:H	2.183
	LYS229:CE—UNKO:C	3.293	GLY226:N—UNKO:O	3.409	SER505:OG—UNKO:H	2.456
	THR459:CG—UNKO:C	3.274	ASN347:ND2—UNKO:O	3.122	GLN526:O—UNKO:H	3.176
	THR459:CG—UNKO:C	3.981	ASN347:ND2—UNKO:O	3.767	GLN526:O—UNKO:H	3.087
	ALA225:C—UNKO:C	3.659	ASN347:ND2—UNKO:O	3.630	GLN526:OE—UNKO:H	3.625
	ALA225:C—UNKO:C	3.725	LYS429:NZ—UNKO:O	3.754	LEU527:N—UNKO:H	3.940
	ALA224:CB—UNKO:C	2.824				
	ALA224:CB—UNKO:C	2.828				
	THR459:CG—UNKO:C	3.769				
	SER477:CB—UNKO:C	3.809				
	SER477:CA—UNKO:C	3.911				
	SER477:C—UNKO:C	3.950				
	GLY478:CA—UNKO:C	3.164				
	TYR528:CB—UNKO:C	3.762				
	TYR528:CB—UNKO:C	3.944				
	TYR528:CA—UNKO:C	3.824				
	TYR528:C—UNKO:C	3.874				
	SER529:CA—UNKO:C	3.313				
	SER529:CA—UNKO:C	3.787				
	SER529:CA—UNKO:C	3.816				
	SER529:CB—UNKO:C	2.865				
	SER529:CB—UNKO:C	2.725				
	SER529:CB—UNKO:C	3.718				
	SER529:CB—UNKO:C	3.922				
	CYS530:CB—UNKO:C	3.976				
	PHE509:CZ—UNKO:C	3.813				
	PHE509:CE1—UNKO:C	3.853				
	LEU527:C—UNKO:C	3.464				
	LEU527:CA—UNKO:C	3.346				
	LEU529:CA—UNKO:C	3.930				
	ASN458:CG—UNKO:C	3.633				
	ASN458:CG—UNKO:C	3.988				
	ASN458:CG—UNKO:C	3.940				
	GLY507:CA—UNKO:C	3.492				
	GLY507:CA—UNKO:C	3.823				
	GLY507:CA—UNKO:C	3.923				
	GLY506:C—UNKO:C	3.697				
	GLY506:C—UNKO:C	3.652				
	GLY506:C—UNKO:C	3.840				
	GLY506:CA—UNKO:C	3.195				
	GLY506:CA—UNKO:C	3.490				

	GLY506:CA—UNKO:C	3.556				
	GLY506:CA—UNKO:C	3.987				
	SER505:CB—UNKO:C	3.715				
	SER505:CB—UNKO:C	3.782				
C-Alkylation	CYS276:CB—UNKO:C	2.935	GLY226:N—UNKO:O	3.775	GLY506:N—UNKO:H	2.688
	CYS276:CB—UNKO:C	3.586	LYS429:NZ—UNKO:O	3.872	SER505:OG—UNKO:H	2.030
	CYS276:CB—UNKO:C	3.946	SER505:OG—UNKO:N	2.525	GLN526:O—UNKO:H	3.628
	CYS276:CA—UNKO:C	3.607	GLY506:N—UNKO:O	3.264	ASN458:ND2—UNKO:H	3.655
	CYS276:C—UNKO:C	3.850	ASN458:OD—UNKO:N	3.988	ASN342:ND2—UNKO:H	3.105
	ASN274:CG—UNKO:C	3.602				
	LYS229:CE—UNKO:C	3.904				
	LYS229:CE—UNKO:C	3.511				
	PHE278:CE2—UNKO:C	3.989				
	PHE278:CA—UNKO:C	3.900				
	ASN347:CG—UNKO:C	3.987				
	PRO346:CG—UNKO:C	3.795				
	PRO346:CD—UNKO:C	3.698				
	ALA225:C—UNKO:C	3.952				
	ASN458:CG—UNKO:C	3.434				
	ASN458:CG—UNKO:C	3.812				
	ASN458:CG—UNKO:C	3.570				
	THR459:CG—UNKO:C	3.206				
	THR459:CG—UNKO:C	3.545				
	THR459:CG—UNKO:C	3.894				
	LYS429:CE—UNKO:C	3.951				
	LEU481:CD2—UNKO:C	3.084				
	SER505:CB—UNKO:C	3.676				
	SER505:CB—UNKO:C	3.774				
	GLY506:CA—UNKO:C	3.100				
	GLY506:CA—UNKO:C	3.677				
	GLY506:CA—UNKO:C	3.536				
	GLY506:CA—UNKO:C	3.849				
	GLY506:C—UNKO:C	3.793				
	GLY506:C—UNKO:C	3.733				
	GLY507:CA—UNKO:C	3.826				
	GLY507:CA—UNKO:C	3.625				
	ALA224:CB—UNKO:C	3.237				
	ALA224:CB—UNKO:C	3.064				
	ALA224:CB—UNKO:C	2.440				
	GLN526:CB—UNKO:C	3.875				
	GLN526:C—UNKO:C	3.614				
	LEU527:C—UNKO:C	3.079				
	LEU527:C—UNKO:C	3.707				
	LEU527:CA—UNKO:C	3.675				
	LEU527:CA—UNKO:C	3.712				
	TYR528:CB—UNKO:C	3.217				
	TYR528:CA—UNKO:C	3.895				
	TYR528:CA—UNKO:C	3.722				
	TYR528:C—UNKO:C	3.878				
	SER529:CB—UNKO:C	3.012				
	SER529:CB—UNKO:C	2.625				
	SER529:CB—UNKO:C	3.584				
	SER529:CA—UNKO:C	3.769				
	SER529:CA—UNKO:C	3.346				
	SER529:C—UNKO:C	3.950				
	GLY478:C—UNKO:C	3.885				

	GLY478:CA—UNKO:C	2.993				
	SER529:OG—UNKO:C	3.162				
	GLY478:CA—UNKO:C	3.733				
	SER477:C—UNKO:C	3.883				
	SER477:CA—UNKO:C	3.567				
	SER477:CB—UNKO:C	3.582				
	TYR528:CA—UNKO:C	3.992				
Ester Formation	PRO346:CD—UNKO:C	2.910	SER505:OG—UNKO:N	1.807	ASN342:ND2—UNKO:H	3.064
	PRO346:CD —UNKO:C	3.610	GLY506:N—UNKO:O	3.905	THR249:OG—UNKO:H	3.562
	PRO346:CG—UNKO:C	3.781	ALA225:N—UNKO:O	3.720	SER505:OG—UNKO:H	1.008
	PRO346:CG—UNKO:C	3.939	ALA224:N—UNKO:O	3.807	GLY506:N—UNKO:H	3.639
	ASN347:CG—UNKO:C	3.649	LYS429:NZ—UNKO:O	3.932	GLN526:O—UNKO:H	3.949
	ASN347:CB—UNKO:C	3.522	GLY226:N—UNKO:O	3.198		
	ASN347:CB—UNKO:C	3.981	THR249:N—UNKO:O	3.478		
	SER345:CA—UNKO:C	3.707	GLY478:N—UNKO:O	3.984		
	SER345:CB—UNKO:C	3.591	PRO346:N—UNKO:O	3.761		
	SER345:CB—UNKO:C	3.919	ASN347:ND2—UNKO:O	2.602		
	PHE278:CZ—UNKO:C	3.763	ASN458:ND2—UNKO:O	3.676		
	PHE278:CE2—UNKO:C	3.708				
	PHE278:CE2—UNKO:C	3.928				
	PHE278:CD2—UNKO:C	3.933				
	PHE278:CD2—UNKO:C	3.647				
	PHE278:CE2—UNKO:C	3.982				
	PHE278:CG—UNKO:C	3.772				
	PHE278:CG—UNKO:C	3.929				
	PHE278:CA—UNKO:C	3.107				
	PHE278:CA—UNKO:C	3.525				
	PHE278:CA—UNKO:C	3.967				
	GLY277:C—UNKO:C	3.615				
	GLY277:C—UNKO:C	3.585				
	GLY277:CA—UNKO:C	3.326				
	GLY277:CA—UNKO:C	3.886				
	CYS276:C—UNKO:C	3.123				
	CYS276:C—UNKO:C	3.784				
	CYS276:CA—UNKO:C	3.220				
	CYS276:CA—UNKO:C	3.982				
	CYS276:CB—UNKO:C	3.174				
	CYS276:CB—UNKO:C	2.819				
	CYS276:CB—UNKO:C	3.839				
	LYS229:CE—UNKO:C	3.485				
	LYS229:CE—UNKO:C	3.626				
	GLY226:CA—UNKO:C	3.973				
	THR249:CB—UNKO:C	3.193				
	THR249:CA—UNKO:C	3.760				
	ALA225:CB—UNKO:C	3.852				
	ALA225:C—UNKO:C	3.781				
	ALA225:C—UNKO:C	3.294				
	ALA224:CB—UNKO:C	2.020				
	ALA224:CB—UNKO:C	2.630				
	ALA224:CB—UNKO:C	3.331				
	ALA224:CB—UNKO:C	3.741				
	ALA224:CA—UNKO:C	3.218				
	GLN526:CB—UNKO:C	3.300				
	TYR528:CB—UNKO:C	3.557				

	TYR528:CB—UNKO:C	3.946				
	TYR528:CA—UNKO:C	3.844				
	TYR528:CA—UNKO:C	3.910				
	LEU527:C—UNKO:C	3.805				
	SER505:CB—UNKO:C	3.217				
	SER505:CB—UNKO:C	3.919				
	THR459:CG—UNKO:C	3.738				
	THR459:CG—UNKO:C	3.496				
	ASN458:CG—UNKO:C	2.951				
	ASN458:CG—UNKO:C	3.767				
	ASN458:CG—UNKO:C	3.333				
	LYS429:CE—UNKO:C	3.945				
	LYS429:CE—UNKO:C	3.990				
	GLY507:CA—UNKO:C	3.784				
	GLY506:C—UNKO:C	3.871				
	GLY506:C—UNKO:C	3.973				
	GLY506:CA—UNKO:C	3.450				
	GLY506:CA—UNKO:C	3.641				
	GLY506:CA—UNKO:C	3.890				
	GLY506:CA—UNKO:C	3.525				
	GLY506:CA—UNKO:C	3.782				
	GLY506:CA—UNKO:C	3.957				
	GLN526:CA—UNKO:C	3.541				
	LEU481:CD2—UNKO:C	2.823				
	LEU481:CD2—UNKO:C	2.809				
	LEU481:CD2—UNKO:C	3.811				
	GLY478:CA—UNKO:C	3.713				
	GLY478:CA—UNKO:C	3.748				
	SER477:C—UNKO:C	3.112				
	SER477:C—UNKO:C	3.958				
	SER477:CA—UNKO:C	2.027				
	VAL476:C—UNKO:C	3.546				
	SER477:CB—UNKO:C	2.239				
	ALA225:C—UNKO:C	3.718				

3.5 Quantitative Structure Activity Relationship

26 compounds of anti-malarial agents (*N*-(4-acylamino/ Arylpropionylamino -3-benzoylphenyl)-[5-(4-nitrophenyl)-2-furyl]acrylic acid amides) were selected as data sets shown in Table 3.9 (Wiesner *et al.*, 2003: Wiesner *et al.*, 2003). Hyper Chem and Chem Draw were used to calculate a number of steric and electronic parameters. The descriptors included partition coefficient i.e. Log P, critical volume, molar refractivity as steric parameter, total binding energy, heat of formation, E_{HOMO}, E_{LUMO} as electronic parameters. The calculated descriptor values are mentioned in Table 3.10. In order to have direct correlation between the descriptor and the compound biological activity the regression coefficient was supposed to be greater than 0.6 and as the regression coefficient value decreased it indicated that there was no correlation among the both variables. Descriptors i.e. electronic and steric parameters were taken as dependent while IC_{50} value as independent variables. The regression values were recorded as 0.133 for Log P, 0.610 for critical volume, 0.635 for molar refractivity, 0.613 for total energy, 0.614 for heat of formation, 0.6 for E_{LUMO} and 0.6071 for E_{HOMO} and the plots are shown in Figure 3.15-3.21. This analysis suggested that there was no correlation between IC_{50} value and Log P but IC_{50} value was found to be directly related to critical volume, molar refractivity, total energy, heat of formation, E_{HOMO} and E_{LUMO} as the regression value of these parameters was greater or equivalent to 0.6

Table 3.9: Data set anti-malarial agents along with the IC_{50} values.

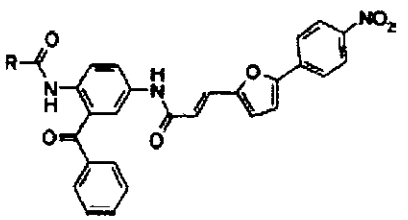

Compound	R	IC_{50} (nM)
4a	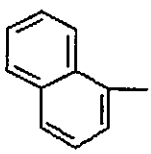	770
4b	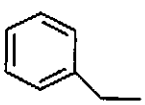	270
4c	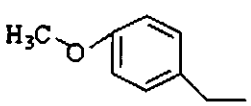	320
4d	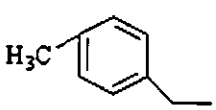	75
4e	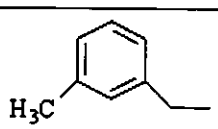	150
4f	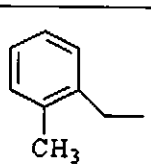	650
4g	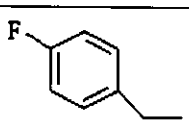	230
4h	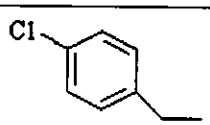	64
4i	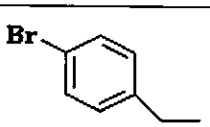	70

4j	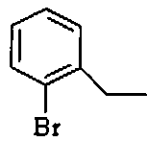	1000
4k	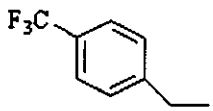	47
4l	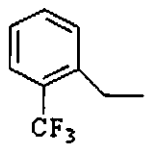	1000
4m	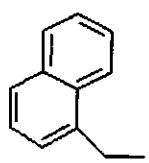	250
4n	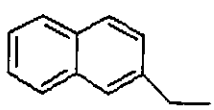	210
4o	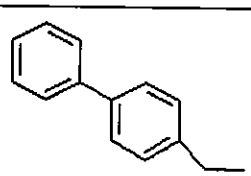	1000
4p	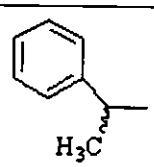	500
4q	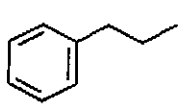	310
4r	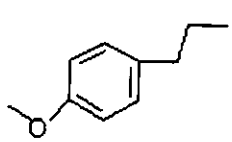	1300
4s	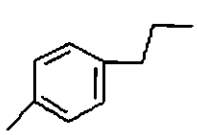	440

4t	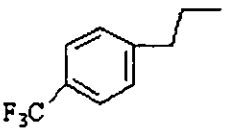	61
4u	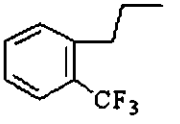	1100
4v	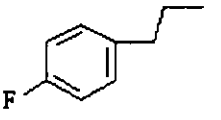	440
4w	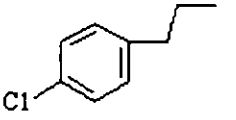	130
4x	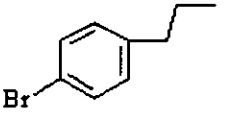	170
4y	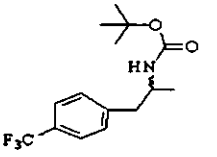	3200
4z	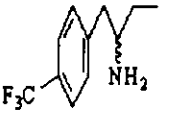	710

Table 3.10: Steric and Electronic descriptors along with IC_{50} value of the data set chosen for QSAR studies.

R	IC_{50} (nM)	Log P	Critical Volume	Molar Refractivity (cm^3/mol)	Total Energy (Kcal/mol)	Heat of Formation (Kcal/mol)	E_{LUMO} (Kcal/mol)	E_{HOMO} (Kcal/mol)
4a	770	5.83	1630.5	175.37	-162040	273.336	0.00331	-0.0297
4b	270	4.78	1540.5	162.51	-153989	216.543	0.03075	-0.02826
4c	320	4.65	1614.5	169.76	-164197	282.949	0.01207	-0.0129
4d	75	5.27	1596.5	168.41	-157441	297.157	0.03834	-0.0225
4e	150	5.27	1596.5	168.41	-157315	333.439	0.02372	-0.02572
4f	650	5.27	1596.5	168.41	-157437	210.928	0.03559	-0.02509
4g	230	4.94	1558.5	162.92	-163661	298.802	0.06027	-0.01259
4h	64	5.34	1589.5	167.12	-160813	336.299	0.06708	-0.00463
4i	70	5.61	1602.5	170.2	-161783	225.594	0.0262	-0.00637
4j	1000	5.61	1602.5	170.2	-161781	227.347	0.02964	-0.0251
4k	47	5.7	1639.5	169.02	-186719	334.053	0.0444	-0.00951
4l	1000	6.46	1639.5	169.02	-186685	227.425	0.04272	-0.0251
4m	250	5.78	1686.5	169.68	-164483	290.120	0.00965	-0.00592
4n	210	5.78	1686.5	169.68	-165618	237.738	0.02572	-0.03266
4o	1000	5.7	1768.5	188.11	-171790	245.659	0.02482	-0.0321
4p	500	5.35	1590.5	167.43	-157308	339.877	0.023	-0.02472
4q	310	5.2	1596.5	167.11	-157312	335.888	0.01942	-0.0185
4r	1300	5.07	1670.5	174.36	-167519	154.731	0.02021	-0.03423
4s	440	5.68	1652.5	173.01	-160765	326.504	0.02394	-0.02773
4t	61	6.12	1695.5	173.62	-190169	257.078	0.05315	-0.02323
4u	1100	6.12	1695.5	173.62	-190134	221.597	0.01737	-0.03149
4v	440	5.36	1614.5	167.51	-167111	292.100	0.0598	-0.01263
4w	130	5.76	1645.5	171.71	-164263	329.454	0.02983	-0.00724
4x	170	6.03	1658.5	174.8	-165232	218.953	0.02258	-0.00352
4y	3200	6.34	2019.5	202.86	-268188	41.949	0.3914	-0.05841
4z	710	5.06	1774.5	181.53	-197705	195.378	0.03362	-0.03716

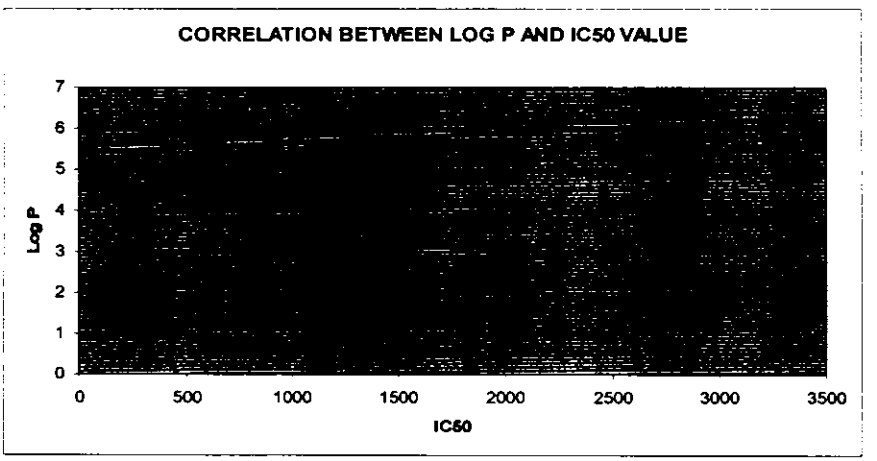

Fig 3.15: Graphical representation showing correlation between Log P and IC_{50} value

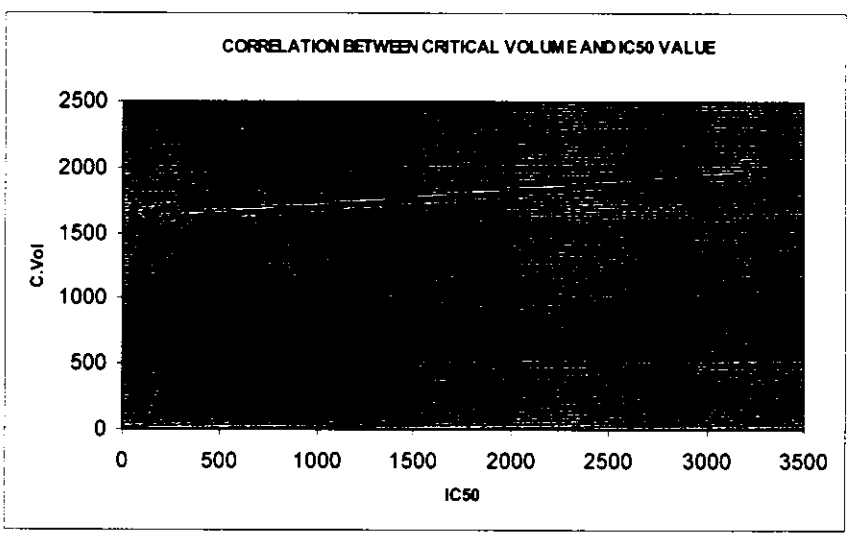

Fig 3.16: Graphical representation showing correlation between critical volume and IC_{50} value

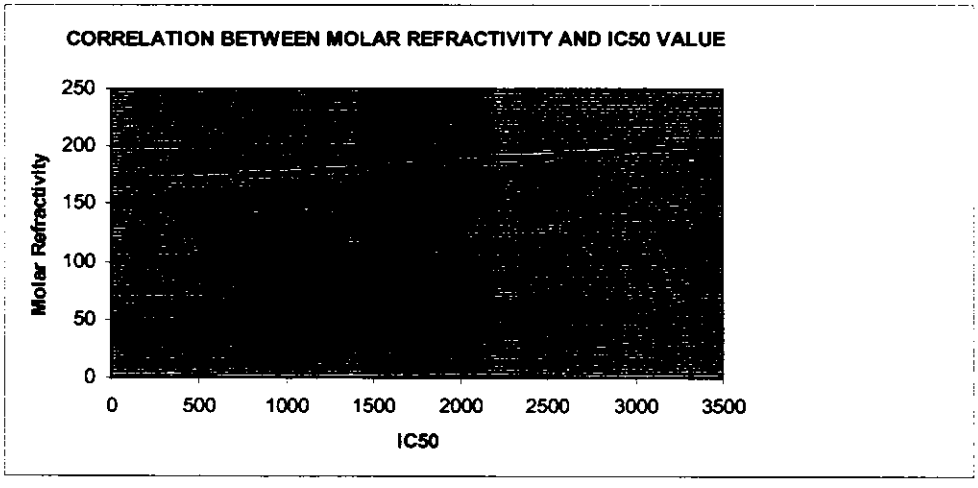

Fig 3.17: Graphical representation showing correlation between molar refractivity and IC_{50} value

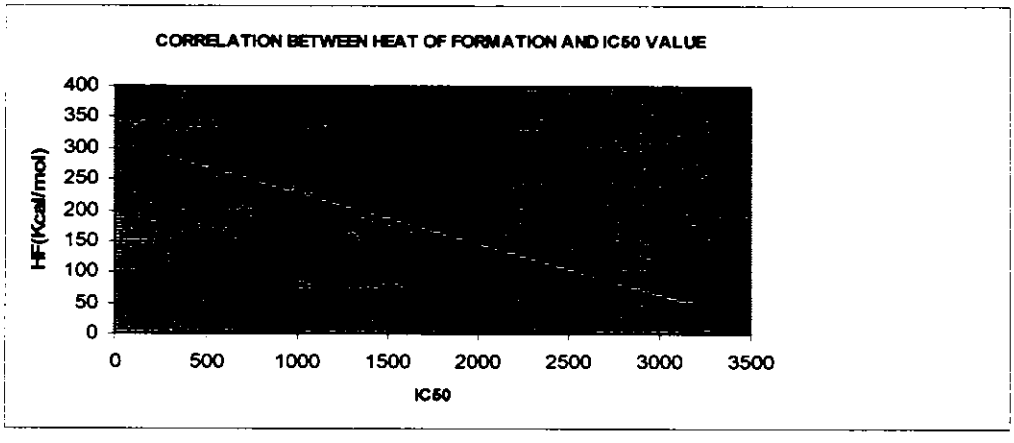

Fig 3.18: Graphical representation showing correlation between heat of formation and IC_{50} value

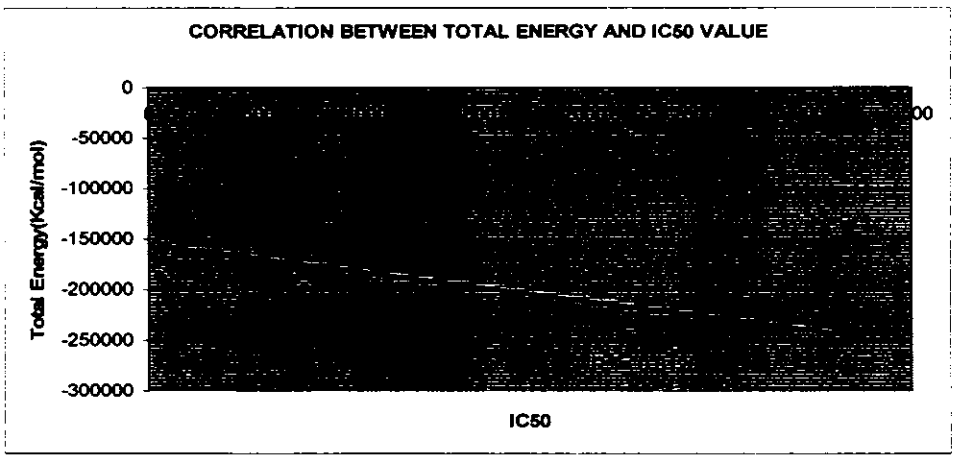

Fig 3.19: Graphical representation showing correlation between total energy and IC_{50} value

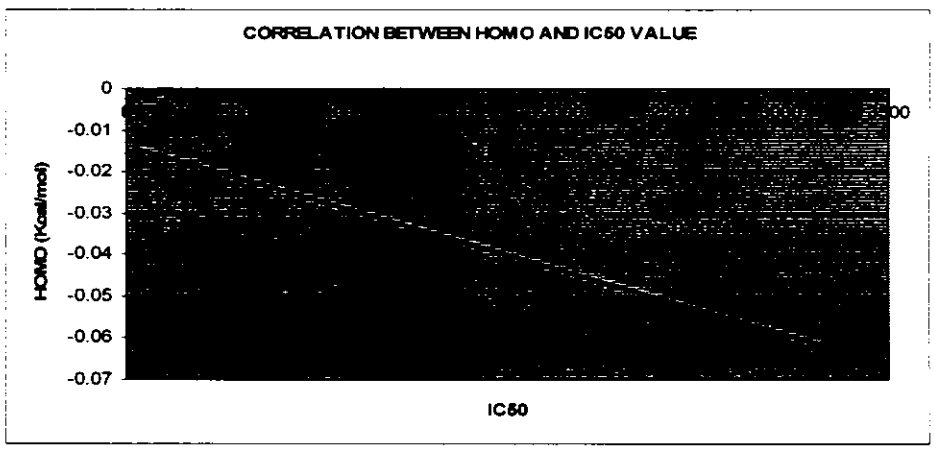

Fig 3.20: Graphical representation showing correlation between E_{HOMO} and IC_{50} value

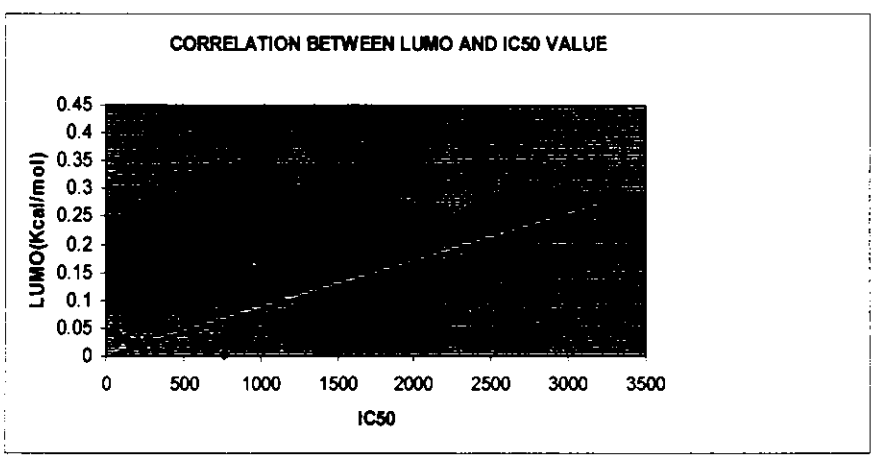

Fig 3.21: Graphical representation showing correlation between E_{LUMO} and IC_{50} value

3.6 Molecular Dynamic Simulation

The molecular dynamic simulation of *plasmodium falciparum* dehydroorotate dehydrogenase bound with triazolopyrimidine-based inhibitor DSM2 was performed, using the GROMOS96 43A1 force field incorporated in the freely available program, GROMACS, in order to understand the inhibition mechanism of inhibitors toward the target. Figure 3.22 shows that the energy is minimized which result in a stability of the structure. The root mean square deviation as a function of the simulation time of the complex with respect to the starting structure was analyzed as shown in figure 3.23. It reveals that the rigid protein structure reach the plateau characteristic at about 400ps and remains below 0.25 nm with respect to their initial coordinates. Figure 3.24 shows that the ligand equilibrates in active site at around 45ps. So the protein/ligand complex show stable dynamics in 1ns simulation and gave almost similar dynamics of protein backbones suggesting sanctity of crystal structure of the complex.

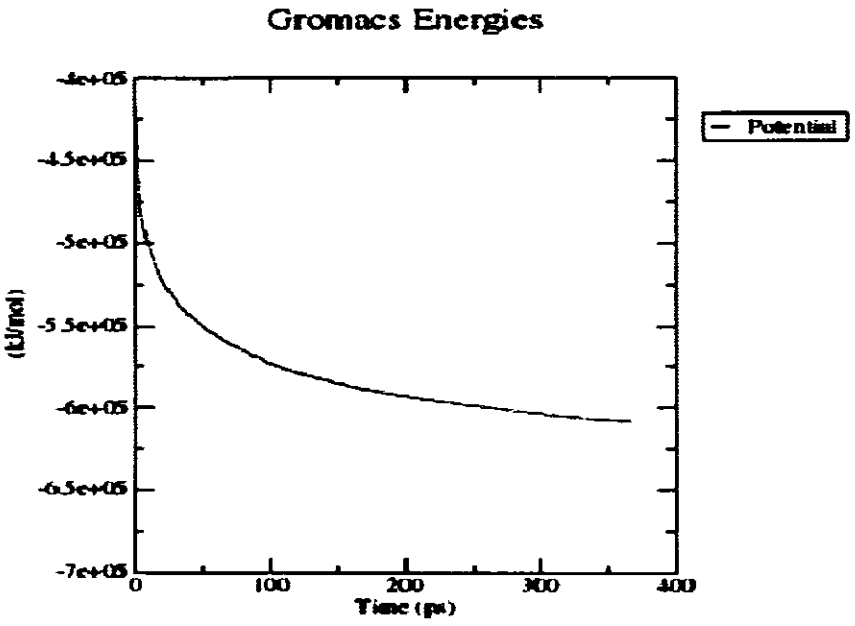

Fig 3.22: Potential Energy

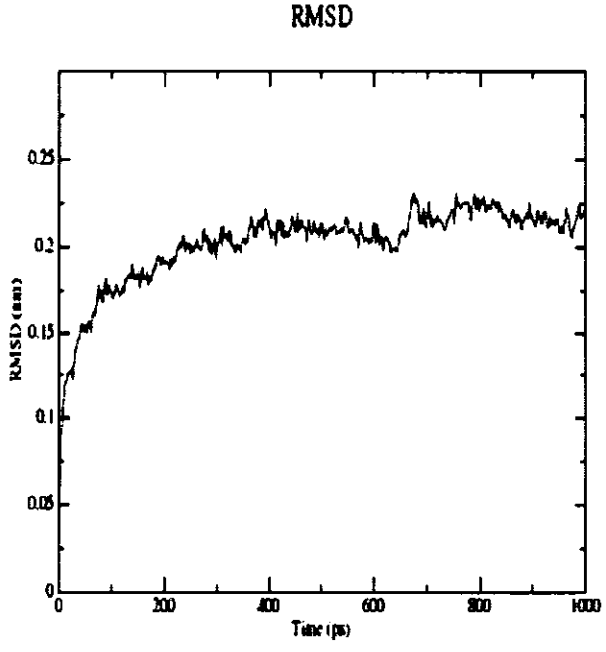

Fig 3.23: Root mean square deviation of protein fit to backbone.

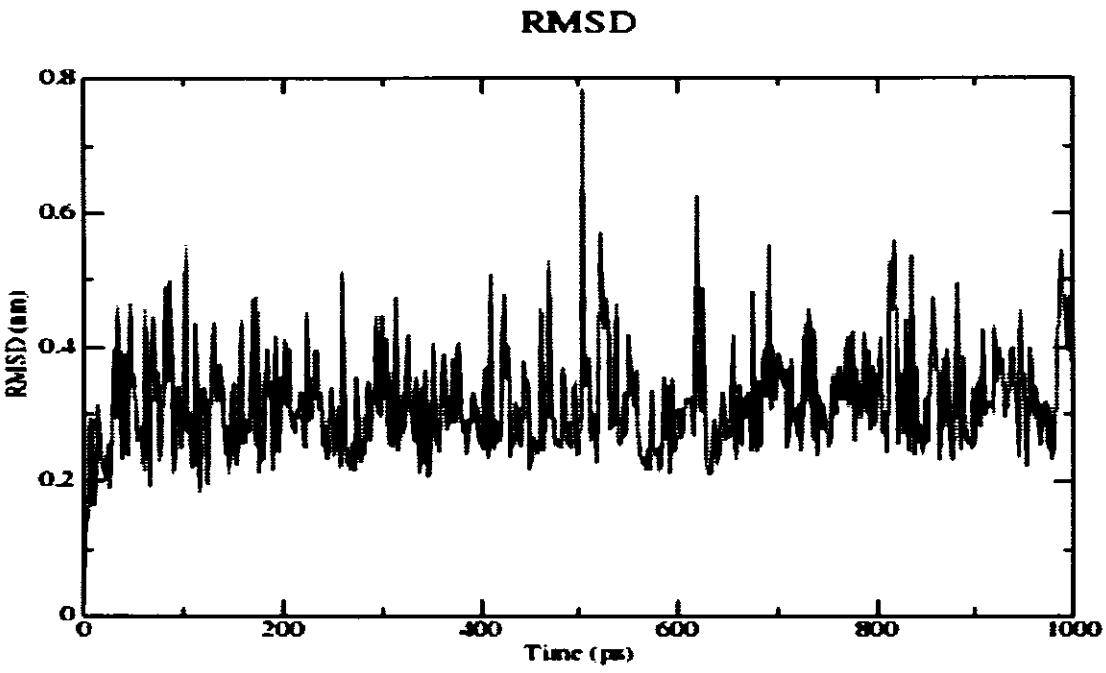

Fig 3.24: Root mean deviation of protein fit to ligand.

CONCLUSION AND FUTURE ENHANCEMENT

Malaria is a mosquito borne disease transmitted by the protozoan parasite Plasmodium which infects the human and insect host alternately. It remains a globally prevalent infectious disease that leads to significant morbidity and mortality as malarial parasites becomes increasingly resistant to several anti-malarial drugs. In the present study, pharmacophore modeling, molecular docking, QSAR and simulation studies have been performed. The aims of this study is to generate pharmacophore model, to identify interaction patterns between the enzyme and ligands at the molecular level for design of new potent DHODH inhibitors, to explore important molecular properties and to identify the stability of protein/ligand complex. So the main purpose of this study is to identify new classes of anti-malarial and develop them as drugs with varied mode of action to overcome resistance problem.

Ligand based pharmacophore modeling was carried on 41 compounds along with 2 standard compounds. A pharmacophore triangle was identified with distances between HBA and HBD range from 4.0 to 4.99, between HBA and Ar/HY range from 3.70 to 4.75 and between Ar/HY and HBA range from 3.7 to 4.6. Identified pharmacophore feature shows that every candidate compound must have 5 hydrophobic volumes, 2 HBA and 1 HBD. It is the novel pharmacophore model identified for anti-malarial inhibitors and this model can be further tested on the other classes therefore a more universal pharmacophore model can be presented.

Molecular docking is used to study how a ligand is interacting with its biological target. Lead compound was identified from the dataset on the basis of having strong binding interaction and lower IC50 value. Three analogues were designed from this lead compound and one analogue have the potential to be the next possible anti-malarial agents as it has

lower binding affinity and strong binding interaction. So it is proposed for clinical trials in order to have a better drug to treat malaria.

Quantitative structure activity relationships are the most important applications of chemo metrics, attempts to find a consistent relationship between biological activity and molecular properties. Thus, QSAR models can be used to predict the activity of new compounds. QSAR studies was done on 26 compounds of anti-malarial agents (*N*-(4-acylamino/ Arylpropionylamino -3-benzoylphenyl)-[5-(4-nitrophenyl)-2-furyl] acrylic acid amides) where the statistical analysis of data suggested that biological activity of compound was directly related to six molecular properties i.e. critical volume, molar refractivity, total energy, heat of formation, E_{HOMO} and $E_{LUMO,}$ while one descriptor i.e. Log P showed no correlation with the activity as the regression value was lower than 0.6. The six descriptors may be evaluated for other classes of compounds to get a broad-spectrum view.

The static view of protein ligand interactions is unrealistic so the dynamic behavior of pfDHODH bound with triazolopyrimidine based inhibitor DSM2 was carried out by bio-molecular simulation packages i.e. GROMACS 4.5.4. The simulation showed stable trajectory indicating a stable equilibrium after energy minimization. The RMSD reach a plateau after a few nanoseconds indicating that it will reach a stable equilibrium after energy minimization although it is more variable indicative of its mobility within the binding pocket. Thus it is proposed to conduct a complete laboratory synthesis of triazolopyrimidine inhibitor and begin clinical trials so that bioactivity of the drug can be reliably outlined.

REFERENCES

- Abagyan R, Totrov M (1994). Biased probability Monte Carlo conformational searches and electrostatic calculations for peptides and proteins. J. Mol. Biol. 235:983–1002.
- Abagyan R, Totrov M, Kuznetsov D (1994). ICM - a new method for protein modeling and design: Applications to docking and structure prediction from the distorted native conformation. J. Comput. Chem. 15:488–506.
- Alonso PL, Djimde A, Kremsner P, Magill A, Milman J, Nájera J, Plowe CV, Rabinovich R, Wells T, Yeung S (2011). A research agenda for malaria eradication: drugs. PLoS Med. 8(1):e1000402.
- Alder BJ, Wainwright TE (1957). Phase Transition for a Hard Sphere System. J. Chem. Phys. 27:1208.
- Baldwin J, Michnoff CH, Malmquist NA, White J, Roth MG, Rathod PK, Phillips MA (2005). High-throughput screening for potent and selective inhibitors of *Plasmodium falciparum* dihydroorotate dehydrogenase. J. Biol. Chem. 280:21847.
- Balint GA (2001). Artemisinin and its derivatives: An important new class of anti-malarial agents. Pharmacol.Ther. 90:261–265.
- Barreca ML, De Luca L, Iraci N, Rao A, Ferro S, Maga G, Chimirri A (2007). Structure-based pharmacophore identification of new chemical scaffolds as non-nucleoside reverse transcriptase inhibitors. J. Chem. Inf. Model. 47 (2): 557–562.
- Barril X, Soliva R (2006). Molecular Modelling. Mol. Biosyst. 2:660–681.
- Batt DG, Copeland RA, Dowling RL, Gardner TL, Jones EA, Orwat MJ, Pinto DJ, Pitts WJ, Magolda RL, Jaffee BD (1995). Immunosuppressive structure-activity

relationships of Brequinar and related cinchoninic acid derivatives. Bioorg. Med. Chem. Lett. 5(14):1549–1554.

- Batt DG, Petraitis JJ, Sherk SR, Copeland RA, Dowling RL, Taylor TL, Jones EA, Magolda RL, Jaffee BB (1998). Heteroatom-and carbon-linked biophenyl analogs of brequinar as immunosuppressive agents. Bioorg. and Med. Chem. Lett. 8(13):1745–1750.
- Baumgartner R, Walloschek M, Kralik M, Gotschlich A, Tasler S, Mies J, Leban J (2006). Dual binding mode of a novel series of DHODH inhibitors. J. Med. Chem 49(4):1239–1247.
- Biagini GA, Fisher N, Berry N, Stocks PA, Meunier B, Williams DP, Bonar-Law R, Bray PG, Owen A, O'Neill PM, Ward SA (2008). Acridinediones: Selective and potent inhibitors of the malaria parasite mitochondrial bc1 complex. Mol. Pharmacol. 73:1347–1355.
- Blaney J, Dixon J (1993). A good ligand is hard to find: Automated docking methods. Perspect. Drug Disc. Des. 1:301–319.
- Boa AN, Canavan SP, Hirst PR, Ramsey C, Stead AMW, McConkey GA. Synthesis of brequinar analogue inhibitors of malaria parasite dihydroorotate dehydrogenase (2005). Bioorganic & Medicinal Chemistry 13:1945–1967.
- Boa AN, Canavan SP, Hirst PR, Ramsey C, Stead AMW, McConkey GA (2005). Synthesis of Brequinar Analogue Inhibitors of Malaria Parasite Dihydroorotate Dehydrogenase. Bioorg. Med. Chem. 13(6):1945—1967.
- Brem R, Dill KA (1999).The effect of multiple binding modes on empirical modeling of ligand docking to proteins. Protein Sci. 8:1134–1143.

- Brooks BR, Bruccoleri RE, Olafson BD, States DJ, Swaminathan S, Karplus M (1983). CHARMM—A program for macromolecular energy, minimization, and dynamics calculations. J. Comput. Chem. 4:187–217.
- Breman JG. The ears of the hippopotamus: Manifestations, determinants, and estimates of the malaria burden (2001). Am. J. Trop. Med. Hyg. 64:1–11.
- Carlos AG, Priscilla WG, Andrew J T, Abdisalan M N, Dave LS, Simon IH, Robert WS (2008).The Limits and Intensity of *Plasmodium falciparum* Transmission: Implications for Malaria Control and Elimination Worldwide. PLoS Medicine. 5:e38.
- Cornell WD, Cieplak P, Bayly CI, Gould IR, Merz KM, Ferguson DM, Spellmeyer DC, Fox T, Caldwell JW, Kollman PA (1996). A second generation force field for the simulation of proteins, nucleic acids, and organic molecules. J. Am. Chem. Soc. 118:2309–2309.
- Chang MW, Ayeni C, Breuer S, Torbett BE (2010). Virtual screening for HIV protease inhibitors: A comparison of AutoDock 4 and Vina. PLoS ONE 5(8):E11955.
- Chen SF, Ruben RL, Dexter DL (1986). Mechanism of action of the novel anticancer agent 6-fluoro-2-(2'- fluoro-1,1'-biphenyl-4-yl)-3-methyl-4-quinolinecarbo xylic acid sodium salt (NSC 368390): inhibition of de novo pyrimidine nucleotide biosynthesis. Cancer Res. 46(10):5014–5019.
- Copeland RA, Marcinkeviciene J, Haque TS, Kopcho LM , Jiang W, Wang K, Ecret LD, Sizemore C, Amsler KA, Foster L, Tadesse S, Combs AP, Stern AM, Trainor GL, Slee A, Rogers MJ, F. Hobbs (2000). Helicobacter pylori-selective anti-bacterials based on inhibition of pyrimidine biosynthesis. J. Biol. Chem. 275:33373–33378.

- Davies M, Heikkila T, McConkey GA, Fishwick CW, Parsons MR, Johnson AP (2009). Structure-based design, synthesis, and characterization of inhibitors of human and *Plasmodium falciparum* dihydroorotate dehydrogenases. J. Med. Chem. 52(9):2683–2693.
- Davis JP, Cain GA, Pitts WJ, Magolda RL, Copeland RA (1996). The Immunosuppressive Metabolite of Leflunomide Is a Potent Inhibitor of Human Dihydroorotate Dehydrogenase Biochemistry. 35:1270–1273.
- Deguchi M, Kishino J, Hattori M, Furue Y, Yamamoto M, Mochizuki I, Iguchi M, Hirano Y, Hojou K, Nagira M, Nishitani Y, Okazaki K, Yasui K, Arimura A (2008). Suppression of immunoglobulin production by a novel dihydroorotate dehydrogenase inhibitor, S-2678. Eur. J. Pharmacol. 601(1–3):163–170.
- Deng X, Gujjar R, El Mazouni F, Kaminsky W, Malmquist NA, Goldsmith EJ, Rathod PK, Phillips MA (2009). Structural plasticity of malaria dihydroorotate dehydrogenase allows selective binding of diverse chemical scaffolds. J. Biol. Chem. 284(39):26999–27009.
- Dixon SL, Smondyrev AM, Knoll EH, Rao SN, Shaw DE, Friesner RA (2006). PHASE: a new engine for pharmacophore perception, 3D QSAR model development, and 3D database screening: 1. Methodology and preliminary results. J. Comput.-Aided Mol. Des. 20:647–671.
- Dondorp AM, Nosten F, Yi P, Das D, Phyo AP, Tarning J, Lwin KM, Ariey F, Hanpithakpong W, Lee SJ, Ringwald P, Silamut K, Imwong M, Chotivanich K, Lim P, Herdman T, An SS, Yeung S, Singhasivanon P, Day NP, Lindegardh N, Socheat D,

White NJ. Artemisinin resistance in *Plasmodium falciparum* malaria (2009). N. Engl. J. Med 361(5):455–467.

- Egan TJ, Kaschula CH (2007). Strategies to reverse drug resistance in malaria. Curr. Opin. Infect. Dis. 20:598–604.
- Ehrlich P (1909). Über den jetzigen Stand der Chemotherapie. Ber. Dtsch. Chem. Ges. 42: 17–47.
- Ewing TJA, Kuntz ID (1997). Critical evaluation of search algorithms for automated molecular docking and database screening. J. Comput. Chem. 18:1175-1189. FEBS Lett. 580:2928–2934.
- Friesner RA, Banks JL, Murphy RB, Halgren TA, Klicic JJ, Mainz DT, Repasky MP, Knoll EH, Shelley M, Perry J K, Shaw DE, Francis P, Shenkin PS (2004). Glide: A new approach for rapid, accurate docking and scoring. 1. Method and assessment of docking accuracy. J. Med. Chem. 47:1739–1749.
- Friesner RA, Murphy RB, Repasky MP, Frye LL, Greenwood JR, Halgren TA, Sanschagrin PC, Mainz DT (2006). Extra precision glide: Docking and scoring incorporating a model of hydrophobic enclosure for protein-ligand complexes. J. Med. Chem. 49:6177–6196.
- Fujioka H, Aikawa M. Structure and Life Cycle (2002). Chem Immunol. Basel, Karger, 80:1–26.
- Fuller JC, Burgoyne NJ, Jackson RM (2009). Predicting druggable binding sites at the protein-protein interface. Drug Discov. Today. 14:155–161.

- Gardner MJ, Hall N, Fung E, White O, Berriman M, Hyman RW, Carlton JM, Pain A, Nelson, KE, Bowman S, Paulsen IT, James K, Eisen JA, Rutherford K, Salzberg SL, Craig A, Kyes S, Chan MS, Nene V, Shallom SJ, Suh B, Peterson J, Angiuoli S, Pertea M Allen J, Selengut J, Haft D, Mather MW, Vaidya AB, Martin DMA, Fairlamb AH, Fraunholz MJ, Roos DS, Ralph SA, McFadden GI, Cummings LM, Subramanian GM, Mungall C, Venter JC, Carucci DJ, Hoffman SL, Newbold C, Davis RW, Fraser CM, Barrell B (2002). Genome sequence of the human malaria parasite *Plasmodium falciparum*. Nature. 419: 498–511.
- Goodsell DS, Olson AJ (1990). Automated docking of substrates to proteins by simulated annealing. Protein. Struct. Funct. Genet. 8:195–202.
- Greene S, Watanabe S, Braatz-trulson J, Lou L (1995). Inhibition of dihydroorotate dehydrogenase by the Immunosuppressive agent leflunomide. Biochem. Pharmacol. 50:861.
- Greenwood BM, Bojang K, Whitty CJM, Targett GAT (2005). Malaria. Lancet. 365:1487–1498.
- Greenwood BM, Fidock DA, Kyle DE, Kappe SHI, Alonso PL, Collins FH, Duffy PE (2008). Malaria: Progress, perils, and prospects for eradication. J. Clin. Invest. 118:1266–1276.
- Greer J, Erickson WJ, Baldwin JJ, Varney MD (1994). Application of the three-dimensional structures of protein target molecules in structure-based drug design. J. Med. Chem. 37:1035–1054.
- Guidelines for the treatment of malaria. World Health Organization: 2006; p253.

- Gund P (1979). Pharmacophoric Pattern Searching and Receptor Mapping. Annual Reports in Medicinal Chemistry. 14: 299–308
- Halgren TA, Murphy RB, Friesner RA, Beard HS, Frye LL, Pollard WT, Banks JL (2004). Glide: A new approach for rapid, accurate docking and scoring. 2. Enrichment factors in database screening. J. Med. Chem. 47, 1750–1759.
- Hansch C, Yoshimoto M (1974). Structure-activity relationship in immunochemistry, 2. Inhibition of complement by benzamidines. J. Med. Chem. 17:1160–1167.
- Hansson T, Oostenbrink C, van Gunsteren W (2002). Molecular dynamics simulations. Curr Opin Struct Biol. 12:190–196.
- Heikkila T, Thirumalairajan S, Davies M, Parsons MR, McConkey AG, Fishwick C, Johnson P (2006). The first de novo designed inhibitors of *Plasmodium falciparum* dihydroorotate dehydrogenase. Bioorganic & Medicinal Chemistry Letters. 16:88–92.
- Heikkila T, Thirumalairajan S, Davies M, Parsons MR, McConkey AG, Fishwick CW, Johnson AP. The first de novo designed inhibitors of *Plasmodium falciparum* dihydroorotate dehydrogenase (2006). Bioorg Med Chem Lett. 16(1):88–92.
- Henry CM (2001). Structure-based drug design. C & EN. 79:69–74.
- Herrmann ML, Schleyerbach R, Kirschbaum B (2000). Leflunomide: an immunomodulatory drug for the treatment of rheumatoid arthritis and other autoimmune diseases. Immunopharmacology. 47:273–289.
- Huey R, Morris GM, Olson AJ, Goodsell DS (2007). A semiempirical free energy force field with charge-based desolvation. J. Comput. Chem. 28:1145–1152.

- Humphrey W, Dalke A, Schulten K (1996). VMD: Visual molecular dynamics. Journal of Molecular Graphics. 14(1): 33–38.
- Humphrey WF, Dalke A, Schulten K (1996). VMD - Visual Molecular Dynamics. J. Mol. Graphics 14:33–38.
- Hurt DE, Widom J, Clardy J (2006). Structure of *Plasmodium falciparum* dihydroorotate dehydrogenase with a bound inhibitor. Acta. Crystallogr. D Biol. Crystallogr 62(3):312–323.
- Hypercube, Inc., HyperChem ®Release 7 for Windows ®, (Jan 2002).
- Idro R, Bitarakwate E, Tumwesigire SAM, John CC (2005). Clinical manifestations of severe malaria in the highlands of southwestern Uganda. Am. J. Trop. Med. Hyg. 72:561-567.
- Drie (2007). Monty Kier and the Origin of the Pharmacophore Concept". Internet Electronic Journal of Molecular Design 6: 271–279.
- Jain AN (2003). Surflex: Fully automatic flexible molecular docking using a molecular similarity-based search engine. J. Med. Chem. 46:499–511.
- Jones G, Willett P, Glen RC (1995). A genetic algorithm for flexible molecular overlay and pharmacophore elucidation. J. Comput.-Aided Mol. Des. 9:532–549.
- Jones G, Willett P, Glen RC (1995). Molecular recognition of receptor sites using a genetic algorithm with a description of desolvation. J. Mol. Biol. 245:43–53.
- Jones G, Willett P, Glen RC, Leach AR, Taylor R (1997). Development and validation of a genetic algorithm for flexible docking. J. Mol. Biol. 267:727–748.

- Jorgensen WL (2004). The Many Roles of Computation in Drug Discovery. Science. 303(5665):1813–1818.
- Karplus M, McCammon JA (2002). Molecular dynamics simulations of biomolecules. Nat. Struct. Biol. 9:646–652.
- Kaur K, Jain M, Kaur T, Jain R. Antimalarials from nature (2009). Bioorg Med Chem. 17(9):3229–3256.
- Kuo EA, Hambleton PT, Kay DP, Evans PL, Matharu SS, Little E, McDowall N, Jones CB, Hedgecock CJ, Yea CM, Chan AW, Hairsine PW, Ager IR, Tully WR, Williamson RA, Westwood R (1996). Synthesis, structure-activity relationships, and pharmacokinetic properties of dihydroorotate dehydrogenase inhibitiors: 2-cyano-3-cyclopropyl-3-hydroxy-N-[3'-methyl-4'-(trifluoromethyl) phenyl]propenamide and related compounds. J. Med. Chem. 39(23):4608–4621.
- Kier LB (1967). Molecular orbital calculation of preferred conformations of acetylcholine, muscarine, and muscarone. Mol. Pharmacol. 3 (5): 487–94.
- Kier LB (1971). Molecular orbital theory in drug research. Boston: Academic Press. 164–169.
- Klebe G, Kubinyi H, Folkers G, Martin YC (Eds) (1998). Comparative Molecular Similarity Indices: CoMSIA In 3D QSAR in Drug Design. Kluwer Academics Publishers, Great Britain 3:87.
- Knecht W, Loffler M (2000). Redoxal as a new lead structure for dihydroorotate dehydrogenase inhibitors: a kinetic study of the inhibition mechanism. FEBS Lett. 467(1):27–30.

- Knecht W, Loffler M. Redoxal as a new leadstructure for dihydroorotate dehydrogenase inhibitors: a kinetic study of the inhibition mechanism (2000). FEBS Letters 467:27-30.
- Knegtel RMA, Wagener M (1999). Efficacy and selectivity in flexible database docking. Proteins. 37:334–345.
- Korenromp E, Miller J, Nahlen B, Wardlaw T, Young M. World malaria report. Geneva: Roll Back Malaria Partnership, World Health Organisation and United Nations Children's Fund (UNICEF); 2005.
- Kramer B, Rarey M, Lengauer T (1999). Evaluation of the FLEXX incremental construction algorithm for protein–ligand docking. Proteins. 37:228–241.
- Kumar S, Guha M, Choubey V, Maity P, Bandyopadhyay U (2007). Antimalarial drugs inhibiting hemozoin ([beta]-hematin) formation: A mechanistic update. Life Sci. 80:813-828.
- Kuntz ID, Blaney JM, Oatley SJ, Langridge R, Ferrin TE (1982) A geometric approach to macromolecule-ligand interactions. J. Mol. Biol. 161:269–288.
- Kuo EA, Hambleton PT, Kay DP, Evans PL, Matharu SS, Little E, McDowall N, Jones CB,
- Kutter E, Hansch C (1969). The use of substituent constants in the quantitative treatment of hapten-antibody interaction. Arch. Biochem. Biophys. 135:126–135.
- Leach AR, Kuntz ID (1992). Conformational analysis of flexible ligands in macromolecular receptor sites. J. Comput. Chem. 13:730–748.

- Liu S, Neidhardt EA, Grossman TH, Ocain T, Clardy J (2000). Structures of human dihydroorotate dehydrogenase in complex with antiproliferative agents. Structure. 8(1):25–33.
- Marcinkeviciene J, Rogers MJ, Kopcho L, Jiang W, Wang K, Murphy DJ, Lippy J, Link S, Chung TDY, Hobbs F Haque T, Trainor GL, Slee A, Stern AM. Copeland R.A (2000). Selective Inhibition of Bacterial Dihydroorotate Dehydrogenases by Thiadiazolidinediones. Biochem. Pharmacol. 60:339–342.
- Marshall GR , Barry CD , Bosshard HE , Dammkoehler RA, Dunn DA (1979).The Conformational Parameter in Drug Design: The Active Analog Approach. Computer-Assisted Drug Design. 9:205–226.
- McGann MR, Almond HR, Nicholls JA, Grant A, Brown FK (2003). Gaussian docking functions. Biopolymers. 68:76–90.
- McLean LR, Zhang Y, Degnen W, Peppard J, Cabel D, Zou C, Tsay JT, Subramaniam A, Vaz RJ, Li Y. Discovery of novel inhibitors for DHODH via virtual screening and X-ray crystallographic structures (2010). Bioorganic & Medicinal Chemistry Letters 20 :1981-1984.
- Meng EC, Shoichet BK, Kuntz ID (1992). Automated docking with grid-based energy evaluation. J. Comput. Chem. 13:505–524.
- Milner E, McCalmont W, Bhonsle J, Caridha D, Carroll D, Gardner S, Gerena L, Gettayacamin M, Lanteri C, Luong T, Melendez V, Moon J, Roncal N, Sousa J, Tungtaeng A, Wipf P, Dow G. Structure–activity relationships amongst 4-position quinoline methanol antimalarials that inhibit the growth of drug sensitive and resistant

strains of *Plasmodium falciparum* (2010). Bioorganic & Medicinal Chemistry Letters. 20:1347–1351.

- Moitessier N, Englebienne P, Lee D, Lawandi J, Corbeil CR (2007). Towards the development of universal, fast and highly accurate docking/scoring methods: A long way to go. Br. J. Pharmacol., 153:S7–S26.
- Morris GM, Goodsell DS, Halliday RS, Huey R, Hart WE, Belew RK, Olson AJ (1998). Automated docking using a Lamarckian genetic algorithm and an empirical binding free energy function. J. Comput. Chem. 19:1639–1662.
- Morris GM, Goodsell DS, Huey R, Olson AJ (1996). Distributed automated docking of flexible ligands to proteins: Parallel applications of AutoDock 2.4. J. Comput. Aided Mol. Des. 10:293–304.
- Moustakas D, Lang P, Pegg S, Pettersen E, Kuntz I, Brooijmans N, Rizzo R (2006). Development and validation of a modular, extensible docking program: DOCK 5. J. Comput. Aided Mol. Des. 20:601–619.
- Muller BA (2009). How modern chemistry has changed drug Development. Curr. Pharm. Des. 15:120–133.
- Murray MC, Perkins ME (1996). Antimalarial activity and synthesis of new trisubstituted pyrimidines. Ann. Rep. Med. Chem. 31:141–150.
- Patel V, Booker M, Kramer M, Ross L, Celatka CA, Kennedy LM, Dvorin JD, Duraisingh MT, Sliz P, Wirth DF, Clardy J. Identification and characterization of small molecule inhibitors of *Plasmodium falciparum* dihydroorotate dehydrogenase (2008). J. Biol. Chem. 283(50):35078-35085.

- Norberg J, Nilsson L (2003). Advances in biomolecular simulations: Methodology and recent applications. Quart. Rev. Biophys. 36:257–306.
- Nelson MT, HumphreyW, Gursoy A, Dalke A, Kale LV, Skeel RD, Schulten K (1996). NAMD: A parallel, object oriented molecular dynamics program. Int. J. Supercomput. Applic. 10:251–268.
- Peters GJ, Schwartsmann G, Nadal JC, Laurensse EJ, van Groeningen CJ, van der Vijgh WJ, Pinedo HM (1990). In vivo inhibition of the pyrimidine de novo enzyme dihydroorotic acid dehydrogenase by brequinar sodium (DUP-785; NSC 368390) in mice and patients. Cancer Res. 50(15):4644–4649.
- Phillips MA, Rathod PK (2010). *Plasmodium falciparum* dihydroorotate dehydrogenase: a promising target for novel anti-malarial chemotherapy. Infect Disord. Drug Targets. 10(3): 226–239.
- Pitts WJ, Jetter JW, Pinto DJ, Orwat MJ, Batt DG, Sherk SR, Petraitis JJ, Jacobson IC, Copeland RA, Dowling RL, Jaffee BD, Gardner TL, Jones EA, Magolda RL (1998). Structure-activity relationships of some tetracyclic heterocycles related to the immunosuppressive agent brequinar sodium. Bioorg. And Med. Chem. Lett. 8(3):307–312.
- Rarey M, Kramer B, Lengauer T (1997). Multiple automatic base selection: Protein–ligand docking based on incremental construction without manual intervention. J. Comput. Aided Mol. Des. 11:369–384.
- Punkvang A, Saparpakorn P, Hannongbua S, Wolschann P, Beyer A, Pungpo P (2010). Investigating the structural basis of arylamides to improve potency against M.

tuberculosis strain through molecular dynamics simulations. European Journal of Medicinal Chemistry. 45:5585–5593

- Rarey M, Kramer B, Lengauer T (1999). Docking of hydrophobic ligands with interaction-based matching algorithms. Bioinformatics. 15:243-250.
- Rarey M, Kramer B, Lengauer T (1999). The particle concept: Placing discrete water molecules during protein-ligand docking predictions. Protein. Struct. Funct. Genet. 34:17–28.
- Rarey M, Kramer B, Lengauer T, Klebe G (1996). A fast flexible docking method using an incremental construction algorithm. J. Mol. Biol. 261:470–489.
- Rarey M, Wefing S, Lengauer T (1996). Placement of medium-sized molecular fragments into active sites of proteins. J. Comput. Aided Mol. Des. 10:41–54.
- Rahman A(1964). Correlations in the Motion of Atoms in Liquid Argon. Phys. Rev. 136:A405-A4
- Richmond NJ, Abrams CA, Wolohan PRN, Abrahamian E, Willett P, Clark RD (2006). GALAHAD: 1. Pharmacophore identification by hypermolecular alignment of ligands in 3D. J. Comput.-Aided Mol. Des. 20:567–587.
- Robert IF, Matthias LH, Costakis GF, Geoffrey MW, Randall EM, Vibeke S, Bernhard JK (1999). Mechanism of action for leflunomide in rheumatoid arthritis. Clin. Immunol.93:198.
- Rosenthal PJ (2001). Antimalarial chemotherapy. Mechanism of action, resistance, and new directions in drug discovery. Humana Press: 400.
- Schellenberg D, Menendez C, Kahigwa E, Font F, Galindo C, Acosta C, Schellenberg JA, Aponte JJ, Kimario J, Urassa H, Mshinda H, Tanner M, Alonso P (1999). African

children with malaria in an area of intense *Plasmodium falciparum* transmission: Features on admission to the hospital and risk factors for death. Am. J. Trop. Med. Hyg. 61:431–438.

- Shoichet BK, Kuntz ID, Bodian DL (1992). Molecular docking using shape descriptors. J. Comput. Chem. 13: 380–397.
- Slater AFG (1993). Chloroquine: Mechanism of drug action and resistance in *Plasmodium falciparum*. Pharmacol. Ther. 57:203-235.
- Snow RW, Guerra CA, Noor AM, Myint HY, Hay SI (2005). The global distribution of clinical episodes of *Plasmodium falciparum* malaria. Nature. 434(7030):214–7.
- Stillinger FH, Rahman A (1974). Improved simulation of liquid water by molecular dynamics. J. Chem. Phys. 60:1545–1557.
- Snow CD, Sorin EJ, Rhee YM, Pande VS (2005). How well can simulation predict protein folding kinetics and thermodynamics? Annu Rev Biophys Biomol Struct. 34:43–69.
- Scott WRP, Hunenberger PH, Tironi IG, Mark AE, Billeter SR, Fennen J, Torda AE, Huber T, Kruger P, van Gunsteren WF (1999). The GROMOS biomolecular simulation program package. J. Phys. Chem. A. 103:3596–3607.
- Taylor TE, Fu WJ, Carr RA, Whitten RO, Mueller JG, Fosiko NG, Lewallen S, Liomba NG, Molyneux ME (2004). Differentiating the pathologies of cerebral malaria by postmortem parasite counts. Nat. Med. 10:143–145.
- Totrov M, Abagyan R (1997). Flexible protein-ligand docking by global energy optimization in internal coordinates. Protein. Struct. Funct. Genet. 29:215–220.

- Totrov M, Abagyan R (1997). Flexible protein-ligand docking by global energy optimization in internal coordinates. Protein. Struct. Funct. Genet. 29:215–220.
- Tramontano A (2006). The role of molecular modelling in biomedical research. FEBS Lett. 580(12):2928–2934.
- Trott O, Olson AJ (2010). AutoDock Vina: improving the speed and accuracy of docking with a new scoring function, efficient optimization and multithreading. Journal of Computational Chemistry. 31:455–461.
- Tsuiji M (2010). Homology modeling of HyperChem, Revision F1; Saitama, JAPAN.
- Verdonk ML, Chessari G, Cole JC, Hartshorn MJ, Murray CW, Nissink JWM, Taylor RD, Taylor R (2005). Modeling water molecules in protein-ligand docking using gold. J. Med. Chem. 48, 6504–6515.
- Verdonk ML, Cole JC, Hartshorn MJ, Murray CW, Taylor RD (2003). Improved protein-ligand docking using gold. Protein. Struct. Funct. Genet. 52:609–623.
- Verkhivker GM, Bouzida D, Gehlhaar DK, Rejto PA, Arthurs S, Colson AB, Freer ST, Larson V, Luty BA, Marrone T, Rose PW (2000). Deciphering common failures in molecular docking of ligand-protein complexes. J. Comput. Aided Mol. Des.14:731–751.
- Walse B, Dufe VT, Svensson B, Fritzson I, Dahlberg L, Khairoullina A, Wellmar U, Al-Karadaghi S (2008). The structures of human dihydroorotate dehydrogenase with and without inhibitor reveal conformational flexibility in the inhibitor and substrate binding sites. Biochemistry. 47(34): 8929–8936.

- Wermuth CG, Ganellin CR, Lindberg P, Mitscher LA (1998). Glossary of terms used in medicinal chemistry (IUPAC Recommendations 1998). Pure and Applied Chemistry. 70 (5): 1129–1143.
- Wiesner J, Fucik K, Kettler K, Sakowski J, Ortmann R, Jomaa H, Schlitzer M (2003). Structure–Activity relationships of novel anti-malarial agents. Part 6: N-(4-Arylpropionylamino-3-benzoylphenyl)-[5-(4-nitrophenyl)-2-furyl]acrylic acid amides. Bioorganic & Medicinal Chemistry Letters. 13(9):1539–1541.
- Wiesner J, Kettle K, Sakowski J, Ortmann R, Jomaa H, Schlitzer M (2003). Structure–Activity relationships of novel anti-Malarial agents: Part 5. N-(4-acylamino-3-benzoylphenyl)-[5-(4-nitrophenyl)-2-furyl] acrylic acid amides. Bioorganic & Medicinal Chemistry Letters. 13(3):361–363.
- Wolber G, Dornhofer AA, Langer T (2007). Efficient overlay of small organic
- Wolber G, Langer T (2005). LigandScout molecules using 3D pharmacophores. J. Comput. Aided. Mol. Des. 20 (12):773–788.: 3-D Pharmacophores Derived from Protein-Bound Ligands and Their Use as Virtual Screening Filters J. Chem. Inf. Model. 45:160–169.
- Wolber G, Langer T (2005). LigandScout: 3-D pharmacophores derived from protein-bound ligands and their use as virtual screening filters. J Chem. Inf. Model. 45 (1):160–169.
- Zhang YK, Plattner JJ, Freund YR, Easom EE, Zhou Y, Gut J, Rosenthal PJ, Waterson D, Gamo FJ, Barturen IA, Ge M, Li Z, Li L, Jian Y, Cui H, Wang H, Yang J. Synthesis and structure–activity relationships of novel benzoxaboroles as a new class of antimalarial agents (2011). Bioorganic & Medicinal Chemistry Letters. 21:644–651.

- Zielesny A (2005). Chemistry Software Package ChemOffice Ultra 2005. J. Chem. Inf. Model. 1474–1477